Technische Universität München
WACKER-Lehrstuhl für Makromolekulare Chemie

Novel developments in Hydrogen Storage, Hydrogen Activation and Ionic Liquids

Amir Doroodian

Vollständiger Abdruck der von der Fakultät für Chemie der Technischen Universität München zur Erlangung des akademischen Grades eines

Doktors der Naturwissenschaften

genehmigten Dissertation.

Vorsitzender: Univ.-Prof. Dr. K. O. Hinrichsen

Prüfer der Dissertation:

1. Univ.-Prof. Dr. Dr. h. c. B. Rieger

2. apl. Prof. Dr. Anton Lerf

Die Dissertation wurde am 28.10.2010 bei der Technischen Universität München eingereicht und durch die Fakultät für Chemie am 03.12.2010 angenommen.

To My Parents and Uncle

تقدیم به پدر و مادرم و دایی مهدی

در دایره اي که آمدن و رفتن ماست آن را نه بدایت نه نهایت پیداست

کس می نزند دمی در این معنی راست کاین آمدن از کجا و رفتن به کجاست

خیام

Acknowledgements

This thesis is carried out during the period of November 2006 until May 2007 in the department of inorganic chemistry of university of Ulm and May 2007 until June 2010 in the department of macromolecular chemistry of TU Munich.
This work could not be accomplished without permission of dissertation, continuous advice and kindly support of Prof. Dr. B. Rieger, who has guided me during the doctoral dissertation with his great knowledge and experience in different fields of chemistry particularly in the chemistry of catalysis and its application in polymer chemistry, hydrogen storage and activation. His insight into organic and inorganic chemistry as well as polymer chemistry has introduced me to accurate thinking and developing new ideas about a lot of chemistry articles.

I would like to thank him for his supports despite all difficulties during the moving from Ulm to Munich and through my investigation in Munich. I want to pronounce my gratitude profoundly.
I would like to express my gratefulness to all those who gave me the possibility to complete this thesis.
I gratefully thank Dr. Carsten Troll, who has advocated technical supplies. I express Dr. Sergei Vagin and Dr. Carly Anderson my appreciation for their supports with good ideas.
I would like to thank all of my colleagues at the university of Ulm as well as Technische Universität München for supporting and friendship.
I am grateful to Dr. Genest for great cooperation, Mr. Krausse for MS measurements, Dr. Raudaschl-Sieber for solid state NMR measurements and Dr. Herdtweck for crystal structures.
I would like to thank Joachim Dengler and Felix Schulz for NMR-Measurement and their grateful ideas, which were very helpful.
And finally all the thanks to all my colleagues in Prof. Rieger's and Prof. Nyken's group for the nice working atmosphere in the university, their cooperation and help.
I would like to present this thesis to my parents and my uncle, who have always supported and motivated me during my study and promotion.

Abbreviations

AB	Ammonia borane
BDPP	1,3-bis (diphenylphosphino)propane
BMIM	Buthyl methyl imidazolium
BPBH	1,6-bis(bis(perfluorophenyl)boryl) hexane
9-BBN	9-Borabicyclo[3.3.1]nonane
CSD	Cambridge Structural Database
DFT	Density functional theory
DMF	Dimethylformamide
DMSO	Dimethylsulfoxide
DMAB	Dimethyl ammonia borane
DSC	Differential scanning calorimetry
EA	Elemental analysis
Equiv.	Equivalent
EMIM	Ethyl methyl imidazolium
EDB	Ethylenediamine bisborane
FLPs	Frustrated Lewis pairs
GC	Gas chromatography
GB	Guanidinium borohydride
GOTB	Guanidinium octahydrotriborate
HOMO	Highest occupied molecular orbital
IR	Infrared spectroscopy
ILs	Ionic liquids
LUMO	Lowest unoccupied molecular orbital
MOFs:	Metal–organic frameworks
MS:	Mass spectroscopy
MGB:	Methyl guanidinium borohydride
MPILs	Metal containing protic ionic liquids
MGCC	Methyl guanidinium tetrachlorocobaltate
MGCZ	Methyl guanidinium tetrachlorozincate
MALDI	Matrix-assisted laser desorption/ionization
NHC	N-heterocyclic carbene

PDI	Polydispersity index
PIM	Organic polymers with intrinsic microporosity
THF	Tetrahydrofuran
TGA	Thermal gravimetric analysis
TOF	Turnover frequency
TEM	Transmission electron microscopy
UV	Ultraviolet spectroscopy
Wt	Weight
Å	Ångstrom (10^{-10} m)

Preface

This dissertation is divided into three chapters. Recently, metal-free hydrogen activation using phosphorous compounds has been reported in science magazine. We have investigated the interaction between hydrogen and phosphorous compounds in presence of strong Lewis acids (chapter one). A new generation of metal-free hydrogen activation, using amines and strong Lewis acids with sterically demanding nature, was already developed in our group.

Shortage of high storage capacity using large substitution to improve sterical effect led us to explore the amine borane derivatives, which are explained in chapter two.

Due to the high storage capacity of hydrogen in aminoborane derivatives, we have explored these materials to extend hydrogen release. These compounds store hydrogen as proton and hydride on adjacent atoms or ions. These investigations resulted in developing hydrogen storage based on ionic liquids containing methyl guanidinium cation. Then we have continiued to develop ionic liquids based on methyl guanidinium cation with different anions, such as tetrafluoro borate (chapter three). We have replaced these anions with transition metal anions to investigate hydrogen bonding and catalytic activity of ionic liquids.

This chapter illustrates the world of ionic liquid as a green solvent for organic, inorganic and catalytic reactions and combines the concept of catalysts and solvents based on ionic liquids. The catalytic activity is investigated particularly with respect to the interaction with CO_2.

Chapter 1

Metal-free hydrogen activation (Frustrated Lewis Pairs)

1.1. Introduction

In 1923, Lewis explained[1] new descriptions of acids and bases categorizing molecules as electron pair donors or acceptors, which is central to our understanding of much of main group and transition metal chemistry. A basic concept of this description in chemical reactions is that the combination of Lewis acids and bases results in the formation of simple Lewis acid-base adducts. A simple demonstration of this concept is the formation of ammonia-borane adducts (NH_3BH_3), upon combination of the Lewis acid borane with the Lewis base ammonia. The use of Lewis acidic boron and aluminium based activators in olefin polymerisation is an example of transition metal coordination chemistry.[2-9] Lewis acids are characterized by low-lying, lowest-unoccupied molecular orbitals (LUMOs) which can interact with the lone electron-pair in the high-lying highest-occupied molecular orbital (HOMO) of a Lewis base. Thus the combination of a simple Lewis acid and Lewis base results in neutralization.[10] In 1942, Brown and co-workers reported that, although most of these combinations of Lewis acids and bases formed classical Lewis adducts, lutidine formed a stable adduct with BF_3 but did not react with BMe_3 (Fig. 1).[11]

Fig.1 Treatment of lutidine with BMe_3 and BF_3. (NR: no reaction)

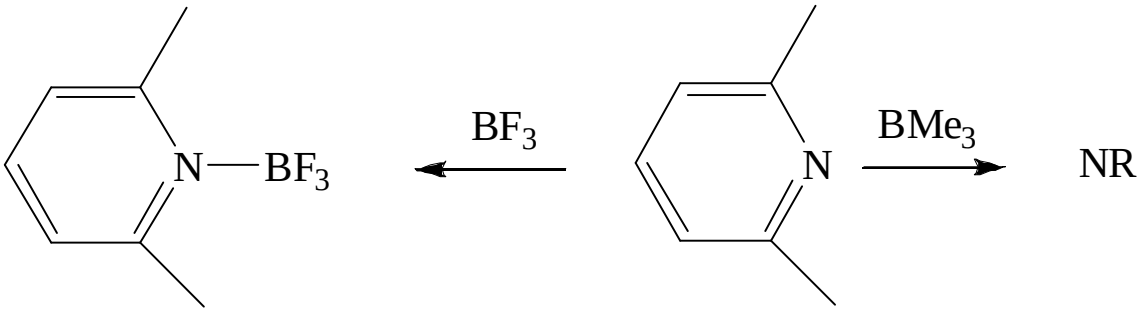

This result was attributed to the steric conflict of ortho-methyl groups of lutidine with the methyl groups of the borane. Wittig and Benz reported[12] o-phenylenebridged phosphonium-borate by treatment of dehydrobenzen with a mixture of the Lewis base triphenylphosphine and the Lewis acid triphenylborane (Fig.2).

Fig. 2 Frustrated Lewis-pair reagents

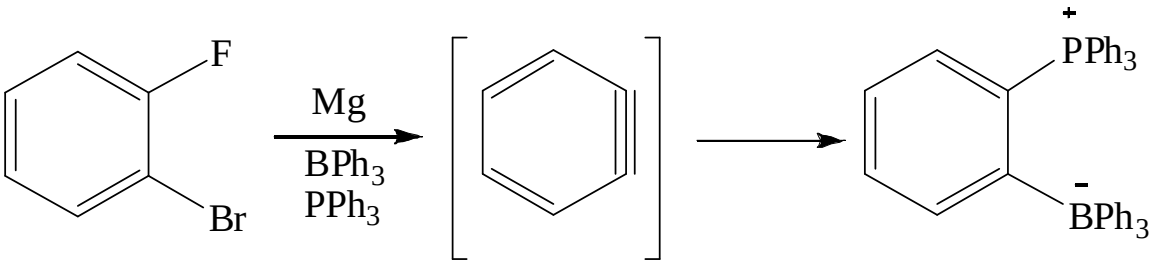

Tochterman reported later that the addition of BPh_3 to a mixture of butadiene and trityl anion did not result in polybutadiene (Fig. 3).

Fig.3 Lewis pairs reagents

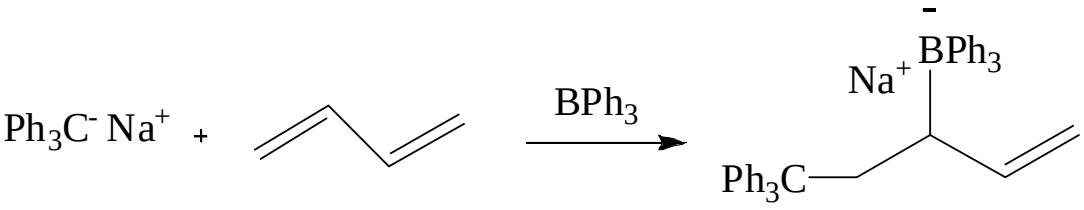

These reports realized the special nature of steric Lewis pairs, that did not yield the classical Lewis adduct.

1.2 Metal-free H_2 activation based on frustrated Lewis pairs

The Stephan and co-workers have reported[13] reversible hydrogen activation, which was derived through an unusual reaction from the nucleophilic aromatic substitution reaction of $B(C_6F_5)_3$ with dimesitylphosphine, which was treated with Me_2SiHCl, yielding zwitterionic species cleanly (Fig. 4).

These Lewis acid and Lewis base functions were incorporated into the same molecule and sterically precluded from quenching each other. This compound can release H_2 cleanly above 100 °C and activate it at room temperature.

To gain further insight into mechanisms, the kinetic data of hydrogen loss using $^{31}P\ \{^1H\}$ NMR in bromobenzen over the temperature range 100 ° to 150 °C were collected. Over this temperature range the enthalpy and entropy of activation were reported $\Delta H^{\neq} = 90 \pm 1$ kJ/mol and $\Delta S^{\neq} = -96 \pm 1$ J/mol.K.

Fig.4 Syntheses of zwitterionic species

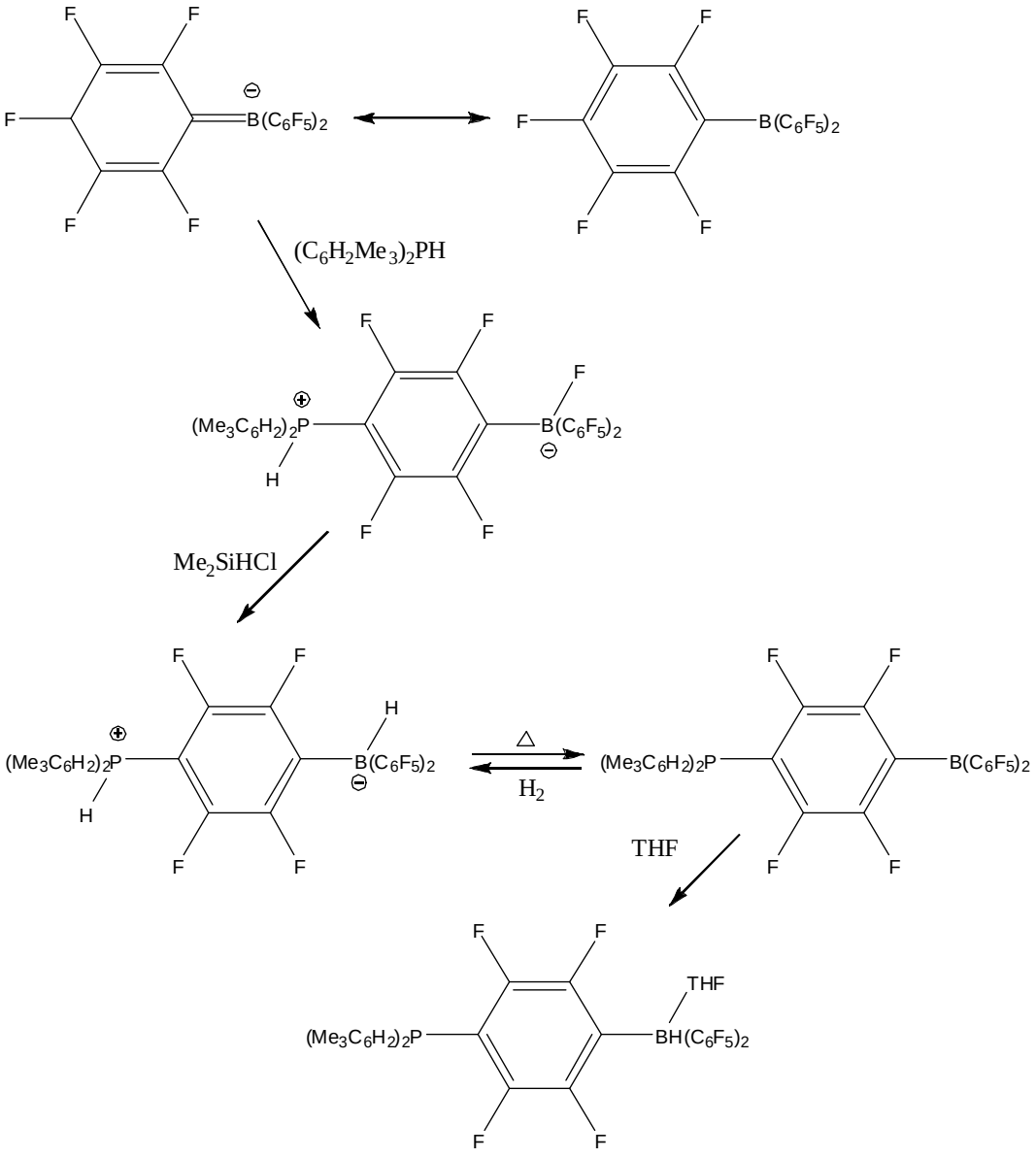

Initially, spin-lattice relaxation time (T_1) showed first-order decay kinetics. The entropy value and the first order kinetics are consistent with an intramolecular process, and the enthalpy value suggests substantial bond breakage in the transition state. Intramolecular H_2 elimination requires proton and hydride on adjacent atoms. This could be achieved by proton migration from P to B, or alternatively by hydride migration from B to P (Fig. 5). This innovation represents the first non-transition-metal system known that both releases and takes up dihydrogen. This combination of a Lewis acid and Lewis base in which steric demands preclude classical adduct formation, was classified under “frustrated Lewis pairs” or “FLPs”.

Fig.5 Possible mechanisms of H_2 release

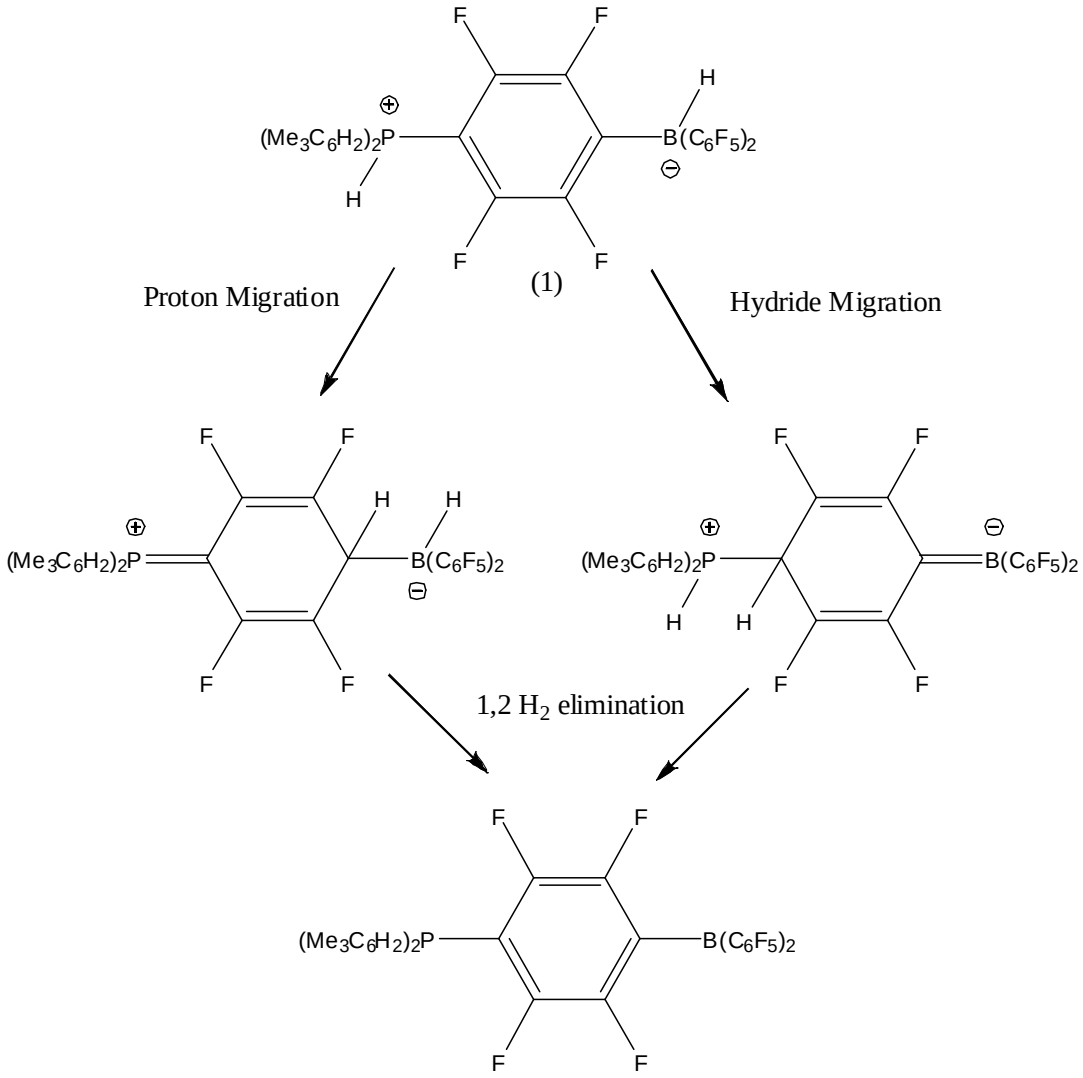

1.2.1 Heterolytic activation of H_2 by phosphine/borane

This observation led to wide investigation on similar FLPs systems. In order to establish working on FLPs based on phosphorous and boron, the Stephan group found[14] that toluene solutions of stoichiometric mixtures of R_3P (R = ^{t}Bu, $C_6H_2Me_3$) with $B(C_6F_5)_3$ showed no evidence of the formation of Lewis acid-base adducts at 25 °C or on cooling to -50 °C. The absence of Lewis adduct formation is consistent with the sterically demanding nature of the phosphines R_3P (R = ^{t}Bu, $C_6H_2Me_3$), which precludes coordination to the Lewis acidic boron center or nucleophilic aromatic substitution at a para-carbon of $B(C_6F_5)_3$. Exposure of these phosphine/borane solutions to an atmosphere of H_2 at 1 atm pressure and 25 °C resulted in the quantitative formation of white precipitates $[R_3PH][HB(C_6F_5)_3]$ (R = t-Bu, $C_6H_2Me_3$)(Fig. 6).

The crystallographic data showed that the cations and anions pack such that the BH and PH units are oriented toward each other with the B$H^{\cdots}$HP approach being 2.75 Å, which is much larger than typical dihydrogen bonding. Despite this orientation in the solid state, heating of these compounds in toluene solutions to 150 °C did not release H_2.

Fig.6 Heterolytic cleavage of H_2 by phosphine and borane

$$B(C_6F_5)_3 + PR_3 \xrightarrow[1\ atm,\ 25\ ^\circ C]{H_2} [R_3PH][HB(C_6F_5)_3]$$

$$R = {}^t\text{Bu},\ C_6H_2Me_3$$

In order to gain insight into the generality of the reaction, several phosphine/borane combinations were reported. For instance, toluene solution mixtures of ^{t}-Bu_3P and BPh_3 led to hydrogen activation in a 33% yield, although longer reaction times are required for H_2 activation, presumably due to the reduced Lewis acidity at Boron.

Following the results of the Stephen group, Erker and co-workers[15] have developed linked phosphine-boranes for hydrogen activation. This system contains a weakly intramolecular interacting phosphane Lewis base/borane Lewis acid pair that splits dihydrogen rapidly at room temperature and low H_2 pressure to yield the ethylene-linked phosphonium–hydridoborate zwitterion. The zwitterion (Fig. 7) serves as an efficient hydrogenation catalyst for a variety of substrates, such as enamines, bulky imines and (less efficiently) silyl enol ethers.[16]

The computational studies described an almost planar four-membered heterocycle containing a rather weak P$^{\cdots}$B linkage. One pair of mesityl and C_6F_5 substituents at P/B, arranged nearly

parallel to each other at the framework, is in an orientation to support the weak P····B contact by an energetically favourable π–π stacking interactions between an electron-rich and an electron-poor arene system.

Fig.7 H_2 activation by linked phosphine-borane

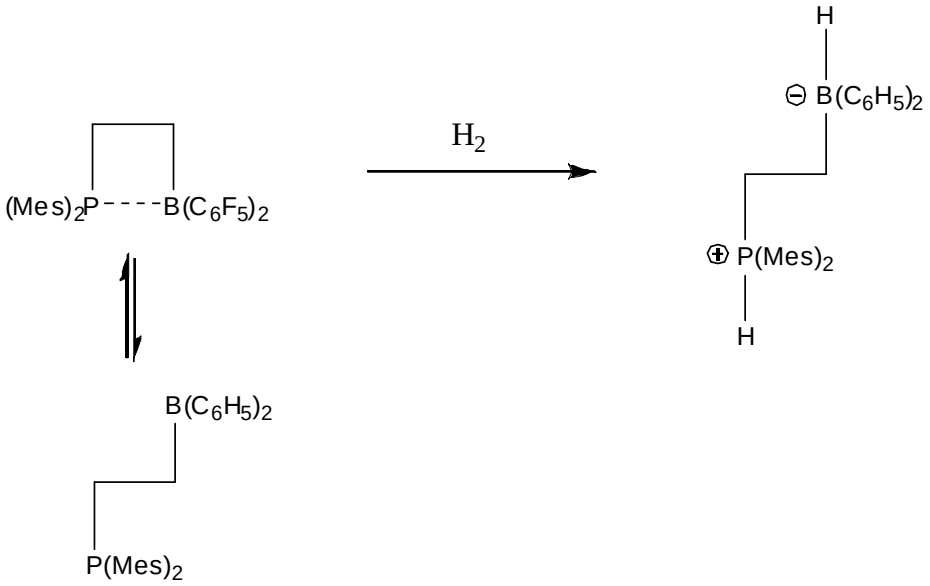

The examination of related alkenylene-linked phosphine/borane systems derived from hydroboration of $^{t}Bu_2P(C{=}CCH_3)$ with $HB(C_6F_5)_2$ led to clean reactions with H_2 at ambient conditions, giving corresponding zwitterionic phosphonium hydridoborate (Fig.8).[15]

Fig.8 H_2 activation with alkenylene-linked phosphine/borane

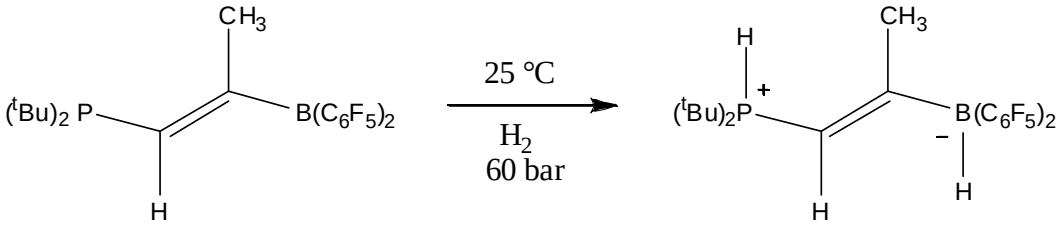

The Erker group has also reported, that when 1,8-bis(diphenylphosphino)naphthalene and $B(C_6F_5)_3$ were stoichiometrically mixed in d_8-toluene, the ^{31}P, ^{19}F and ^{11}B NMR spectra remained practically unchanged, suggesting that no Lewis adduct was formed, and exposure of this solution

to an atmosphere of H_2 at 2 atm pressure and 25 °C resulted in the quantitative formation of the mono-phosphonium/hydridoborate salt (Fig. 9).[17]

A solution of this salt in d_6-benzene can release hydrogen at 60 °C, resulting in a virtually quantitative formation of 1,8-bis(diphenylphosphino)naphthalene and $B(C_6F_5)_3$, indicating stoichiometric loss of H_2.

Fig.9 Reversible hydrogen activation with 1,8-bis(diphenylphosphino)naphthalene and $B(C_6F_5)_3$

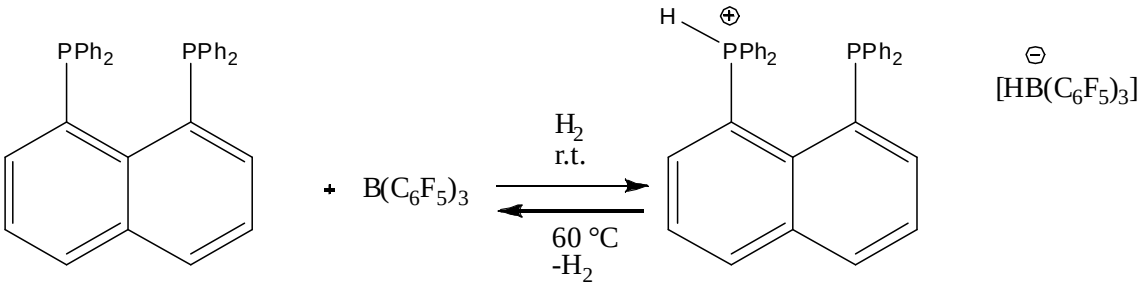

Hydrogen activation based on bulky amines as Lewis base and tris(pentafluorophenyl) borane has been developed in our research group. Exposure of solutions of stoichiometric mixtures of diisopropylethylamine, diisopropylamine, or 2,2,6,6-tetramethylpiperidine and $B(C_6F_5)_3$ in toluene to hydrogen were investigated by ^1H, ^{11}B, and ^{19}F NMR spectroscopy. The reactions of diisopropylethylamine and diisopropylamine with $B(C_6F_5)_3$ gave mixtures of the salt or and the zwitterion as expected (Fig. 10).[18]

Fig.10 Interactions between bulky amines and $B(C_6F_5)_3$

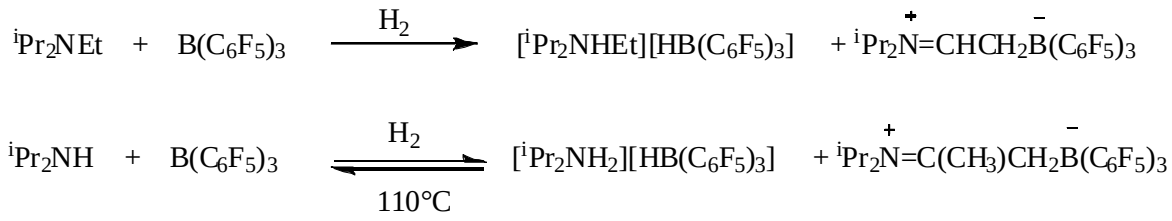

Interestingly, the exposure of a solution of 2,2,6,6-tetramethylpiperidine and $B(C_6F_5)_3$ in toluene to an atmosphere of H_2 (1 atm) at 20 °C resulted in the quantitative formation of the salt (Fig. 11).

Later, the first ansa-aminoborane, able to reversibly activate H_2 under mild conditions through an intramolecular mechanism was reported.[19] The structural and theoretical findings show that the

dihydrogen interaction in molecular tweezers is partially covalent in nature (Fig. 12).

Fig.11 Heterolytic cleavage of H_2 by bulky amines and $B(C_6F_5)_3$

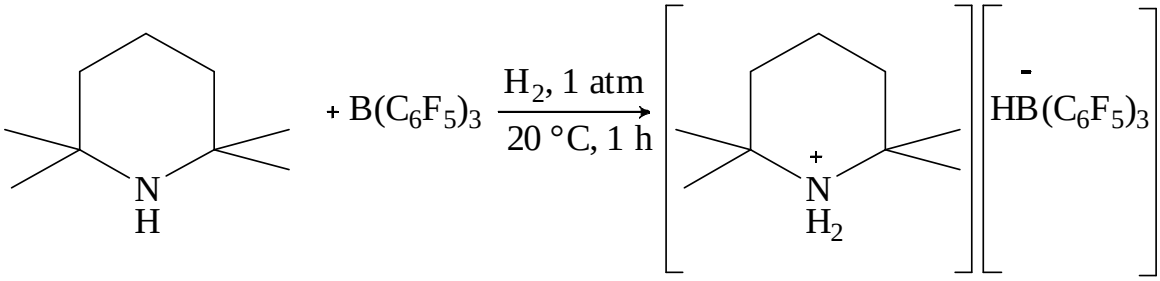

Fig.12 Reversible H_2 activation based on ansa-aminoborane

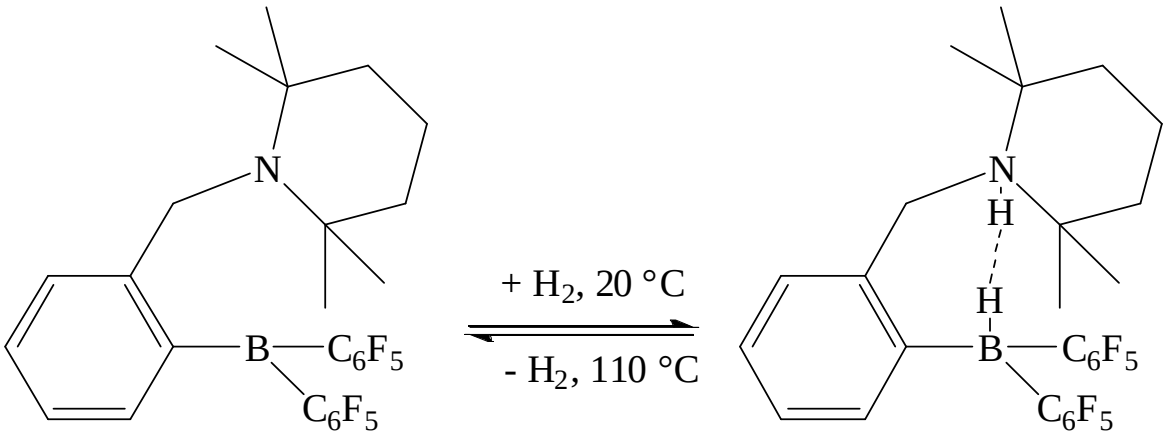

1.3 Scope of this work

Due to spliting of hydrogen with FRs, the goal of this investigation is activation of hydrogen molecules between bifunctional sterical demanding Lewis acid and Lewis base, which are bridged via dihydrogen bonding to give a polymer-like structure (Fig. 13). The starting materials are diphosphanes, which are commercially available and diboranes, which were prepared by hydroboration reaction.

Fig. 13 Polymer based on dihydrogen-bridging

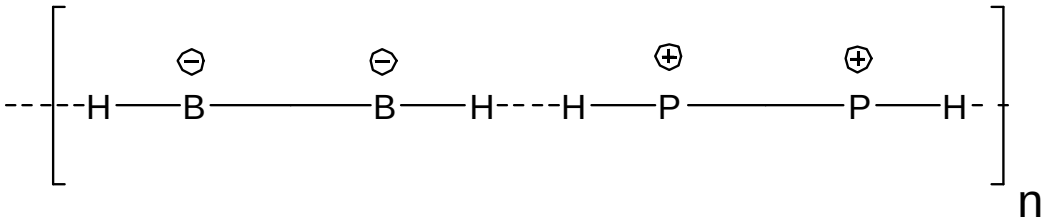

1.4 Results and discussion

In our research, we have focused on alkane-bridged diborane and diphosphane compounds in order to activate hydrogen, resulting in a chain of zwitterionic species, bridging via dihydrogen bonding. For this issue, we have synthesized the 1,6-bis(bis(perfluorophenyl)boryl) hexane (**1**), and investigated the interaction with 1,3-bis (diphenylphosphino)propane (**2**) as lewis base (Fig 14).

Fig. 14 Structure of **1** and **2**

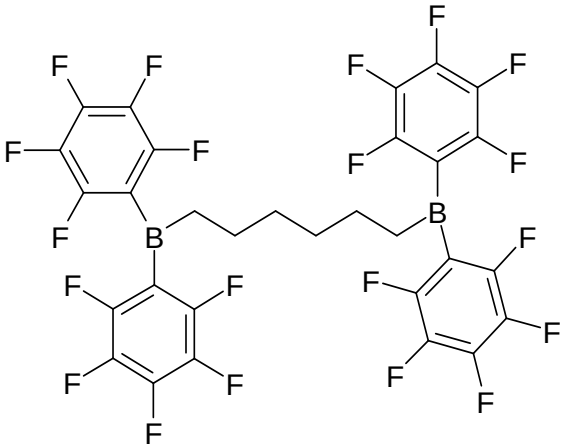

1,6-bis(bis(perfluorophenyl)boryl) hexane (**1**)

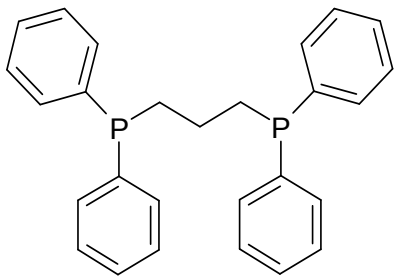

1,3-bis (diphenylphosphino)propane (**2**)

By hydroboration of 1,5-hexadien with Piers` borane ($HB(C_6F_5)_2$), **1** can be isolated in good yield (Fig. 15).

Bis(pentafluoropheny1)borane was prepared from the known chloroborane $(C_6F_5)_2BCl$ [20] in the absence of Lewis bases by reaction with hydride sources such as $[Cp_2Zr(Cl)H]_n$, Bu_3SnH and $Me_2Si(Cl)H$ (Fig. 16).

Traditional metathetical methods for transformations of this type[21] were not advisable because they necessitated the use of donor solvents which were difficult to remove completely (if at all) owing to the high Lewis acidity.[22]

The most convenient hydride transfer[23] agent proved to be $Me_2Si(CI)H$ since it also served as solvent for the reaction and the by-product, Me_2SiCl_2, was easily removed. The product was observed to precipitate over the course of one hour and was isolated in high yield by filtration.

Fig.15 Hydroboration of 1,5-hexadien

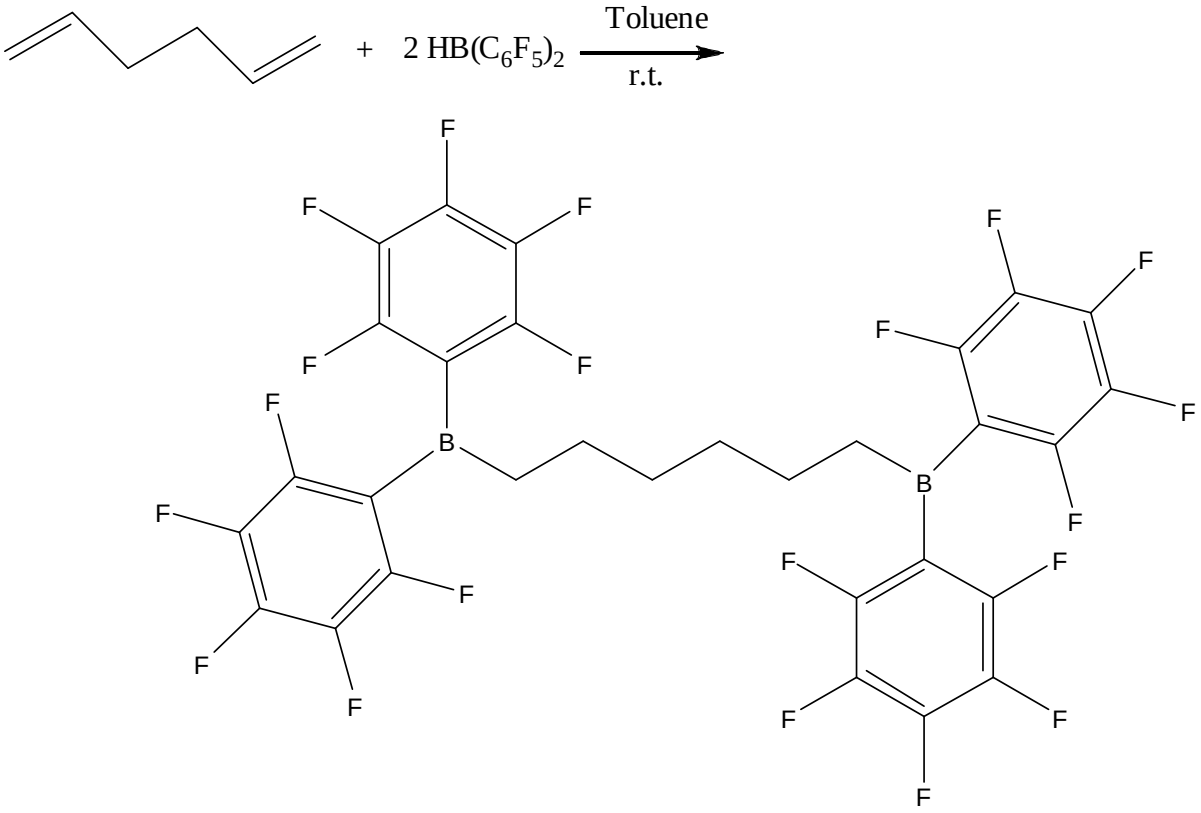

Fig.16 Synthesis of $(C_6F_5)_2BH$ **.**

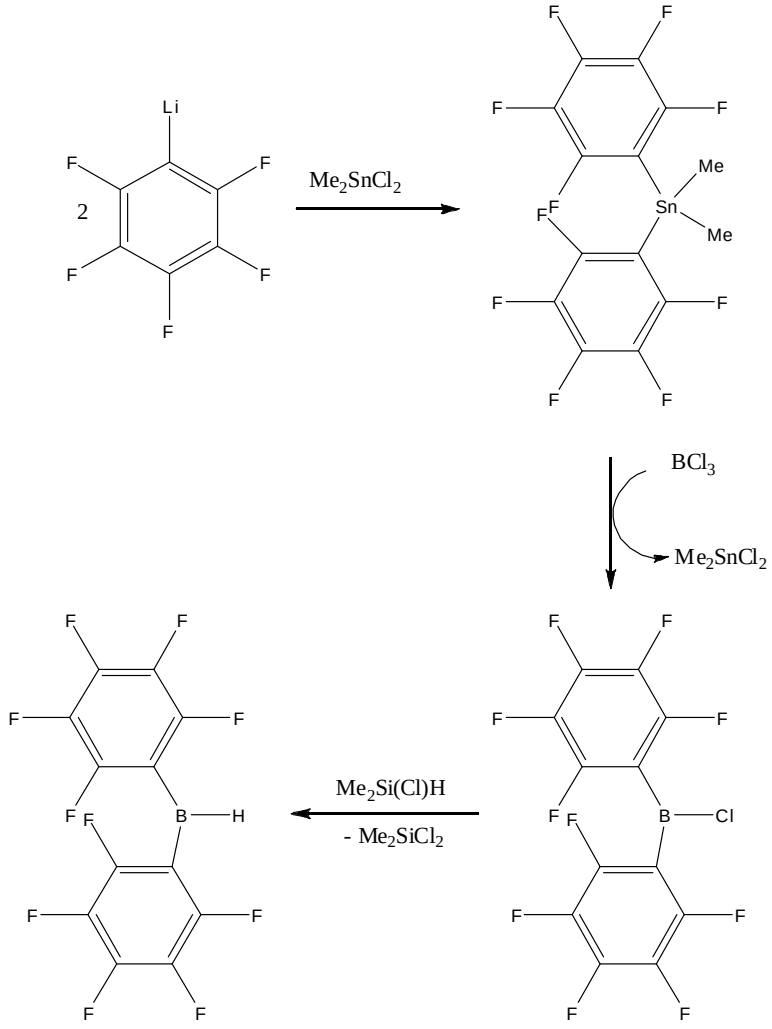

A solution of **1** in toluene was added to a toluene solution of **2**. A white precipitate was formed in a short time. The spectroscopic investigation in $CDCl_3$ using ^{31}P NMR confirmed the simple Lewis acid-base adducts. The ^{31}P NMR data of **2** was measured at – 5 ppm but this signal was shifted after adding the **1** to 5 ppm, which indicated internal adduct formation. Exposure of this system to an atmosphere of H_2 exhibited no change in ^{31}P NMR. Although the acidity and basity of **1** and **2** due to similarity to active species published by Stephan[14] seem to be enough for H_2 activation, presumably the required steric effect for precluding of Lewis acid/base quenching was failed. This is probably due to open side of borane at carbon, which intensifies the nucleophilic attack, therefore leading it to form the Lewis acid-base adducts.

Taking into account that more sterically demanding groups need to prevent the Lewis acid/base

reaction, we have decided to use tris(pentafluorophenyl) borane as it is a stronger acid with more steric effect.

Crystallographic data[24] of $B(C_6F_5)_3$ exhibited alleviating steric interactions between three ortho fluoro groups on opposing aryl rings, thus leading to more steric demand and stronger Lewis acid in comparison to the **1** (Fig. 17).

Fig.17 Molecular structure of tris (pentafluorophenyl) borane

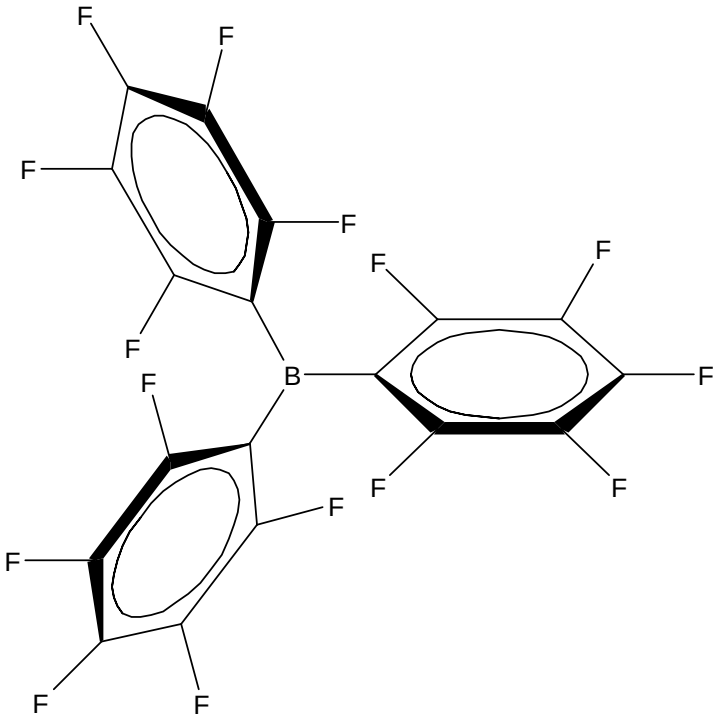

Unfortunately, the reaction again resulted in the Lewis acid-base adducts, which was investigated by ^{31}P NMR. The ^{31}P NMR was measured at – 5 ppm for **2**, however addition of Tris (pentafluorophenyl) borane shifted this signal to 7 ppm. A $CHCl_3$ solution of product under H_2 was investigated using ^{1}H NMR in order to approve the reactivity of product at presence of H_2. ^{1}H NMR showed only starting material; therefore, activation of hydrogen based on this system was not possible.

The variation of Lewis acidity by using of triphenyl borane led to the simple Lewis acid-base adducts, which was investigated using ^{31}P NMR. The ^{31}P NMR was shifted from – 5 ppm to 2 ppm similar to the above demonstrated reactions.

These experiments showed that the electron pair of phosphorous can attack the vacant orbital of the boron-compound and generate the Lewis acid-base adducts. The reason is probably a shortage of steric effect, as reported by Stephan and Erker. They have shown that the interaction between very bulky phosphorous such as $^{t}Bu_3P$ or Mes_3P and strong Lewis acid boron compounds leads to the activation of small molecules, due to the suitable distance between electron pairs of phosphorous and the vacant orbital of boron.

Looking at the values of bond angles at phosphorus in all known simple phosphines shows that they vary from slightly above 90 ° to slightly below 104 °,[25-28] but the C-P-C bond angles in trimesitylphosphine assume values from 107.9 ° to 111.2 ° (average 109.7 °).[26] This extraordinary expansion of the valence bond angles, which is obviously due to non-bonded repulsive interaction among the three bulky mesityl (2,4,6-trimethylphenyl) groups, represents the greatest flattening of the phosphorus pyramid in trimesitylphosphine.

The same effect can be detected in tri(tert-butyl)phosphine. The tert-butyl groups are arranged in a pseudosymmetric way generated by a threefold rotation axis passing through the P atom. The C-P-C angles are widened to 107.1, 107.4 and 107.8 ° due to steric effects. The P-C distances are more than 0.06 Å longer than in simple phosphines. This reflects the bulkiness of the tert-butyl groups.[29]

For definition of coordination of the Lewis acid **1** at the Lewis base **2**, we have searched the literature to find the difference between **2** and sterical demanding Lewis base based on phosphorous such as tri(tert-butyl)phosphine and trimesitylphosphine. The crystal structure of **2** merely as ligand coordinated at metal centres was reported.[30-33] In a search of Cambridge Structural Database (CSD), we did not find any registred crystal structure of **2**, but similar structures such as 1,2-Bis(diphenylphosphino)ethane and 1,4-Bis(diphenylphosphino)butane were reported.[34,35]

In both cases, the presence of the lone pair on phosphorus justifies the values of the C-P-C angles which are all around 100 ° less than the tetrahedral value of 109.5 °, with the $C(sp^2)$-P-$C(sp^3)$ angles slightly larger than the $C(sp^2)$-P-$C(sp^2)$ angle. The phenyl rings are perfectly planar in both compounds and nearly perpendicular to one another; therefore, the required steric effect to prevent forming of Lewis acid-base adducts can not be provided by alkyl bridged biphosphane.

Discussion of hydrogen activation based on other type of Lewis base such as sulphide is lacking in the literature. Our attempts were concentrated on sterically hindered sulphide compounds as Lewis base and $B(C_6F_5)_3$ as Lewis acid in order to activate hydrogen.

For this issue, we opted for commercially available diisopropyl sulphide. When a toluene solution of diisopropyl sulphide was added to a toluene solution of $B(C_6F_5)_3$, a white precipitate was formed immediately at room temperature. A THF-D_8 solution of precipitate was investigated by ^1H NMR and ^{19}F NMR. In this case, we have detected no change in the NMR spectroscopy, which implies to H_2 activation.

As a result it is necessary to point out, that only sterically hindered Lewis acids and bases based on amine or phosphine are able to activate small molecules. These innovative results inspired a new area in chemistry, which is nowadays well known as frustrated Lewis pairs.

1.5 Conclusion

Stephan et al. have reported reversible hydrogen storage using a zwitterionic species based on phosphorous-boron compounds. We have focused on alkane-bridged diborane and diphosphane compounds in order to activate hydrogen, resulting in a chain of zwitterionic species based on dihydrogen bonding. For this issue, we have synthesized **1**, and investigated the interaction with phosphorous-based Lewis acids. A solution of **1** and **2** in toluene formed a white precipitate in a short time. The spectroscopic investigation in $CDCl_3$ using ^{31}P NMR confirmed the simple Lewis acid-base adducts. Therefore, we have added more sterical demanding boron such as tris-(pentafluorophenyl) borane to examine the hydrogen activation. Unfortunately, the reaction resulted again in a Lewis acid-base adducts. The reason is a shortage of steric effect on **2**, which is explained by crystal structure. As other nucleophil compounds steric demanding sulphur compounds were investigated. A white precipitate was immediately formed by adding a solution of diisopropyl sulphide in toluene to a toluene solution of $B(C_6F_5)_3$ at room temperature, which implied to a Lewis acid-base adduct. Unfortunatly, the hydrogen activation based on these systems was failed due to sterical effect, but the hydrogen storage as another issue can be considered.

These systems possess very low gravimetric capacity as hydrogen storage materials, but studying the basic reactions of hydrogen additions to non-metal systems can result in insight into the design of reversible systems with higher storage capacities. Due to our experience in boron-nitrogen and boron-phosphorous chemistry we have investigated aminoborane derivatives as hydrogen storage materials, which are explained in next chapter.

1.6 General Experimental Methodology

All reactions and product manipulations were performed under an atmosphere of dry argon using standard Schlenk techniques or in an inert atmosphere glovebox. Solvents were dried via molecular sieves 4 Å. H_2 gas was dried over a molecular sieves 4 Å before streaming in Schlenk flask.

1,6-hexadien, tris(pentafluorophenyl) borane, 1,3-bis(diphenylphosphino)propane, borontrichloride, dimethylsilanechloride, diisopropyl sulphade were purchased and used as received. Solution NMR spectra were collected at room temperature using Bruker ARX300 spectrometer.

^{1}H, ^{13}C NMR spectra are referenced to $SiMe_4$ by referencing the residual solvent peak. ^{11}B NMR spectra were referenced externally to $BF_3.Et_2O$. ^{19}F NMR spectra are referenced to C_6F_6 and ^{31} P NMR to H_3PO_4.

Synthesis of $Me_2Sn(C_6F_5)_2$

Bromopentafluorobenzene (5.0 mL, 40.1 mmol) was added via syringe to a 100 mL two-necked roundbottom flask equipped with a large egg-shaped stir bar. The flask was evacuated, and Et_2O (15-20 mL) was condensed into the vessel at -78 °C. The solution was stirred to dissolve the solidified C_6F_5Br.

Butyllithium (25 mL of a 1.6 M hexanes solution, 40.1 mmol) was added dropwise at – 78 °C via syringe under an argon purge over 10 min. The reaction was stirred at -78 °C for 45 min, and Me_2SnCl_2 (4.4 g, 20.05 mmol) was added to the solution as a concentrated ether solution. The reaction was stirred for 15 min at -78 °C, then allowed to warm to ambient temperature, and stirred for an additional 12 h.

A small volume of untreated, reagent grade (i.e., wet) hexanes (5 mL) was added to the white suspension to quench any unreacted C_6F_5Li. The solvent was removed under reduced pressure, and the solid was extracted with hexanes (3 * 30 mL). The solvent was removed from the collected extracts; distillation of the residue under reduced pressure gave a clear, colorless liquid that crystallized on standing (9.19 g, 19.0 mmol) in 95% yield.

^{1}H NMR: δ(ppm) = 0.88 (s, 6H, ^{117}Sn (7.7%) and ^{119}Sn (8.4%) satellites, J = 31.9 Hz and J = 32.4 Hz).

^{19}F NMR: δ(ppm) = -122.2 (dd, J = 8.7 Hz and J = 25.0 Hz, F_o), -150.4 (tt, J = 2.3 Hz and J =

20.0 Hz, F_p), -159.5 (m, F_m).

Synthesis of $ClB(C_6F_5)_2$

$Me_2Sn(C_6F_5)_2$ (9.19 g, 19.0 mmol) was placed in a 100 mL thick-walled glass bomb and evacuated. Hexane (50 mL) was condensed into the vessel, and the bomb was tared on a balance. BCl_3 (2.23 g, 19.0 mmol) was condensed into the vessel. Once the appropriate amount of BCl_3 was condensed into the bomb, the vessel was back-filled with argon and closed. After the contents were stirred at room temperature for 1 h, the bomb was placed in a thermostated oil bath set to 120.0 °C and heated for 48 h. The bomb was removed from the oil bath and allowed to cool to ambient temperature while crystals of Me_2SnCl_2 were formed. After allowing crystallization to occur for several hours, the supernatant liquid was removed from the crystals via cannula into a vessel flushed with argon. The crystals in the glass bomb were washed once with hexanes (10 mL), and then the wash was transferred to the vessel via cannula. The solvent was removed under reduced pressure, leaving a residue that was transferred to a sublimation apparatus. Residual Me_2SnCl_2 was removed by sublimation under an atmosphere of argon at an oil bath temperature of 35 °C. The crystals of Me_2SnCl_2 were removed from the coldfinger, and the procedure was repeated until no more Me_2SnCl_2 could be obtained. Sublimation of the remaining white powder under full vacuum at an oil bath temperature of 60 °C produced $ClB(C_6F_5)_2$ as a colorless, crystalline solid (4.90 g, 12.9 mmol) in 63% yield.

^{19}F NMR: δ(ppm) = -129.6 (dtt, *J* = 4.9 Hz, *J* = 6.6 Hz, and *J* = 20.9 Hz, F_o), -143.9 (tt, *J* = 6.6 Hz and *J* = 21.2 Hz, F*p*), -160.4 (m, F*m*)

^{11}B NMR: δ(ppm) = 59.1

Synthesis of $HB(C_6F_5)_2$

(10.2 g, 108 rnmol) $Me_2Si(CI)H$ was condensed at - 78 °C into an evacuated flask containing $(C_6F_5)BCl$ (7.00 g. 18.4 mmol). The flask was warmed to room temperature, upon which the chloroborane dissolved and a white precipitate formed.

The reaction mixture was stirred for 1 h, then filtered to give 6.14 g (17.7 mmol, 96%) of the borane as a white crystalline powder.

^{1}H NMR (C_6D_6): δ(ppm) = 4.2 (br**)**

^{11}B NMR (C_6D_6): major component δ(ppm) = 18.0; minor component δ(ppm) = 60.0

^{19}F NMR (C_6D_6): δ(ppm) = -130.5(2F), -143.4(1F). -161.7(2F)

MS: m/z = 346 (M^+)

Synthesis of 1,6-bis(bis(perfluorophenyl)boryl) hexane(1)

To a suspension of $HB(C_6F_5)_2$ (0.65g, 1.88 mmol) in dry toluene (10 mL) 1,5-hexadien (0.11 ml) was added in a Schlenk tube, and the suspension was stirred until all of the solid had dissolved (approximately 15 min). After 15 h, the solvent was removed under reduced pressure and the white solid was washed twice with 10 ml dry hexane (3*10).

^{1}H NMR (300 MHz, $CDCl_3$): δ(ppm) = 2.25 (m, 4H), 1.73(m, 4H), 1.38 (m, 4H)

^{13}C NMR (300 MHz, $CDCl_3$): δ(ppm) = 146.3, 140.2, 126.9, 117.6 and 109.4 (C_6F_5), 40.1, 32.1, 32.5 and 32.1(CH_2)

^{11}B NMR (300 MHz, $CDCl_3$): δ(ppm) = 81.7

^{19}F NMR (300 MHz, $CDCl_3$): δ(ppm) = -130.7 (d, J = 17.1 Hz, F_o), -146.6 (t,J = 20.5 Hz, F_p), -160.1 (m, F_m)

Interaction between 1,6-bis(bis(perfluorophenyl)boryl) hexane (1) and 1,3-bis (diphenylphosphino)propane (2) in solution

1,6-(bis(perfluorophenyl)boryl)hexane (0.400 g) and 1,3-bis (diphenylphosphino)propane (0.213 g) were placed in a 100 mL Schlenk flask. 15 mL degassed toluene was added and after several minutes a white precipitation has detected. No visual and experimental changes were detected with exposure to H_2 atmosphere.

The ^{31}P NMR data of **2** was measured at – 5 ppm but this signal was shifted after adding the **1** to 5 ppm.

Similar observations were detected using 1,3-bis (diphenylphosphino)propane and tris(pentafluorophenyl) borane or triphenyl borane. ^{31}P NMR was shifted from -5 ppm to 7 ppm or 2 ppm, respectively.

1.7 Literature

1) G. N. Lewis, Valence and the Structure of Atoms and Molecules, Chemical Catalogue Company, Inc., New York, 1923.

2) M. Bochmann, S. J. Lancaster, M. D. Hannant, A. Rodriguez, M. Schormann, D. A. Walker and T. J. Woodman, Pure Appl. Chem., 2003, 75, 1183.

3) E. Y.-X. Chen and T. J. Marks, Chem. Rev., 2000, 100, 1391.

4) M.-C. Chen, J. A. S. Roberts and T. J.Marks, J. Am. Chem. Soc., 2004, 126, 4605.

5) P. A. Deck, C. L. Beswick and T. J. Marks, J. Am. Chem. Soc., 1998, 120, 1772.

6) S. J. Lancaster, A. Rodriguez, A. Lara-Sanchez,M. D. Hannant, D. A. Walker, D. H. Hughes and M. Bochmann, Organometallics, 2002, 21, 451.

7) R. E. LaPointe, G. R. Roof, K. A. Abboud and J. Klosin, J. Am. Chem. Soc., 2000, 122, 9560. 8) H. Li and T. J.Marks, Proc. Nat. Acad. Sci. U. S. A., 2006, 103, 15295.

8) M. Schloegl, S. Riethmueller, C. Troll, M. Moeller, B. Rieger, Macromolecules, 2004, 37, 11, 4004-4007.

9) S. Deisenhofer, T. Feifel, J. Kukral, M. Klinga, M. Leskelae, B. Rieger, Organo-metallics, 2003, 22, 17, 3495-3501.

10) J. N. Brønsted, Recl. Trav. Chim. Pays-Bas 1923, 42, 718 – 728.

11) H. C. Brown, H. I. Schlesinger, S. Z. Cardon, J. Am. Chem. Soc. 1942, 64, 325 – 329.

12) G. Wittig, E. Benz, Chem. Ber. 1959, 92, 1999 – 2013.

13) G. C. Welch, R. R. S. Juan, J. D. Masuda, D. W. Stephan, Science 2006, 314, 1124 – 1126.

14) G. C. Welch, D.W. Stephan, J. Am. Chem. Soc. 2007, 129, 1880 – 1881;

15) P. Spies, G. Kehr, K. Bergander, B. Wibbeling, R. Fröhlich, G. Erker, Dalton Trans. 2009, 1534 – 1541.

16) H. Wang, R. Fröhlich, G. Kehr and G. Erker, Chem. Commun., 2008, 5966.

17) D. W. Stephan, G. ErkerAngew. Chem. Int. Ed. 2010, 49, 46–76.

18) V. Sumerin, F. Schulz, M. Nieger, M. Leskelä, T. Repo, B. Rieger; Angew. Chem. Int. Ed. 2008, 47, 6001 –6003.

19) V. Sumerin, F. Schulz,M. Atsumi, C. Wang, M. Nieger, M. Leskelä, T. Repo, P. Pyykkö, B. Rieger; J. Am. Chem. Soc. 2008, 130, 14117–14119.

20) R. D. Chambers. T. Chivers, J. Chem. Sot. 1965, 3933.

21) K. Smith, A. Pelter, Z. Jin, Angew. Chem. 1994, 106, 913; Angew. Chem. Int. Ed.

1994, 33, 851.
22) K. Ishihara. N. Hananki, H. Ydmamoto, Synlett 1993, 577.
23) D. J. Parks, R. E. von H. Spence,W. E. Piers; Angew. Chem. Int. Ed. 1995, 34, 809-811.
24) W. E. Piers, T. Chivers, Chemical Society Reviews, 1997, 26, 345-354.
25) E. D. Morris, C. E. Nordman, Inorg. Chem., 8, 1673 (1969)
26) I. Y. M. Wang, C. 0. Britt, A. l. Cowley, J. E. Boggs, J. Chem. Phys., 48, 812 (1968).
27) J. J. Daly, J. Chem. Sot., 3799 (1964).
28) F. K. Ross, L. Manojlovic-Muir, W. C. Hamilton, F. Ramirez, J. F. Pilot, J. Amer. Chem. Sot., 94, 8738 (1972).
29) J. F. Blount, Tetrahedron Letters, 1975, 11, 913 – 916.
30) J. Bruckmann, C. Kroger, Acta Cryst. (1995). C51, 1152-1155.
31) W. Keim; P. Kraneburg; G. Dahmen; G. Deckers; U. Englert; K. Linn; T. Spaniol; G. Raabe; C. Krueger; Organometallics (1994), 13(8), 3085-94.
32) L. Chunbang; M: E. Cucullu; R: A. McIntyre; E. D. Stevens;S. P. Steven Organometallics (1994), 13(9), 3621-7.
33) W. A. Herrmann; C. Brossmer; T. Priermeier; K. Oefele; Journal of Organometallic Chemistry (1994), 481(1), 97-108.
34) C. Pellizzi, G. Pellizzi; Acta Cryst. (1979). B35, 1785-1790
35) A. V. Rivera, D. Gómez C., E. Rodulfo de Gil and T. Suárez, Acta Cryst. (1988). C44, 277-279.

Chapter 2.
Hydrogen Storage Material

2.1 Introduction

The manufacturing and use of hydrogen is an important process in transformational[1-6] and biological[7] systems.

Using hydrogen as an alternative to traditional energy resources such as oil and natural gas has in the recent years been the focus of research groups in all technologically advanced countries of the world. It is believed that in one side, hydrogen can supply the growing demand for energy and, the other side, prevent climate change. In fact, hydrogen can be made from different sources, including fossil fuels, water and renewable energy such as wind and solar energy.

It is non-toxic and, as an energy carrier, environmentally pleasing, since water is merely a by-product when hydrogen is converted into energy.

In spite of that, the instantaneous incorporation of hydrogen into economical energy faces a number of challenges. The most important of these challenges is the lack of large-scale infrastructure to support its transportation.

The cost of hydrogen storage and delivery is too high for many energy applications; thus the introduction of a "hydrogen economy", in which hydrogen is a major energy carrier, is threatened. The hydrogen economy infrastructure consists of five components: Production, Storage, Delivery, Conversion and Application (Fig. 18).

Because the technology of hydrogen production and conversion is already established, the serious challenge at the current time seems to be storage and delivery. For instance the transportation of pure hydrogen with existing natural gas transmission may be unsuitable. Therefore, other options, such as mixing with natural gas, a compressed gas or cryogenic liquid, as well as possibile hydrogen carriers (methanol, ethanol and other organic liquids), are being considered.

To date, none of these options satisfies the needs of users, thus, the interest and investment in hydrogen related-research and development is growing. The potential hydrogen storage materials, which are able to free hydrogen with a high percentage of weight at low temperature like ammonia borane, hydrides, amides, metal-organic framework, etc. have been explored extensively.

Fig.18 Hydrogen economy infrastructure

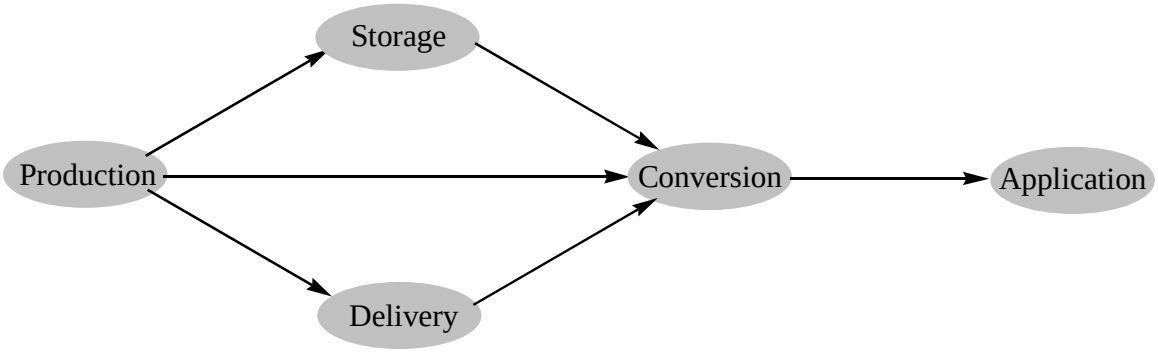

One of the most promising scenarios for the implementation of hydrogen as a hydrogen- based propulsion system for vehicles is the onboard-storage of hydrogen.[8] For transportation applications, an energy carrier should have a high energy content in as compact a volume as possible, to preserve available passenger space, and as small a mass as possible to maintain fuel efficiency.

The current targets set by the U.S. Department of Energy (DOE) specify that the vehicles should have a similar range (480 km or 300 miles), operate at close to ambient conditions, and be quickly and safely refuelled. As hydrogen has approximately three times the gravimetric energy density of petrol, and fuel cells are expected to perform at least twice as efficiently as internal combustion engines, only 5–10 kg of hydrogen must be stored (although 4 kg or less would be required by smaller, more practical passenger cars).[9] The 2010 energy density targets for the hydrogen storage system (including the container and necessary components) are 7.2 MJ kg^{-1} and 5.4 MJ L^{-1}, which translates to 6.0 wt % and 45 kg H_2 per m^3.[10] The goals for 2015 are even more demanding: 9.0 wt % and 81 kg H_2 per m^3, which approach the expectations of the automotive industry.[11]

This daunting task is easily put into perspective by noting that the mass density of elemental hydrogen is only 70.8 kg m^{-3} in its liquid state at 20 K (1 atm), and that 5 kg of hydrogen gas fills a volume of 56 m^3 under ambient conditions. Furthermore, both of these insights ignore the contribution of the mass of the necessary container.

There are currently four leading methods to store hydrogen: physical means, sorbents, metal hydrides, and so-called chemical hydrides. All four will be concisely summarised, and then chemical hydrides with B–N bonds will be discussed in greater detail. Details of the potential of

ammonia borane compounds as a hydrogen storage material, as well as the advantages of using similar systems, will be discussed in succession.

2.2 Hydrogen Storage

2.2.1 Physical hydrogen storage

Physical hydrogen storage requires strong tanks, which makes safe transporting at high pressure or even liquid hydrogen possible. Problematically, compressed hydrogen gas tanks sufficient to provide the equivalent energy content derivable from conventional liquid-filled gasoline tanks are heavy and volumetrically large. Moreover, although currently being used in prototypes,[12] the use of high-pressure (350 bar) hydrogen tanks in consumer automobiles lessens their attractiveness.

The tanks must be lightweight to maintain a high gravimetric capacity. Carbon-fibre reinforced composites seem to be suitable for this purpose, having the capability of transporting hydrogen up to 700 bar, but the toughness of this material leads to difficulties in manufacturing and shaping. In the other hand, because of the high density of liquid hydrogen in comparison to compressed gas, maintaining a low temperature requires other equipment, which limits the volumetric and gravimetric storage capacity.

2.2.2 Sorbents

A wide range of nanoporous materials have been studied as potential hydrogen storage materials. The associated hydrogen molecule can be physisorbed onto a high-surface-area porous structure of lightweight materials. In general, these materials utilize the adsorption of molecular hydrogen, while the bonding of hydrogen molecules to the surface is relatively weak (van der Waals), which is less than 1.4 kcal mol^{-1}, hence low temperatures (normally 77 K for liquid nitrogen temperature) are necessary to obtain reasonable hydrogen uptake.[13] This is their biggest disadvantage in contrast to their ready reversibility.

Nanotubes (SWCNT),[14] nanofibres, solid foams, and activated carbon, which are by weight, primarily carbon, have been extensively investigated. The maximum adsorption is about 5 wt % hydrogen at 77 K, as shown by various methods employed within the same study.[15]

Zeolites are another type of microporous materials[16] based on hydrate aluminate and silicate. They allow control over the pore size and make preparation easier. Since zeolites consist of atoms heavier than carbon, the gravimetric capacity is limited.

The zeolite structures could be used as a template to shape carbon networks,[17] but the templating

can not be successful because of the structural disorder. The hydrogen uptake using zeolite-like carbon materials reaches to 6.9 wt % at 77 K and 20 bar.

An emerging field is using organic polymers with intrinsic microporosity (PIMs),[18] which are made of rigid monomers to maintain microporosity, yielding a gravimetric storage capacity of up to 3 wt % at 77 K and 15 bar.[19] Increasing the pore size leads to higher storage capacity because of increased surface area (Fig. 19).

Fig.19 PIMs make up rigid monomers

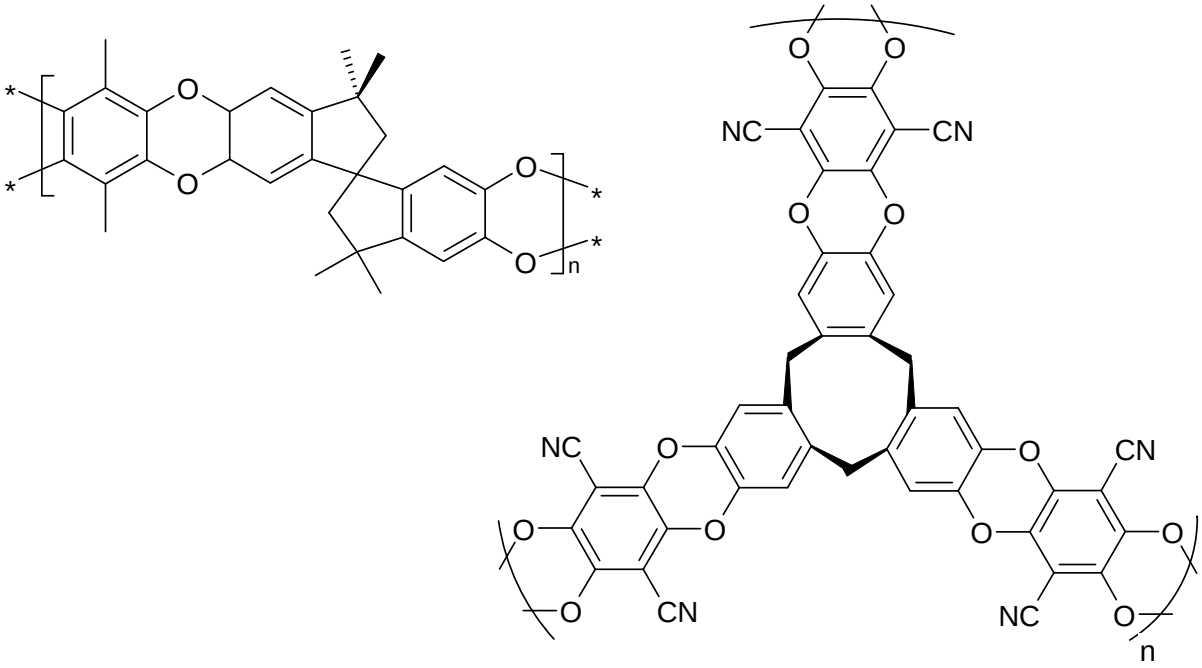

Increased attention is being focused on metal–organic frameworks (MOF) as candidates for hydrogen storage materials. This is a result of their many favourable attributes, such as high porosity, reproducible and facile syntheses, amenability to scale-up, and chemical modification for targeting desired properties. The manufacturing of metal–organic framework coordination polymers enables the new family of nanoporous materials and the concept of so- called ‘reticular design’. Nowadays several hundred different types of MOF are known. The self-assembly of metal ions, which act as coordination centres, linked together with a variety of polyatomic organic bridging ligands, results in nanoporous host materials robust solids with high thermal and mechanical stability.

The simple preparation and high yield and scalability make the MOFs one of the most interesting

hydrogen storage materials. The void regions could be tuned using different ligands extended to the length between metal centers. The tunable void size using different ligands and robustness at a great range of temperatures make MOFs suitable for gas storage (Fig. 20). Considerations of the geometric requirements for a target framework and implementation of the design and synthesis of such a framework have been termed reticular synthesis.

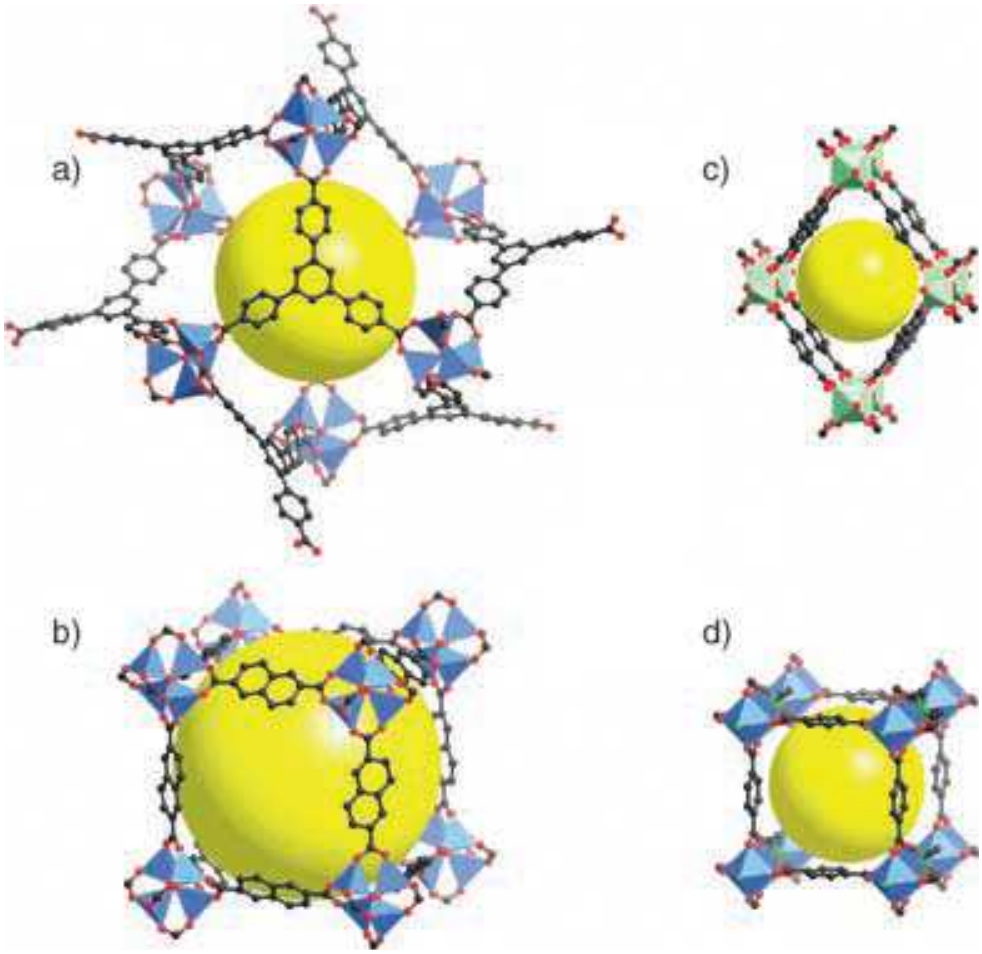

Fig.20 Examples of metal–organic frameworks (MOFs) studied for hydrogen adsorption include a) MOF-177, $Zn_4O(btb)_2$ (btb=benzene- 1,3,5-tribenzoate); b) IRMOF-8, $Zn_4O(ndc)_3$ (ndc=naphthalene-2,6-dicarboxylate); c) MIL-53, M(OH)(bdc) ($M=Al^{3+}$ or Cr^{3+}); and d) Zn_2-$(bdc)_2$(dabco) (dabco=1,4-diazabicyclo[2.2.2]octane). Pores in the evacuated crystalline frameworks are illustrated by yellow spheres that contact the van der Waals radii of the framework atoms (C: black, N: green, O: red, Zn: blue polyhedra, M: green octahedra).

2.2.3 Metal hydrides

Fundamental research on metal hydrides and complex hydrides has recently become very

important in the attempts to develop practical hydrogen storage materials with higher gravimetric hydrogen capacity. These materials often have a poor gravimetric capacity, requiring heating at high temperatures to release hydrogen, and reversibility is impractical. First of all, $NaAlH_4$ has been proposed as a hydrogen storage material[20] and many attempts has been made to promote hydrogen storage reactions based on metal hydrides.[21]

One way to achieve higher gravimetric capacity is using lighter main-group elements. These complex metal hydrides, such as alanates, amide, and borohydride compounds, have been evaluated as reversible hydrogen storage materials**.**[22] Li_3N can absorb roughly two equivalents of hydrogen to form lithium amide ($LiNH_2$) and two equivalents of lithium hydride at elevated temperatures (200–250 °C) to enhance hydrogen uptake to 9.3 wt % (Eq. 1).[23] Under vacuum and at temperatures below 200 °C releases 6.3 wt % of hydrogen, the remaining 3 wt% could be removed by heating above 320 °C.

$$Li_3N \underset{}{\overset{H_2}{\rightleftharpoons}} Li_2NH + LiH \overset{H_2}{\rightleftharpoons} LiNH_2 + 2LiH$$

Eq.1 Reversible hydrogen storage using Li_3N

The features of alkali borohydride $LiBH_4$, $NaBH_4$, and KBH_4, are relatively well explored;[24] while sodium and potassium cannot be rehydrided, lithium borohydride is hydrogenated at 600-650 °C at 100-160 bar.[25]

$Ca(BH_4)_2$ releases 9.6 wt % of hydrogen heated to 400 °C according to Eq.2 supported by the thermogravimetry.[26]

$$3\ Ca(BH_4)_2 \rightleftharpoons CaB_6 + 2\ CaH_2 + 10\ H_2$$

Eq.2 Reversible hydrogen storage using Li_3N

By adding of catalytic amounts of the dopants, $TiCl_3$ and Pd, the ‘spent fuel’ can be rehydrogenated at 700 bar and 400–440 °C in 60% yield.

New investigation has concentrated on a mixture of metal hydride as a potential hydrogen storage material. Ternary mixtures of MgH_2, $LiNH_2$ and $LiBH_4$ show increasing rates and a greater extent of hydrogen release compared to binary systems of MgH_2, $LiNH_2$ and $LiBH_4$ components. Depending on the amount of MgH_2 in the mixture, 8-11 wt % hydrogen was released at elevated temperatures. The magnesium compound contains borohydride and amines, $Mg(BH_4)_2$. $2NH_3$ has

a maximum storage capacity[27] of 16 wt %, although it releases to 13.1 wt % hydrogen above 150 °C. The hydrogen release has been reported to be endothermic, therefore, rehydrogenation process may be possible.

2.2.4 Chemical hydrides

Hydrides of metals and elements lighter than metal are hypothesized as hydrogen storage, which later result higher gravimetric storage capacity. The necessary cleavage of covalent element–hydrogen bonds, however, puts more stringent requirements on reversibility. The Gibb`s free energy (ΔG) of hydrogen release in a reversible system must be at or near 0 kcal/mol. These compounds will have a positive entropic term (ΔS) as hydrogen gas is released. Thus, a slightly endothermic dehydrogenation process (ΔH > 0) is necessary to obtain a reversible system under operating conditions. The reaction enthalpies are usually either too endothermic or exothermic for reversible hydrogen release in chemical hydrogen storage. The other challenge is the kinetics in some cases. Recently, there have been several examples of isolable compounds that add hydrogen under mild conditions. The digermyne compound (Fig. 21) can add two hydrogen molecules, as reported by Power and co-wokers.[28] The following work of Himmel and co-workers[29] exhibits a facile hydrogen addition across two diaryltin molecules. Schoeller and co-workers designed N-heterocyclic carbene analogues, with an N-aryl group substituted with a carbon group, which add hydrogen under mild heating.[30]

Fig.21 Non-metal compounds that add hydrogen under mild conditions

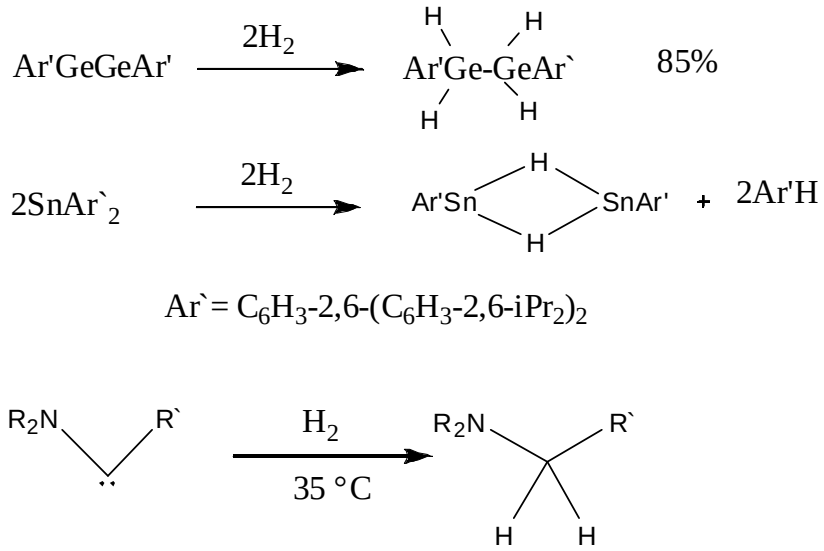

2.2.5 B-N compounds

The previously mentioned hydrogen storage materials (Zeolite, MOFs, PIM's, Metal and chemical hydride) possess low gravimetric capacities for on-board hydrogen storage requirements. There are several B-N compounds with the potential to meet these requirements. Both boron and nitrogen are lightweight elements with the capability of bearing multiple hydrogens. Thus, these compounds are well studied and developed.

B-H and N-H bonds possess hydridic and protic characters, respectively, resulting in facile hydrogen release.[31-33]

Several classes of B–N materials that may be suitable for hydrogen storage applications will be explained in this work, and then the simplest B–N compounds, amine boranes, will be discussed in more detail. The preparation, structure, characterisation and properties of guanidinium borohydride and methylguanidinium borohydride as hydrogen storage materials[34] will also be demonstrated in this work, as developed in our group.

2.2.5.1 Hydrazine borane compounds

Both hydrazine borane and -bis(borane) have been synthesised by the addition of hydrazine salts to borohydride (Fig. 22). These compounds are of interest as commercial propellants.[35]

Fig.22 Synthesis of hydrazine bis(borane) and hydrazine monoborane

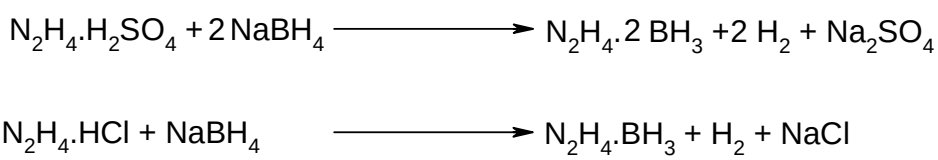

Hydrazine borane (-bis(borane)) comprises hydrogen storage capacity of 13.1 [13.4] wt% assuming loss of 3 [4] eq. of H_2. Unfortunately, hydrazine bis(borane) is shock-sensitive and explosive[36]; it explodes as air heats up[37] and therefore is not suitable for hydrogen storage applications.

2.2.5.2 Amine triborane compounds

In his pioneer studies, Kodama et al. reported high yield synthesis of ammonia-triborane (H_3N-B_3H_7).[38] Tetraborane (B_4H_{10}) is treated with ammonia to yield ammonia-triborane and a half

equivalent of diborane. Unfortunately, tetraborane is a volatile, unstable and toxic compound and toxic that is explosive in air, which makes this method of synthesis impractical. An alternate synthesis treats $Bu_4NB_3H_8$ with 0.5 eq. I_2 with glyme to yield glyme-B_3H_7, Bu_4NI[39] and 0.5 eq. of H_2. The glyme is displaced by ammonia to yield the product. (Eq. 3,4)

$$Bu_4\overset{+}{N}\ \overset{-}{B_3H_8} + 0.5\ I_2 + \text{glyme} \longrightarrow (\text{glyme})B_3H_7 + Bu_4NI + 0.5\ H_2 \quad \text{Eq.3}$$

$$(\text{glyme})B_3H_7 + NH_3 \longrightarrow NH_3B_3H_7 + \text{glyme} \quad \text{Eq.4}$$

Ammonia-triborane, $NH_3B_3H_7$, forms two crystalline modifications, a disordered, tetragonal form stable at about 25 °C, and an ordered, monoclinic form stable at lower temperatures. Single crystal x-ray diffraction studies of both modifications show that the molecule contains a triangle of boron atoms with a non-coplanar NH_3 group attached to one corner. The arrangement of hydrogen atoms suggests that the B_3H_7 group is a rather strongly distorted fragment of the B_4H_{10} molecule, but the alternative description of $NH_3B_3H_7$ as a bridge substituted diborane, $(H_3NBH_2)B_2H_5$, can not be entirely ruled out (Fig. 23).[40]

Fig. 23 Crystallographically redetermined structure of ammonia-triborane.

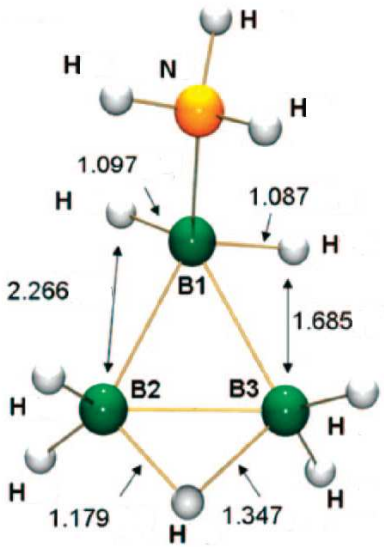

Ammonia-triborane comprises 10.6 wt % hydrogen (assuming 3 eq. H_2 are released), but any kinetic measurements were reported. Kodama mentioned that upon treatment with sodium in ammonia, one equivalent of hydrogen is released. Ammonia-triborane releases 7.85 equivalent of H_2 after 120 min in 1 M HCl or various metal catalysts lead to release approximately 7.5

equivalent of H_2 after 25 min.[39]

Ammonium hydrotriborate ($[NH_4][B_3H_8]$) has been reported as a stable colourless crystalline solid.[41] This is in contrast to thermally unstable $[NH_4][BH_4]$, which decomposes at temperatures above – 40 °C. Ammonium hydrotriborate underwent dehydrogenation to form $NH_3B_3H_7$ and H_2 in benzene or ether. Surprisingly, it is apparently stable in water and alcohols. It possesses a potential hydrogen storage of 13.9 wt % (assuming loss of 4 eq. H_2 by dehydrocoupling). Dehydrogenation has been carried out by adding metallic Si or Al (Eq. 5,6)[42] Upon treatment with Si 5 eq. of hydrogen gas are released, giving 9.9 wt % H_2. These polyborane compounds are likely to be explosive, as many related compounds have been used as rocket propellants.

$$(CH_3)_n H_{4-n} NB_3H_8 + n\,Si \longrightarrow n\,SiC + BN + 2\,B + (6-n)\,H_2 \qquad \text{Eq. 5}$$

$$(CH_3)_n H_{4-n} NB_3H_8 + (4n/3)\,Al \longrightarrow (n/3)\,Al_4C_3 + BN + 2\,B + (6-n)\,H_2 \qquad \text{Eq. 6}$$

2.2.5.3 Amine compounds of higher-order polyboranes

There are many polyborohydride compounds known, many of which can be a good candidates for hydrogen storage, depending on their stability and their ability to release hydrogen. For instance, upon treatment of ammonia with decaborane leads to tris (ammoniate) of decaborane (TAD). This compound has a $[NH_4][B_{10}H_{13}(NH_3)_2]$ formulation, with a loosely bounded NH_3 group.[43] TAD is stable under ambient conditions and releases one equivalent of hydrogen and one equivalent of ammonia upon heating to 75 °C. Complete dehydrogenation occurs by addition of hydrazine and heating to 800 °C.[44]

Ammonium salts of $(B_{11}H_{14})^-$, $(B_{12}H_{12})^{2-}$ and $(B_{10}H_{10})^{2-}$ were all synthesized and hydrolyzed in the presence of a metal catalyst to yield hydrogen, ammonium borate, and boric acid (Fig. 24).[45]

Fig.24 Hydrolysis of ammonium polyborane salts

$$[NH_4][B_{11}H_{14}] + 32\,H_2O \longrightarrow [NH_4][BO_2] + 10\,B(OH)_3 + 24\,H_2 \qquad 6.55\ wt\,\%$$

$$[NH_4]_2[B_{12}H_{12}] + 34\,H_2O \longrightarrow 2\,[NH_4][BO_2] + 10\,B(OH)_3 + 23\,H_2 \qquad 5.82wt\,\%$$

$$[NH_4]_2[B_{10}H_{10}] + 28\,H_2O \longrightarrow 2\,[NH_4][BO_2] + 8\,B(OH)_3 + 21\,H_2 \qquad 6.34wt\,\%$$

2.2.5.4 Amine borane compounds

Low molecular-weight species with high contents of covalently bound hydrogen are promising candidates for hydrogen storage. For this reason, ammonia borane (NH_3BH_3) (AB) as a high potential capacitor of hydrogen (19.6 wt %) has been investigated extensively.

By varying the substituents on B and N, a variety of properties can be altered, such as melting and decomposition points as well as dehydrogenation enthalpy and nature of the reaction products. Nöth and Beyer investigated the physical properties of a variety of alkylamine boranes obtained by addition of the alkylammonium salt to lithium borohydride (Tab. 1).[46]

Tab.1 Physical properties of some alkylamine boranes

Alkylamine borane	Melting point /°C	Decomp. point/°C
H_3NBH_3	104	~ 100
H_2MeNBH_3	56	70
H_2EtNBH_3	19	30-40
$H_2{}^nPrNBH_3$	45	50-70
$H_2{}^iPrNBH_3$	65	90-100
$H_2{}^nBuNBH_3$	- 48	10-15
$H_2{}^tBuNBH_3$	96	120-140
HMe_2NBH_3	37	150
HEt_2NBH_3	- 18	200
$H^nPr_2NBH_3$	30	140
$H^iPr_2NBH_3$	23	250
$H^nBu_2NBH_3$	15	120
$H^tBu_2NBH_3$	19	150

Carboni and co-workers reported an alternative way to synthesis these compounds by treatment of $H_3B.L$ (L=Me_2S, THF, Me_3N) with the amine derivatives.[47] The physical behaviors of these compounds are confusing. For example, H_2EtNBH_3 is one of the least stable, while HEt_2NBH_3 is one of the most stable amine boranes.

Manners and co-workers reported[48] the effect of B- and N- substituents on the ΔG and ΔH of dehydrogenation of $HR_2NBR´_2H$. The process of reversibility is too difficult because of B-N strong bonding. The ΔG of dehydrogenation can be reduced with differing of the substituents on $HR_2NBR´_2H$. This study shows that $HR_2NBR´_2H$ compounds with electron donating groups on

nitrogen (resulting in a more Lewis-basic amine) and electron-withdrawing groups on boron (resulting in a more Lewis-acidic borane) are best suited for reversible dehydrogenation. Taking into account the DSC measurements of Rieger and co-workers, which exhibit the decreasing of enthalpy by substitution of electron withdrawing groups on boron and nitrogen,[49] the reversibility process of dehydrogenation is still a big challenge. Hydrogen loss from amine borane can be achieved by solvolysis (Acid- and metal-catalysed) or thermolysis. The product distribution depends on the reaction conditions (Temperature, concentration) and presence of additives or catalysts. The resulting product of thermal and catalytic decomposition as well as controlling the structure of product is reported in the literature.

A) Thermal solvolysis of amine borane

There have been several reports of amine borane dehydrogenation. The dehydrogenation of AB (NH_3BH_3) as a high potential capacitor of hydrogen (19.6 wt %) has been reported in the solid state and in solution. Thermolysis occurs at temperatures[50] that are too high (around 110, 150, and 1400 °C for the first, second, and third equivalents of H_2) and reactions of amine boranes with alcohol or water are thermodynamically enhanced. However, high temperatures (above the boiling point of water) are necessary to induce hydrolysis with slow rates under neutral or basic conditions.[51] Hydrolysis results in strong B-O bonds that make regeneration difficult.

Varma and co-workers have reported recently thermally-induced solvolysis in two different ways.[52] The first capitalized on an exothermic hydrogen release to induce a self-sustained reaction, and the second relied on pressurising water to increase its boiling point.

B) Acid-catalysed solvolysis

The oldest known process for dehydrogenation from amine boranes is acid-catalysed hydrolysis.[53]

It is suggested that the acid functions by protonating the amine, which releases BH_3 for subsequent hydrolysis (Eq. 8). The nature of the amine in the complex has a profound influence on the reaction rate. For example $_3HBNH_3$ is hydrolysed 600 times faster than H_2MeNBH_3 and 4.8 $*10^4$ times faster than HMe_2NBH_3.

$$H_3N{\cdot}BH_3 + H^+ + 3\ H_2O \longrightarrow 3\ H_2 + B(OH)_3 + NH_4^+ \qquad \text{Eq. 7}$$

C) Metal-catalysed solvolysis

Many metals and metal complexes have been reported to catalyse amine borane solvolysis (Table 2).[54] The investigations on non-precious metals show that in nickel heterogeneous systems, hollow spheres of nickel exhibit substantial catalytic activity versus nickel powder. The recent focus on catalyst development has been in the use of non-precious metals.

The rate of hydrogen release could be increased to three equivalents within 30 min by using of Pt hollow spheres.[55] Solvolysis can be catalysed by iron nanoparticles. The iron nanoparticles can be synthesized by borohydride reduction of $FeSO_4$.

Tab.2 Catalysed amine borane solvolysis

	Amine borane	catalyst	solvent	Eq. of H_2	Temp/°C	Time
1	$H_2{}^tBuNBH_3$ Me_3NBH_3	10% Pd/C (50%wet)	MeOH	3	30	100 min 20 h
2	Various	10% Pd/C (50%wet) Raney Ni	H_2O,various alcohols	High efficiency	20	5min (MeOH) to 190 min (^{t}BuOH)
3	$_3HNBH_3$	Pt (20% on C) $[Rh(1,5\text{-cod})(\mu\text{-Cl})]_2$ Pd	H_2O	3 2.7 2.5	20	2 min 20 min 250 min
4	$_3HNBH_3$	Dowex CO_2	H_2O	2.8 no $_3HNBH_3$ left	20	8 min 7 days
5	$_3HNBH_3$	Co (10% on C) Ni (10% on γ-Al_2O_3)	H_2O	2.9 2.9	20	60 min 60 min
6	$_3HNBH_3$	$Ni_{0.88}Pt_{0.12}$	H_2O	3	20	30 min
7	3HNBH3	Rh Colloids Ir Colloids Co Colloids	H_2O	2.8 3 3	20	40 s 105 min 60 min
8	$_3HNBH_3$	$RuCl_3$	MeOH	3	20	5 min
9	$_3HNBH_3$	Fe nanoparticles	H_2O	3	20	8 min
10	$_3HNBH_3$	Co, Ni, Cu nanoparticles	H_2O	3	20	20-300 min

These nanoparticles slowly catalyse solvolysis of AB. It was found that $FeSO_4$ reduction forms crystalline material in the absence of AB, but forms amorphous nanoparticles in the presence of it, which may account for the difference in activity.

D) Thermal dehydrogenation of amine boranes

The dehydrogenation of AB is an exothermic process (ΔH = - 5.09 kcal mol^{-1})[56] as the dative B-N bond is converted into a stronger covalent one. In contrast ethane, which is isoelectric to AB, under goes an endothermic dehydrogenation. Cleavage of two strong C-H bond is not totally

compensated for by formation of H_2 and the C=C π-bond. Taking into account the intramolecular hydrogen release from AB in the gas phase the activation barrier (32-33 kcal mol^{-1})[57] is larger than the B-N dissociation energy (25.9 kcal mol^{-1}).[58] According to this result, AB should dissociate into NH_3 and BH_3 before H_2 loss.

Theoretically the newly formed BH_3 can catalyse AB dehydrogenation through a six-membered transition state at a barrier 6.1 kcal mol^{-1} higher in energy than separated AB and BH_3 (Fig. 25).

Fig.25 Mechanism of BH_3 catalysed AB dehydrogenation

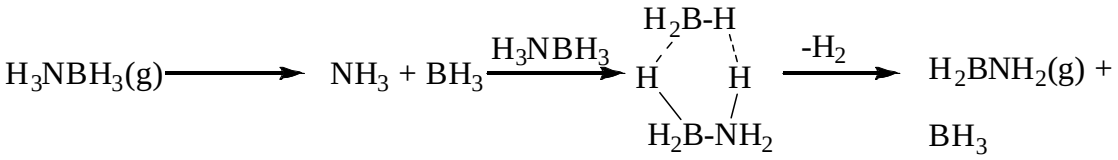

Thermolysis of amine boranes such as AB and methylamine borane (H_2MeNBH_3) have been shown to proceed in the condensed phase by an intermolecular mechanism that involves initial formation of a diaminoboronium borohydride salt (Fig. 26).

Fig. 26 Formation of the diaminoboronium borohydride salt

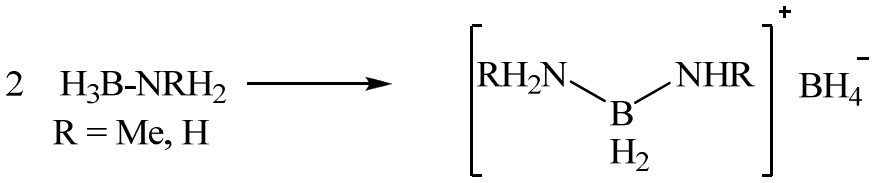

This salt undergoes further reaction with additional amine borane molecules to make aminoborane chains, formation a new B-N bond for each hydrogen molecule released. Computational studies show the low energy coiled and helical conformations are favoured products of presumed linear polyaminoborane.[59] Dehydrogenation of amino borane leads to different oligomeric products depending on reaction conditions (Fig. 27).

Thermodynamic calculations of formation of smaller oligomers in both gas and condensed phase were investigated by Dixon and co-workers.[60] Larger oligomeric products formed in condensed phase, were calculated by Miranda and Ceder.[61]

These products result from both a polymeric ammonia borane cycle (ammonia borane to PAB to PIB; see Fig. 48 for structures) and a cyclic oligomeric pathway (ammoniaborane to CTB,

borazine or 1,4-polyborazylene). While the overall reaction enthalpies depend on the products formed, all reactions in the study are estimated to be mildly exothermic [-1.6 to -20 kcal mol^{-1}]. Direct rehydrogenation will not be possible under practical conditions and amine boranes will need to be regenerated in a chemical process. A few products, such as borazine, are volatile. Loss of these products leads to contamination of the hydrogen stream (potentially poisoning the fuel cell), and material loss (limiting regeneration efficiency).

Fig.27 a), b) Some products of dehydrogenation from AB

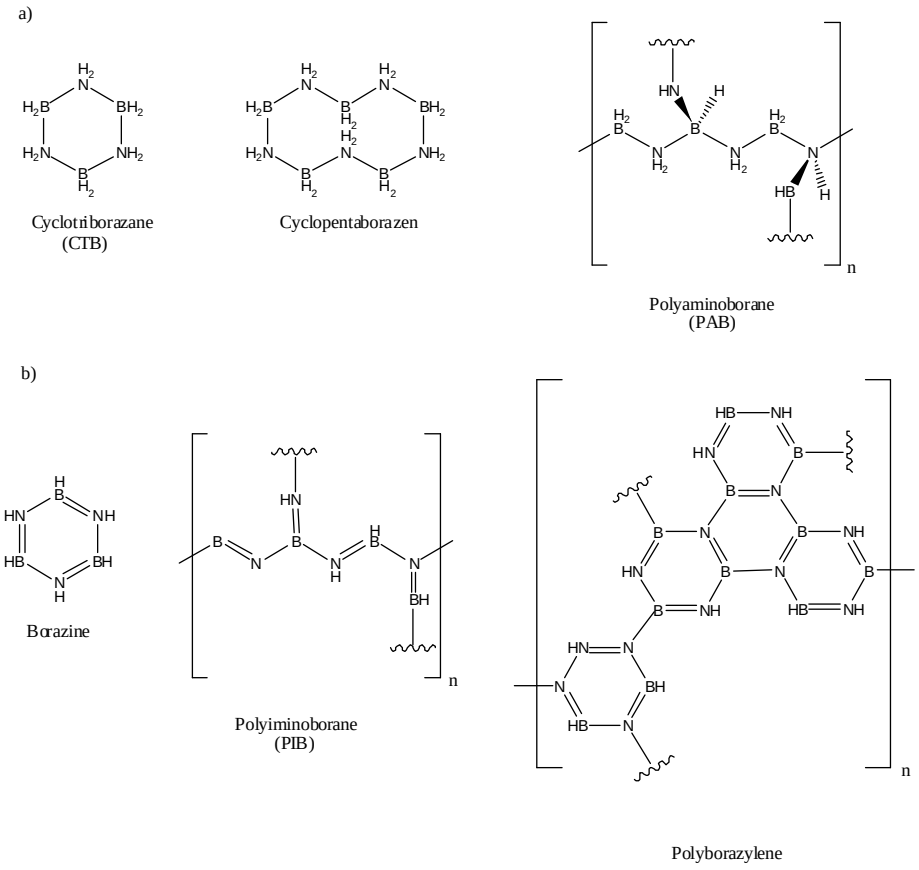

E) Solid state thermolysis

Thermolysis of alkylamine borane between 90 to 120 °C leads to a mixture of cyclic amino- and iminoborane oligomers as well as undefined products.[62] Borazine compounds have been reported by heating N- and B-substituted amine borane (H_2RNBH_3 or H_3NBRH_2) to 200 °C in good yield.[63] The thermolysis of methyl ammonia borane revealed that hydrogen is released in two stages, one at ~100 °C, and the second at 190 °C. For the latter, a competing pathway to borazine formation was identified as dehydrogenative cross-linking of $(HMeNBH_2)_3$ to give an insoluble polymer.[64]

The investigations show three-step decomposition[65] for AB demonstrated in figure 28.

Fig.28 Thermolysis of AB

$$H_3N{-}BH_3 \xrightarrow[107\text{-}117\ ^\circ C]{-H_2} 1/n\ "(H_2BNH_2)_n" \quad (1)$$

$$"(H_2BNH_2)_n" \xrightarrow[150\ ^\circ C]{-H_2} "(HBNH)_n" \quad (2)$$

$$"(HBNH)_n" \xrightarrow[> 1400^\circ C]{-H_2} BN \quad (3)$$

The first peak between 107 °C and 117 °C shows an initial weight loss of 1.1 eq. of dihydrogen, which equates to 7.2 wt %. The second equivalent is lost over a broader temperature range, with a maximum rate at 150 °C. The rest of the hydrogen released at much higher temperatures. The decomposition temperatures and products of dehydrogenation are dependent on the rate by which the temperature is elevated. IR and MS analysis of the volatile thermolysis products for the first dehydrogenation step exhibit traces of B_2H_6, $H_2N{=}BH_2$ borazine and hydrogen.[66] ^{11}B solid state NMR studies showed the formation of diammoniate of diborane $[BH_2(NH_3)_2][BH_4]$. This molecule forms from two ammonia boranes by a hydride transfer, which initiates hydrogen loss and B-N bond formation.[67]

The dehydrogenation rate can be improved by including the additives. Benedetto and co- workers showed that AB milling with Pt (1%) extended the hydrogen release at low temperatures (23 % increase in H_2 release at 140 °C).[68] Autrey and co-workers found that addition of nanocomposite of mesoporous silica to the AB (1:1 by weight) accelerates the hydrogen release at 50 °C with a half-reaction time of 85 min compared to a half-reaction time of 290 min at 80 °C for neat AB.[69] The heating rate of 1 °C /min decreased the peak of dehydrogenation temperature from 110 °C to 98 °C. Encapsulation of AB in a 24 wt% carbon cryogel lowered this peak to 90 °C and there was no decomposition at elevated temperatures.[70] The volumetric measurements exhibit 9 wt % loss of hydrogen, but there was no evidence for borazine formation (mass spectrometry).

F) Solution thermolysis of ammonia borane

Thermal decomposition of AB in a variety of polar and aprotic solvents results in a mixture of cyclic amino- and iminoborane oligomeric dehydrogenation products.[71] The dehydrogenation is

very slowly but Sneddon and co-workers found that ionic liquids provide advantageous media for AB dehydrogenation in which both the extent and rate of hydrogen release are significantly increased.[72]

In contrast to the solid-state reactions, AB dehydrogenations in bmimCl showed no induction period with hydrogen evolution beginning immediately upon placement of the sample in the heated oil bath. Separate samples heated for only 1 h at 85, 90, and 95 °C evolved 0.5, 0.8, and 1.1 equiv of H_2, while samples heated at these temperatures for 3 h produced 0.95, 1.2, and 1.5 equiv. Heating for 22 h gave a total of 1.2, 1.4, and 1.6 equiv. of H_2, respectively, which are values significantly greater than the 0.9 equiv. ultimately obtained in the solid-state reactions. Including the bmimCl weight, the final values correspond to the evolution of 3.9, 4.5, and 5.4 wt % H_2. ^{11}B NMR monitoring of these reactions provided evidence for rapid formation and stabilisation of DADB ($[BH_2(NH_3)_2][BH_4]$) in ionic liquids. ^{11} B NMR analysis of pyridine extracts of the colorless non-volatile residue indicated linear and branched acyclic aminoborane chains, such as $H_3N(BH_2NH_2)_nBH_3$ and $H_3NBH(NH_2BH_3)_2$, in addition to DADB. Volatile products such as borazine resulting from solid-state reactions can poison a fuel cell, but it is significant that in the bmimCl reactions only traces of borazine were detected.

G) Acid-catalysed dehydrogenation of ammonia borane

Treatment of AB with strong Lewis or Bronsted acid leads to effectively dehydrogenation. Addition of $B(C_6F_5)_3$ at 25 °C in ether affords the boronium cation salt $[BH_2(NH_3)(OEt_2)][BH(C_6F_5)_3]$. Strong Bronsted acids, such as trifluoromethane sulfonic acid (HOTf), protonate a B–H bond in AB yielding hydrogen and the analogous boronium triflate. These boronium cations are more reactive versions of that found in DADB and can, as a result, initiate hydrogen release from AB even at 25 °C. Computational studies showed that the cation interacts initially with a B–H bond of AB, drawing a protic N–H in proximity to a hydridic B–H, resulting in loss of hydrogen. Further molecules of AB then interact similarly with the resultant cationic complex to build the aminoborane chains stepwise (Fig. 29).

The relative concentration of acid needs to be kept low (0.5 mol %) to avoid chain termination to aminodiborane, $B_2H_5(\mu\text{-}NH_2)$, and concentrated solutions afford high yields of borazine at 60 °C in 4 h.[73]

H) Anionic dehydropolymerisation of ammonia borane

Recently, Sneddon and co-workers reported that generation of catalytic amounts of metal complex $[H_2NBH_3]^-$ anion increases the rate of hydrogen release. These metal complexes have also been investigated as hydrogen storage materials.[74] Treatment of AB in situ with LiH, $LiNH_2$ or proton sponge [1,8-bis(dimethylamino)naphthalene] generates the anion. The use of the proton sponge eliminated the formation of $LiBH_4$ and NH_3 side products identified when $LiNH_2$ or LiH was used as the base. The mechanism of this reaction is currently unknown but it has been assumed that the increased hydricity of the B-H bond in $[NH_2BH_3]^-$ leads to facile hydrogen release.[75]

Fig.29 A Lewis-acidic $[H_2BNH_3]^+$ molecule interacts with ammonia borane to lose hydrogen and form a new compound that is capable of attack at two positions

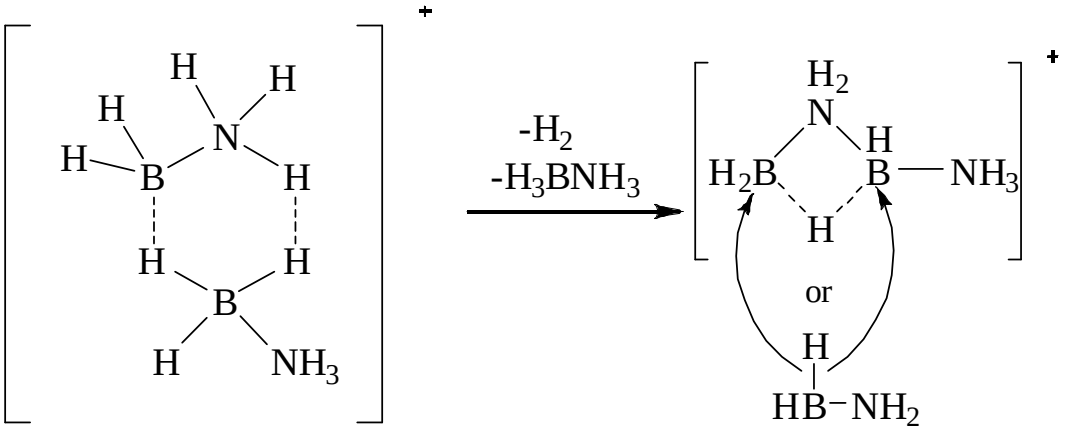

I) Metal-catalysed dehydrogenation of amine boranes

Both the extent and rate of hydrogen release can be controlled by application of metal-catalysed dehydrogenation of amine boranes.

The dehydrogenation of a variety of amine boranes using $Ru_3(CO)_{12}$ at 60 °C was reported by Laine and Blum.[76] Roberts and co-workers found conversion of $HMeBuNBH_3$ to the corresponding aminoborane using heterogeneous Pd/C catalyst at 120 °C.[77] A selection of reported metal catalysts is shown in Table 4; despite this wide range of metal catalysts, there has yet to be catalyst capable of both a high rate and large extent of hydrogen release.[78-86] Moreover this system is to be practical by low catalyst loading, and at last the engineering of hydrogen releas has been only developed for solid catalysts, so effective heterogenisation strategies will be required.

The metal complex catalyst precursor will often undergo changes under significantly reduced conditions of amine borane dehydrogenation. The active species is much different from the precatalyst. Manners and co-workers[79] found that $[Rh(1,5\text{-cod})(\mu\text{-Cl})]_2$ catalyses the dehydrogenation of a variety of amine boranes at low temperatures, but the analogous Ir or Rh precursors with different supporting ligands showed lower activity under the same operating conditions.

Tab.3 Selection of reported metal catalysts for amine borane dehydrogenation

	Catalyst (mol%) Equiv.H_2	Substrate	Conditions	Products [ref.]	
1	Cp_2TiMe_2 (0.5%)	HMe_2NBH_3	16 h, 25 °C	No reaction [79]	0
2	Cp_2Ti (2%)	HMe_2NBH_3	4 h, 20 °C	$(Me_2NBH_2)_2$ [83]	1
3	Cp_2Ti (2%)	$H(i\text{-}Pr)_2NBH_3$	1 h, 20 °C	$^{i}Pr_2NBH_2$ [83]	1
4	$\{[Cp(SiMe_3)_2]_2Ti\}N_2$ (2%)	HMe_2NBH_3	7 min, 23 °C[a]	$(Me_2NBH_2)_2$ [84]	1
5	$\{[Cp(SiMe_3)_2]_2Ti\}N_2$ (2%)	H_3NBH_3	161 h, 65 °C[a]	CTB[b], borazine [84]	NR[c]
6	[indenyl-$(SiMe_3)_2]_2Zr$	HMe_2NBH_3	147 h, 65 °C[a]	$(Me_2NBH_2)_2$ [84]	1
7	$[P(^{i}Pr)_3]_2Br_2(CH_3CN)(NO)Re$ (1%)	HMe_2NBH_3	4h, 85°C	$(Me_2NBH_2)_2$ [78]	1
8	$Ru_3(CO)_{12}$ (0.2%)	H_3NBH_3	85 h, 60 °C	$BN_{1.13}H_{4.7}$ [76]	NR
9	$Ru_3(CO)_{12}$ (0.1%)	Me_3NBH_3, $PrNH_2$	32 h, 60 °C	[–N(Pr)B(H)–]$_3$ (57%)[76]	NR
10	$Ru_3(CO)_{12}$ (0.1%)	Me_3NBH_3, $MeNH_2$	9.5 h, 60 °C	[–B(NMeH)N(Me)–]$_3$, $B(NHMe)_3$[d] [76]	NR
11	trans-$RuMe_2(PMe_3)_4$ (0.5%)	HMe_2NBH_3	16 h, 25 °C	$(Me_2NBH_2)_2$ [79]	1
12	$FeH(PMe_2CH_2)(PMe_3)_3$ (9%)	H_3NBH_3	96 h, 25 °C	CTB, borazine, polyborazylene[d,81]	NR
13	$[Rh(1,5\text{-cod})(\mu\text{-Cl})]_2$ (0.5%)	HMe_2NBH_3	8 h, 25 °C	$(Me_2NBH_2)_2$ [79]	1
14	$[Rh(1,5\text{-cod})(\mu\text{-Cl})]_2$ (5%)	HMe_2NBH_3	>2 h, 25 °C	$(Me_2NBH_2)_2$ [79]	1
15	$RhCl_3$ (0.5%)	HMe2NBH3	22.5 h, 25 °C	$(Me_2NBH_2)_2$ (90%)[79]	0.9
16	$HRh(CO)(PPh_3)_3$ (0.5%)	HMe_2NBH_3	160 h, 25 °C	$(Me_2NBH_2)_2$ (5%)[79]	0.05
17	$[Cp^*Rh(\mu\text{-Cl})Cl]_2$ (0.5%)	HMe_2NBH_3	112 h, 25 °C	$(Me_2NBH_2)_2$ [79]	1
18	$[Rh(1,5\text{-cod})(\mu\text{-Cl})]_2$ (0.5%)	$H(1,4\text{-}C_4H_8)NBH_3$	24 h, 25 °C	$[(1,4\text{-}C_4H_8)NBH_2]_2$ (73%)[e,79]	NR
19	$[Rh(1,5\text{-cod})(\mu\text{-Cl})]_2$ (0.5%)	$HMe(PhCH_2)NBH_3$	24 h, 25 °C	$[Me(PhCH_2)NBH_2]_2$ (79%)[e,79]	NR
20	$[Rh(1,5\text{-cod})(\mu\text{-Cl})]_2$ (1%)	H_2MeNBH_3	60 h, 45 °C	$(MeNBH)_3$ (40%)[e,79]	NR
21	$[Rh(1,5\text{-cod})(\mu\text{-Cl})]_2$ (0.6%)	H_2PhNBH_3	16 h, 45 °C	$(PhNBH)_3$ (56%)[e,79]	NR
22	$[Rh(1,5\text{-cod})(\mu\text{-Cl})]_2$ (0.6%)	H_3NBH_3	60 h, 45 °C	Borazine (10%),e PIB, polyborazylene[79]	NR
23	$[Rh(1,5\text{-cod})(\mu\text{-Cl})]_2$ (1%)	$H^{i}Pr_2NBH_3$	24 h, 25 °C	$(^{i}Pr)_2NBH_2$ (49%)[e,79]	NR
24	$[Ir(1,5\text{-cod})(\mu\text{-Cl})]_2$ (0.5%)	HMe_2NBH_3	136 h, 25 °C	$(Me_2NBH_2)_2$ (95%)[79]	0.95
25	$(POCOP^{f})Ir(H)_2$ (0.5%)	H_3NBH_3	14 min, 20 °C	Cyclopentaborazane[86]	1
26	$Ni(1,5\text{-cod})_2$, 2 NHC[g] (9%)	H_3NBH_3	3 h, 60 °C	Polyborazylene[d,81]	2.8
27	Pd/C	$HMe^{t}BuNBH_3$	1 h, 120 °C	$[Me^{t}BuNBH_2]_2$ [77]	1
28	Pd/C (0.5%)	HMe_2NBH_3	68 h, 25 °C	$(Me_2NBH_2)_2$ (95%)[79]	0.95
29	$(IDipp)^{h}CuCl$ (12.5%)	HMe_2NBH_3	24 h, 20 °C	$(Me_2NBH_2)_2$[d,81]	NR

[a] Inferred from reported TOF values. [b] CTB is cyclotriborazane. [c] NR is ''not reported.'' [d] Yield of products not quantified; other products possible. [e] Isolated yields, actual yield will be higher but other products detected. [f] k^3-2,6-$[OP(t\text{-}Bu)_2]_2C_6H_3$. [g] Enders' carbene: (1,3,4-triphenyl-4,5-dihydro-1H-1,2,4-triazol-5-ylidene). [h] IDipp is 1,3-bis(2,6-diisopropylphenyl)-1,3-dihydro-2H-imidazol-2-ylidene.

The dehydrogenation of DMAB using $[Rh(1,5\text{-cod})(\mu\text{-Cl})]_2$ exhibits an induction period, during the formation of a black suspension. TEM analysis indicated Rh aggregation. Addition of Hg led to complete loss of activity and the UV-Vis spectrum confirmed the Rh colloids.

This evidences proves the Rh(0) as the catalytically active species. Following the EXAFS measurements, exhibit the soluble Rh(0) clusters under different conditions are also shown to catalyse this reaction.[80] These observed $Rh_{4\text{-}6}$ clusters were precipitated during the reaction, due to a ligand exchange process with formed products, but redissolved by treatment with DMAB. The process of colloids or clusters forming is strongly dependent on the variations in conditions.

Minor changes in supporting ligands can profoundly influence the catalytic activity. Baker and co-workers found that the catalytic activity of Ender´s carbene Ni complex (Enders' carbene: 1,3,4-triphenyl-4,5-dihydro-1H-1,2,4-triazol-5- Ylidene) is 11.5 times faster than the IDipp Ni-complex (IDipp: 1,3-bis(2,6-diisopropylphenyl)-1,3-dihydro- 2H-imidazol-2-ylidene.) and 8.8 times faster than the Ni-IMes complex (IMes: 1,3-bis(2,4,6-trimethylphenyl)-1,3-dihydro 2Himidazol-2-ylidene;).[82] Also, the Enders' Ni complex was 4.1 times faster than an Rh(NHC) complex and 1.9 times faster than an Ru(NHC) complex. The Enders' carbene Ni complex has the largest extent of dehydrogenation (>2.5 equiv.) yet seen. The Ni-NHC system exhibits an unprecedented extent of dehydrogenation to a soluble cross-linked borazine structure at 60 °C.

The most logical reaction pathway involves initial formation of a σ-complex[87] B-H bond activation, and β-H elimination from the N-H bond (Fig. 30). The implication from the observed isotope effects showed that the latter two steps have competitive rates (i.e., $k_1 \approx k_2$).

Fig.30 Proposed initial steps of metal-catalyzed AB dehydrogenatio

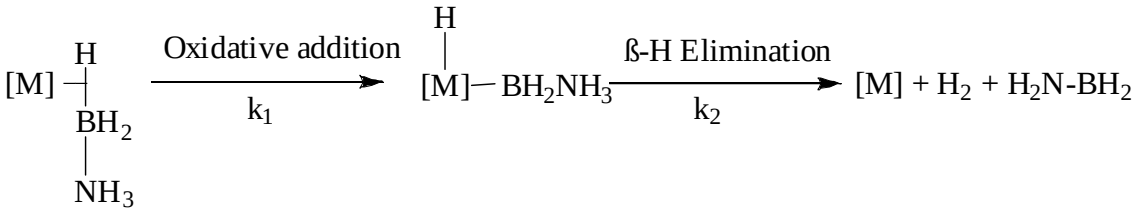

The solvent and substrate using titanocen-based catalysts reported by Manners[83] and co-workers and developed by Chirik and co-workers applying other Cp-based ligands and Zr[84,85] is significant. Chirik and co-workers mentioned that $\{[\eta^5\text{-}C_5H_3(SiMe_3)_2]_2Ti\}N_2$ has a TOF of 4420 h^{-1} in benzene-d_6 and 0.29 h^{-1} in THF for the dehydrogenation of DMAB. Also, AB was found to have a much slower rate than DMAB. $(POCOP)IrH_2$ is an extremely active catalyst for AB

dehydrogenation, as reported by Heinekey, Goldberg and co-workers.[86]

The disadvantage of this system is that only a single equivalent of hydrogen is released per equivalent of AB. During the reaction a colorless solid is continuously precipitated. The x-ray powder diffraction and IR data of this compound differs from previously reported for cyclopentaborazane ($[H_2NBH_2]_5$),[88] but it is clear from the solid state ^{11}B NMR data (-18 ppm) and the measured amount of hydrogen released that an $[H_2NBH_2]_n$ product is formed. It has been suggested that the white precipitate is a polymeric compound similar to the products formed from alkylamine borane dehydrogenation.

The mechanisms of metal-catalysed dehydrogenation have been investigated by computational methods for the (POCOP)IrH_2 system. It is generally believed that transition-metal-catalyzed AB dehydrogenation initiates through oxidative B-H activation at the transition-metal centre followed by ß-H elimination from the N-H bond. Dehydrogenation pathways based on computational studies[89] are represented in Figure 31.

In the $Ni(NHC)_2$ case Hall and Yang have proposed four main steps: transfer of H^+ from N to C(Carbene); transfer of H from C to Ni; transfer of H from B to Ni; and release of H_2 and H_2B-NH_2 (Figure 32).

The proposed mechanisms are merely focused on the initial loss of hydrogen. The extent of dehydrogenation and the role of metal complex are still controversial subjects.

Fig.31 Dehydrogenation pathways (POCOP)IrH_2 for AB dehydrogenation

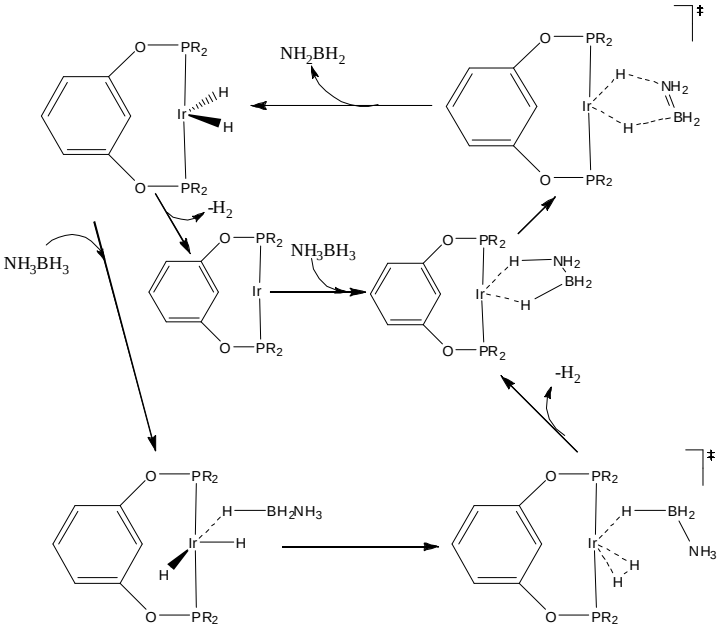

Fig.32 Predicted Reaction mechanism and relative enthalpies of ammonia-borane dehydrogenation catalyzed by $Ni(NHC)_2$

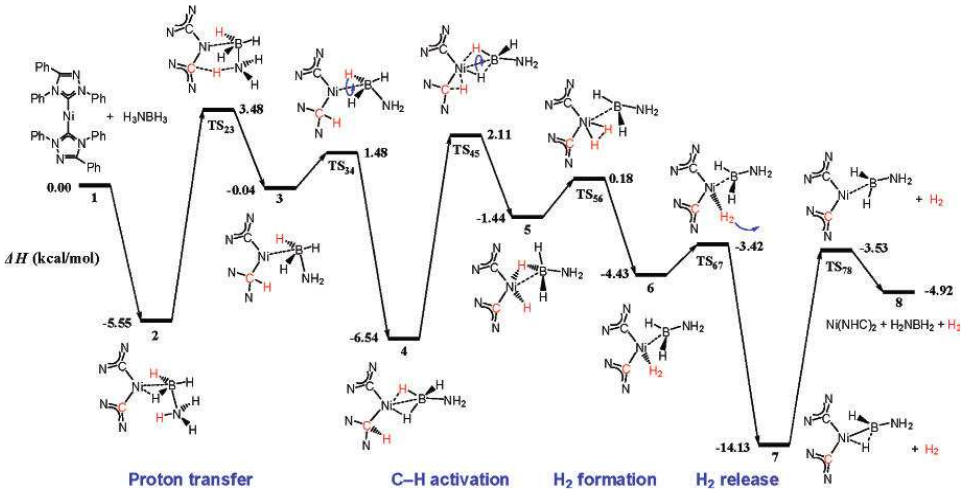

2.2.6 Regeneration of spent fuel

The products of the solvolysis method are usually very stable B-O bonds, which make regeneration of spent fuel possible only by using strong reducing agents. Ramachanran and co-workers established a system based on transition metal catalysed solvolysis of AB to yield $[NH_4][B(OMe)_4]$. Treatment of this compound with NH_4Cl and Lithium aluminium hydride AB can be isolated (Fig. 33).[90]

Fig.33 Solvolysis and subsequent regeneration of ammonia borane.

$$H_3N\text{-}BH_3 + 4\,MeOH \xrightarrow{\text{Solvolysis}} NH_4B(OMe)_4 + 3\,H_2$$

$$NH_4B(OMe)_4 + LiAlH_4 + NH_4Cl \xrightarrow{THF} Al(OMe)_3 + H_3N\text{-}BH_3 + MeOH + H_2 + LiCl + NH_3$$

The alternative for regeneration of solvolysis spent fuel was reported by Sneddon and co-workers and Mertens and co-workers.[91] BNH_x spent fuel generated by metal-catalysed dehydrogenation was successfully digested to form H_2, NH_4Br, BBr_3 as well as $[H_2NBBr_2]_3$ using $HBr/AlBr_3$ in CS_2. Mertens and co-workers[92] reported that the addition of an ether solution of HCl to THF solution of spent fuel leads to BCl_3, NH_4Cl and H_2. Due to the decomposition of BCl_3 in THF the yield of this regeneration is low.

A super acid solution used by Sneddon and co-workers increased the yield of BCl_3 to > 60 %.

The reduction of BCl_3 to B_2H_6 requires high temperatures (600-700 °C) and the resulting products are always a mixture of different boron hydrochlorides. However, adding a Lewis-base such as NMe_3 reduces the hydrochlorination temperature to 200 °C but high pressure is still required.[93]

The reduction of BX_3 can be carried out in a similar way using the chemical hydrides. Mertens and co-workers reported a complete reduction to Ph_3NBH_3 in the presence of a weak acid such as NPh_3 and MgH_2 at 80 °C after 20 min. The final step is displacement of R_3N with ammonia to yield AB.

2.3 Dihydrogen bonding and hydrogen release

The dihydrogen bonding was reported[94-103] as an unusual type of hydrogen bonding, in which a σ M-H bond (where M is less electronegative than H) acts as electron donor (Fig.34).

Fig.34 Dihydrogen bonding

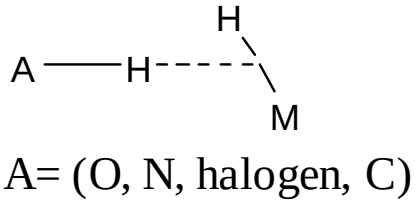

A= (O, N, halogen, C)

This hydridic-to-protonic interaction, also called dihydrogen bonding, proton-hydride bonding, H···H hydrogen bonding, or hydrogen-hydrogen bonding, has strength and directionality comparable with those found in conventional hydrogen bonding. Consequently, it can influence structure, reactivity, and selectivity in solution and solid state, finding thus potential utilities in catalysis, crystal engineering, and materials chemistry.

Epstein and co-workers reported the ability of boron hydrides to act as proton acceptors in hydrogen bonds.[104-106] They studied the interaction of NEt_3BH_3, $P(OEt)_3BH_3$ and $Bu_4N^+BH_4^-$ with different alcohol as proton donors by IR and NMR spectroscopy.

Crabtree et al. have reported[107] 26 intermolecular N-H···H-B short contacts in the range 1.7-2.2 Å. He has suggested the term “dihydrogen bonds”. The investigation of the crystalline structure showed a strong preference for a bent geometry with NH···H-B angles typically between 95 and

120 °, and N-H···HB angles tending to be larger (150-170°). Theoretically, they have also investigated the NH_3BH_3 dimer, which shows a C_2 symmetrical geometry with two identical H···H interactions and contact distances of 1.82 Å (Fig.35).

Fig.35 C_2 isomer of the NH_3BH_3 dimer

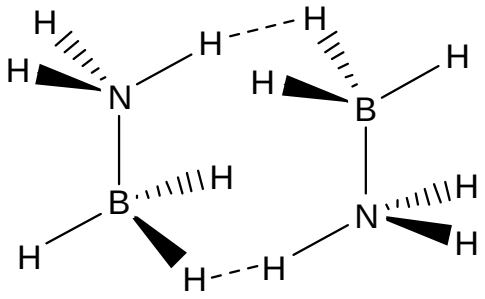

As part of my work the physical and chemical features of GB have been demonstrated previously. The crystal structure of GB shows the alternating BH_4^- and $C(NH_2)_3^+$ ions connecting by multipoint dihydrogen bonding, which can be described in terms of stacks and layers of one-dimensional GB tapes (Fig. 36). The two out of plane borohydride hydrogens are essentially bridging two guanidinium ions in a planar tape. The distance of dihydrogen bonding is reported to be between 2.06 and 2.16 Å.

This three-dimensional dihydrogen bonding extended in space is assumed to be the reason for dehydrogenation of these compounds. In the next chapter, the stability of dihydrogen bonding, as well as the possible reversibility via changing the substitution will be demonstrated.

Fig.36 A one-dimensional GB tape depicting close hydrogen–hydrogen bonding interactions

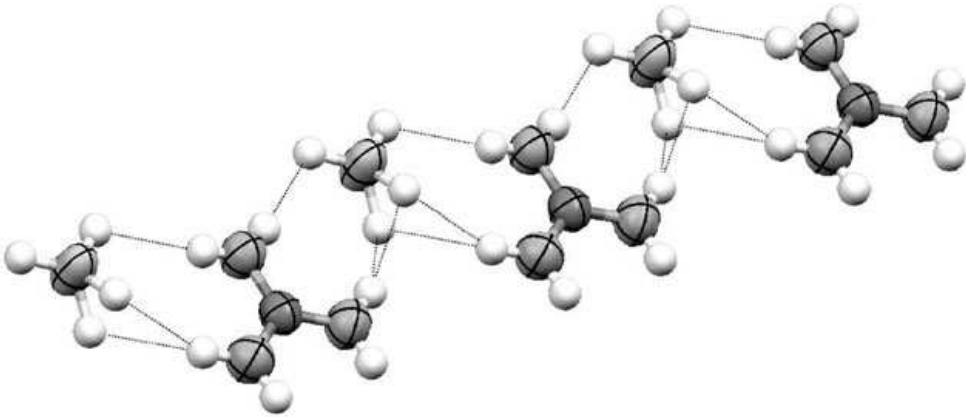

2.4 Scope of this work

The goal of this investigation is developing hydrogen storage materials based on B-N compounds, which can release pure hydrogen under both thermal and catalytic conditions with high gravimetric capacities. Usually, thermal or catalytic dehydrogenation of B-N compounds contains impurities in gas stream such as ammonia, which damage membrane of fuel cell.

The rehydration of spent fuel of B-N hydrogen storage materials is another issue in this work. This can be explored, if the product of dehydrogenation can be controlled to a unique structure. The B-N compounds often generate a big range of products as illustrated in introduction.

To achieve these goals, we have sythesized and analyzed the guanidinium and guanidinium derivatives based B-N compounds.

2.5 Guanidinium and methyl guanidinium borohydride based hydrogen storage Material

Dupont and co-workers have reported[108] the first hydrogen storage materials based on ILs. They have used classical hydrogenation and dehydrogenatin of benzene substituted ILs with commercially available noble metal catalysts, such as Rh/C (5%) and Pd/C (5%) (Fig. 37).

Fig.37 Hydrogenation and dehydrogenation of Benzene containing IL

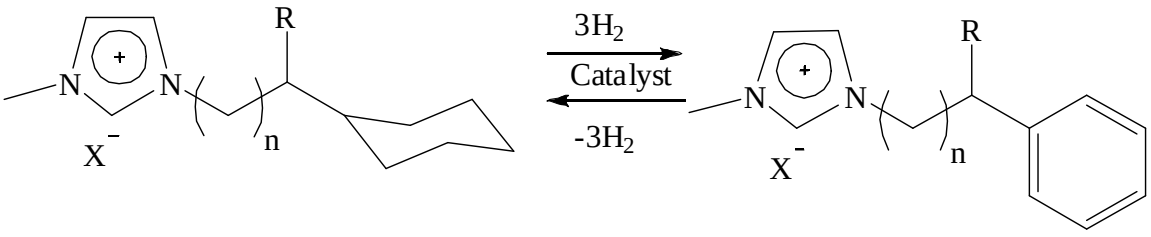

To date, there are relatively few works, that exploit the advantageous features of ionic liquids – lower vapour pressure, high density and low viscosity combined with hydrogen storage.

Herein, methylguanidinium borohydride $(N_3H_8C)C^+BH_4^-$ (MGB) an ionic liquid (m.p. -5 °C, ρ 20 °C = 0.95 g/ml) (Fig. 38) is presented, which releases 9.0 wt % H_2 under both thermal and catalytic conditions. To the best of our knowledge, MGB presents the first ionic liquid based on BH_4^- with an effective hydrogen storage capacity. The ionic liquid is compared with guanidinium borohydride $(N_3H_6)C^+BH_4^-$ (GB), which, with 10.7 wt %, possesses a significant potential for application as hydrogen source.

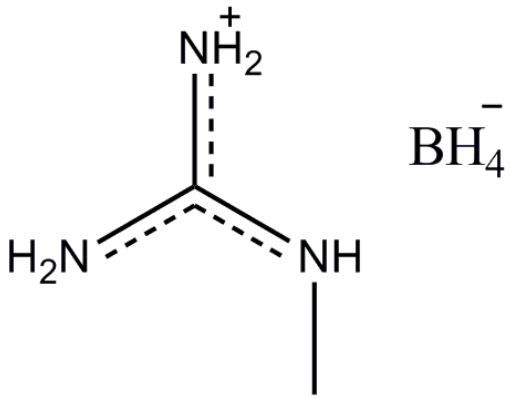

Fig.38 Structural formula of methylguanidinium borohydrid (MGB)

The preparation of GB by ion exchange between $Ca(BH_4)_2$ and guanidinium carbonate in water, or by reaction of $NaBH_4$ and guanidinium sulfate in isopropanol, respectively, has been already detailed by Titov et al.[109,110] An alternative metathesis-based methodology is presented herein. Mixing guanidinium chloride with sodium borohydride in THF at 0 °C affords two discrete phases: the upper phase consisting of THF, and the lower phase comprising guanidinium borohydride with 2.5 equivalents of THF (as determined by NMR spectroscopy, CD_2Cl_2 external standard). Removal of volatile components under vacuum affords GB as a white solid. A parallel synthesis was used for the preparation of MGB by mixing THF slurries of methyl guanidine hydrochloride and sodium borohydride at room temperature, which affords the product as a yellow viscous liquid. The molecular structure of GB, comprising alternating $^-BH_4$ and $(NH_2)_3C^+$ ions interconnected by multipoint dihydrogen bonding, has been previously explained by Jackson and Groshens.[111] GB is a slightly hygroscopic, air stable, colorless crystalline solid. A melting point of 102 °C with decomposition was observed while heating the sample at a rate of about 10 °C min^{-1}. Under 60 °C, no gas evolution was detected for days. Very slow hydrogen evolution started at about 60 °C. After 24 h and 48 h, 0.25 % and 2.1 % of the available hydrogen were released, respectively.

The thermal decomposition of GB was reported by Jackson and Groshens in a good yield, but the amount of ammonia in gas stream is problematic for fuel cell application. Therefore, to improve the purity of liberated gas, a mixture of GB with other hydride additives (MgH_2, $NaBH_4$, $LiAlH_4$) in different ratios was investigated. The mixture exhibited no improvement in thermal decomposition reaction. A remarkable improvement in the purity of the hydrogen product was

reported from mixtures of GB and ethylenediamine bisborane (EDB). The addition of EDB to GB resulted in a decrease in the ammonia production without affecting the gravimetric hydrogen yield of mixture. This mixture is able to release about 4 equivalents H_2 per mole of GB and EDB (Tab. 4).

Tab.4 GB-EDB reaction products

wt % GB	wt % EDB	wt % H_2 yield	mol % NH_3	$\frac{\text{mol } H_2 \text{ generated}}{\text{mol (GB + EDB)}}$
100	0	10.6	4.1	3.94
89.5	11.5	10.4	2.7	3.89
60.0	40.0	10.4	0.10	4.11
46.0	54.0	9.60	0.069	3.87
40.0	60.0	10.1	0.026	4.12

The kinetic dehydrogenation in our studies of MGB and GB were performed in homogeneous diglyme solution and the evolved hydrogen was measured volumetrically. The amount of evolved hydrogen depends on the temperature, concentration and nature of catalyst (Fig. 39).

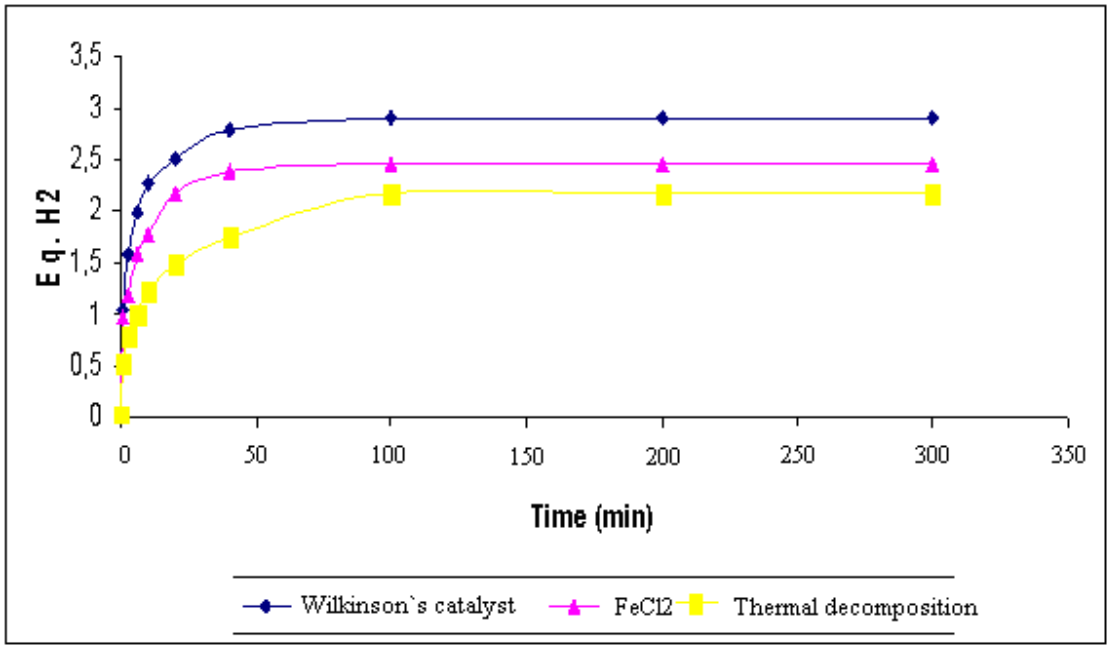

Fig.39 Kinetic of thermal and catalytic dehydrogenation of GB

During the gradual dehydrogenation of MGB, a white precipitate was formed from the yellow

solution. The kinetic measurements in homogenous diglyme solution at 75 °C show within 20 minutes 2.9 equivalents hydrogen evolution for Wilkinson`s and 2.4 for $FeCl_2$, respectively (Tab. 5). Using bipolar coupling of hydride and proton theoretically four equivalents H_2 can be released, which leads to B–N direct bonding (B-N dehydrocoupling).

Tab.5 Amount of hydrogen gas evolved from MGB with $FeCl_2$ and $(PPh_3)_3RhCl$ catalysts

Mol %	**Catalyst**	**Temperature**	**Equiv. H_2**
1 mol %	Wilkinson`s catalyst	75 ℃	2.9
1 mol %	$FeCl_2$	75 ℃	2.4
Thermal	–	75 ℃	2.3

The amount of hydrogen evolved from GB in dry diglyme at 75 °C by loading with Wilkinson`s and $FeCl_2$ catalyst equates to 3.9 (10.3 wt %) and 2.0 (5.3 wt %) equivalents, respectively, thus quantitative H_2 evolution and higher dehydrogenation rates of GB using improved catalysts can be achieved. However the observed dehydrogenation rates demonstrated are still insufficient for practical application.

TGA and DSC measurements of GB have been previously explained by Groshens.[111] TGA-MS analysis of MGB shows a 10.84 % weight loss (theoretical dehydrocoupling: 8.97 %). The weight loss during the TGA-Measurement differs from the theoretical calculated value, because the compound generates volatile substances by dehydrogenation, which exit through the internal gas stream. GB shows a 10.64 % weight loss (theoretically dehydrocoupling: 10.65 %) reached in the temperature range between 40 °C and 180 °C, accompanied by a shoulder up to 200 °C, which can not be assigned to a dehydrocoupling process (Fig. 40).

The purity of evolved gas has been established by MS analysis in the range of 2 g/mol to 60 g/mol using TGA-MS coupling, which indicated hydrogen as the predominant product. In the temperature range from 40 °C to 120 °C the presence of ammonia was below the detection limit for both MGB and GB in the evolved gas stream. Upon further heating of the compounds, traces of ammonia were detected in the 120 °C to 580 °C temperature range in both cases (indicating the onset of decomposition); however, the mass loss observed for both MGB and GB is continuous ($m/z > 60$) until complete decomposition of the compounds is reached (approximately 800 °C).

The DSC curve of MGB demonstrates two exothermic processes which are connected by an endothermic process at 80 °C. It is tentatively proposed that the exothermic H_2 evolution is superimposed with several phase transitions processes, the enthalpy contributions of which are

not easy to compensate.

The overall liberated energy (ΔQ) for MGB over the range 20 °C to 200 °C is therefore determined as - 85 KJ/mol. The thermal dehydrogenation of MGB and GB were broadly similar, with the continuous precipitation of a white solid product from the diglyme solution over the course of the reactions. In both cases, the insoluble product is assumed to be oligomeric or crosslinked in nature, as confirmed by mass spectrometric analysis (m/z > 60 for all observed products).

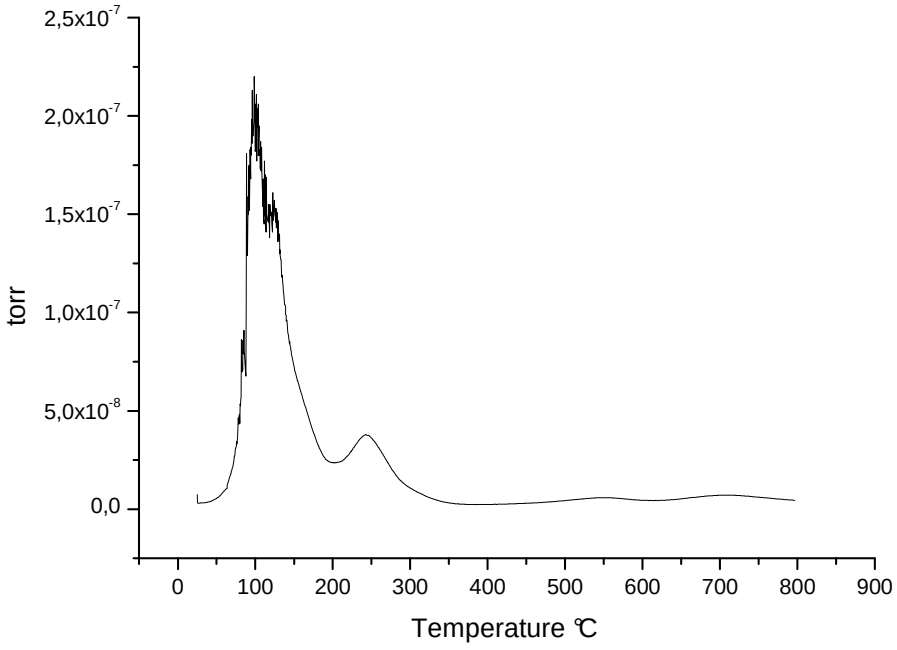

Fig.40 Evolution of hydrogen gas from MGB as detected by TGA-MS

The solution phase is found to contain unreacted guanidinium borohydrides in both cases (as determined by multinuclear NMR spectroscopy). The obtained insoluble products from the dehydrogenation of MGB and GB were characterized with the aid of solid state ^{11}B MAS NMR spectroscopy. The ^{11}B MAS NMR spectrum of the thermal dehydrogenation of MGB exhibits sharp signals at - 38 ppm, - 27 ppm, -15 ppm, -1 ppm and 10 ppm. The ^{11}B MAS NMR spectrum of GB shows similar shifts. The three products of catalytic and thermal decomposition each show two principle signals at around - 39 ppm and - 4 ppm with a shoulder at - 7 ppm. Minor signals appear at - 28 ppm, - 16 ppm and + 9 ppm. The spectra differ only by the relative intensity of the observed signals (Fig. 41). As a result of improved signal intensity and simplified calculations,

the theoretical spectra of GB were compared with the observed ^{11}B NMR spectroscopic shifts of MGB and GB. Although GB lacks a methyl group, this substituent has a minimal effect on the observed chemical shifts, thus enabling comparisons. The solid state ^{13}C NMR spectrum of GB exhibits two signals, attributed to the guanidinium moiety at + 159 ppm and methyl group at + 28 ppm, which indicate no appreciable change in carbon character during the dehydrogenation reaction.

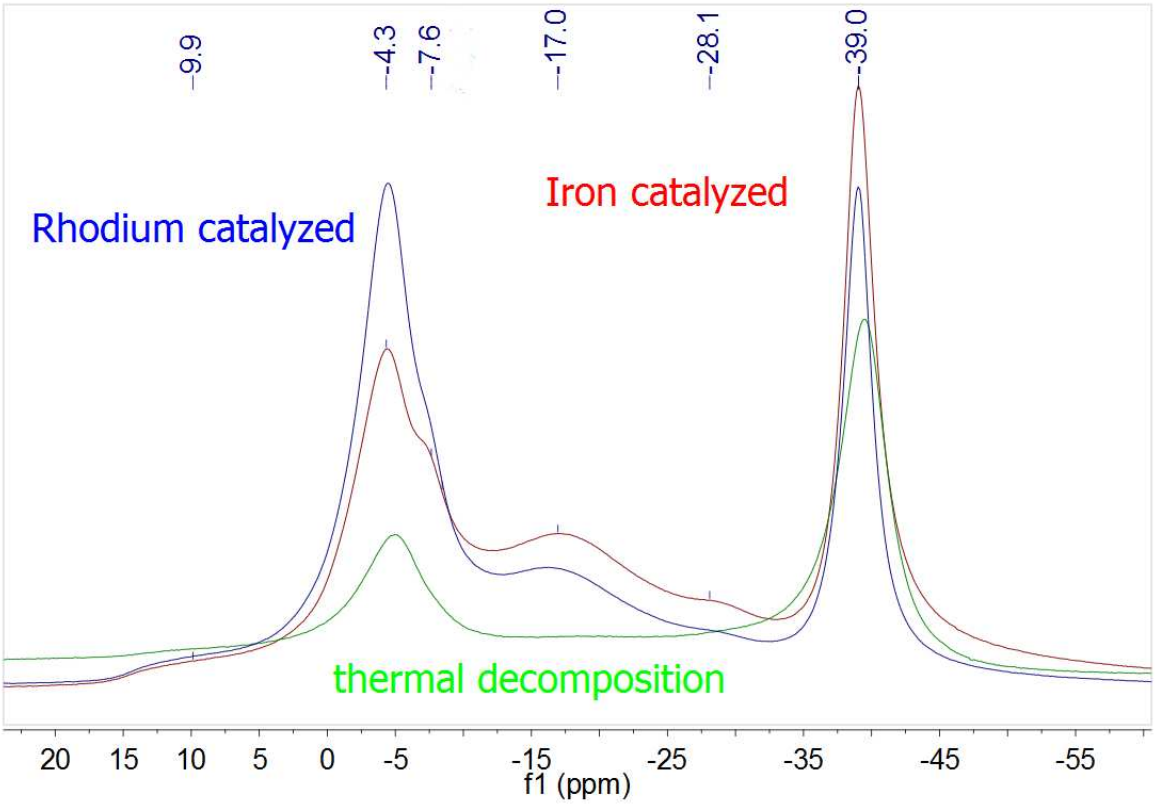

Fig.41 ^{11}B solid state NMR spectra of the decomposition products of 1 by thermal (75 °C), iron-catalyzed (2 mol % catalyst 75 °C) and rhodium-catalyzed (0.1 mol % catalyst, 75 °C) dehydrogenation

The results of RI-MP2/GIAO 11B NMR spectroscopic chemical shift calculations (Turbomole, TZVP-Basissatz)[112,113] on possible dehydrocoupling reaction products of GB are illustrated in Fig. 42. The calculations based on TZVP-Niveau are employed successfully already for prediction of 11B NMR spectra.[114] The sharp signals at - 39 ppm are attributed to residual BH_4^-, which remains unreacted in the product mixture. The second signal at - 4 ppm with a shoulder at - 8 ppm is assigned to tetravalent boran nitrogen substances, which the shift increases with the number of coordinated nitrogen, from - 8.5 ppm for bisubstituted, over - 6.0 ppm for 3 to - 3.5

ppm for tetravalent bonded guanidinium units (Fig.42 b-c).

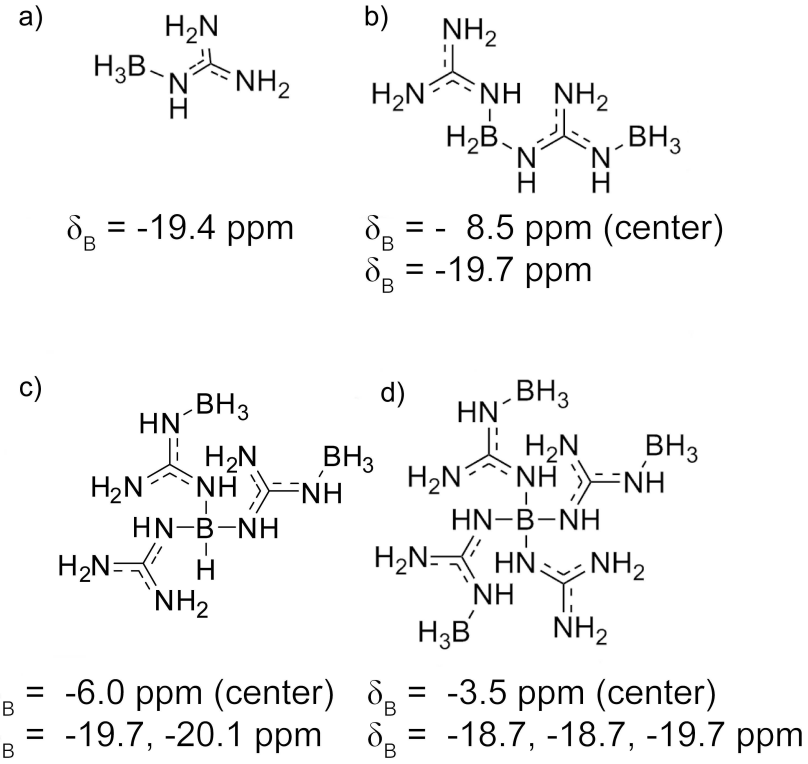

Fig.42 Calculated ^{11}B NMR spectroscopic chemical shifts for proposed structures arising from dehydrogenation of guanidinium borohydride

The calculations show a signal at - 19.4 ppm for the single guanidinium unit coordinated at BH_3 (Fig. 42a). Taking into account that the calculated results shifted 1-3 ppm, to a number of higher frequency, the cited signal is therefore assigned to the measured resonance at -17 ppm. Because all species with more guanidinium units comprise terminated BH_3 groups, the signals between -17 ppm and - 24 ppm can be assigned. The ESI-MS characterization of the solid dehydrogenation products from compounds MGB and GB were performed in warm isopropanol. In both cases, product dissolution was initially limited; however the solubility notably increases over time (days). It is assumed that the improved solubility, in both cases, is a direct result of hydrolysis of the oligomeric products. The predominant formation of dimeric or trimeric boron-bridged species is in accordance with branched oligomers as dehydrocoupling products. Herein, we have

introduced the first ionic liquids with covalently bound hydrogen. Thermal or catalytic decomposition of compounds MGB and GB, in contrast to that of ammonia borane, affords a series of well defined, solid products. The high capacity of pure hydrogen renders these compounds interesting targets for hydrogen storage applications.

2.6 Guanidinium octahydrotriborate as chemical hydrogen storage

The high hydrogen density of guanidinium octahydrotriborate (GOTB) makes it an attractive candidate for chemical hydrogen storage. This compound releases 6.2 equiv. H_2. It is a crystalline hygroscopic compound with a density of 0.86 g/cm^3. It is soluble in isopropanol, THF, diglyme or water and insoluble in saturated hydrocarbons, benzene and toluene.

The syntheses were reported by Titov and co-workers[115] by treatment of $C(NH_2)_3BH_4$ with B_2H_6 in THF or by exchange reaction of solvated NaB_3H_8 with $[C(NH_2)_3]_2SO_4$ in isopropanol.

Herein we obtain the product by the exchange reaction of NaB_3H_8 and $C(NH_2)_3Cl$ in isopropanol (Eq. 8).

Eq.8 Synthesis of GOTB

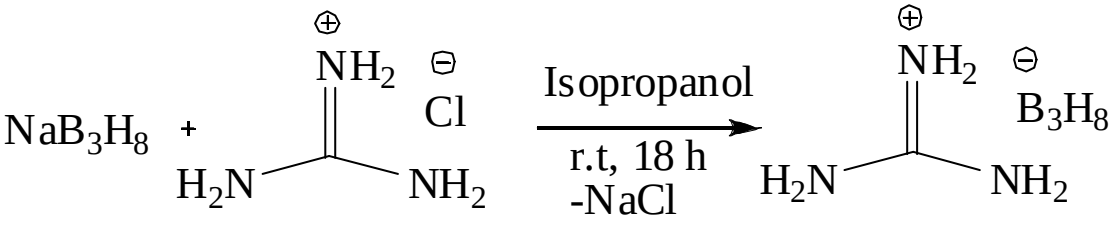

Its decomposition by heating started at 100 °C and terminated after 2 h by liberation of 6.5 equiv. gas. MS-analysis showed 6.2 mol of H_2, 0.3 mol of N_2 and traces of CH_4. The IR-absorption bands of brown residue at 1400 cm^{-1} and 800 cm^{-1} are characteristic for BN compounds. The decomposition occurred at lower temperatures but with a longer induction period.

The dihydrogen bonding formed by proton of guanidinium and hydride of triborane can reveal interesting information about the length and stability of this bonding. This information is lacking in the literature on the crystal structure and dihydrogen bonding. Our attempts to prepare and measure a single crystal of GOTB ended in failure. But the crystal structures of octahydrotriborate-salts are explained in the literature.[116-120] As reported by Frei and co-

workers[120] the crystal structure of CsB_3H_8 exhibited the general arrangement of cations Cs^+ and anions $(B_3H_8)^-$ correspond to a rock salt structure with an orthorhombic distortion.

No disorder of the fluxional $(B_3H_8)^-$anion, as frequently observed in compounds with complex cations, was reported. The study indicated that the triangular anion has Cs symmetry with two asymmetric hydrogen bridges and three BH, groups. The two hydrogen-bridged B-B connectivities are significantly shorter (179 pm) than the non-bridged one (185 pm) (Fig. 43).

Fig.43 Crystal structure of octahydrotriborate in CsB_3H_8 and different configuration of fluctuational B_3H_8-anion in solution

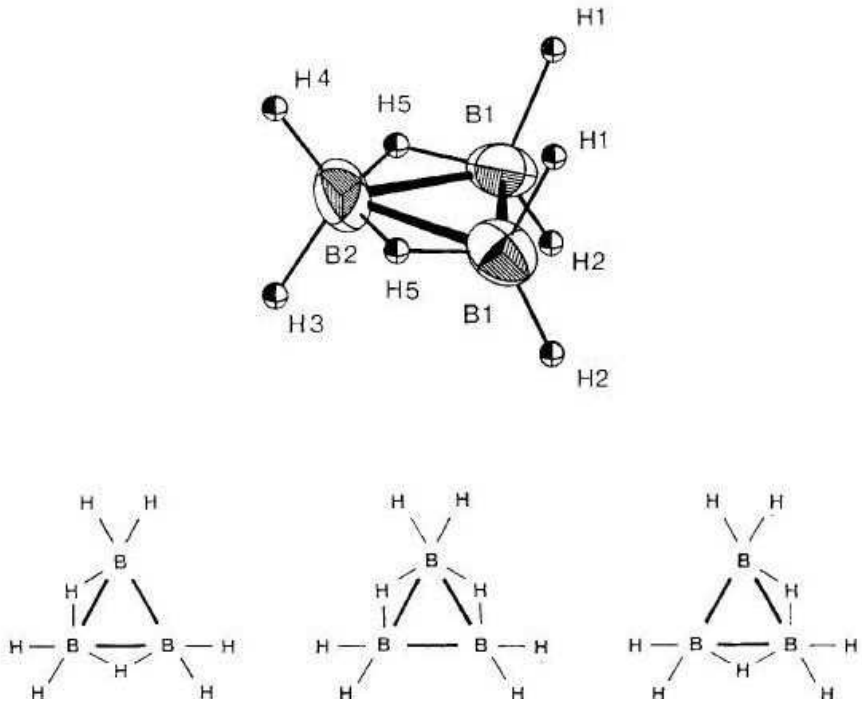

2.7 Conclusion

We have introduced the first ionic liquids with covalently bound hydrogen (MGB). This releases 9.0 wt % H_2 under both thermal and catalytic conditions. The ionic liquid is compared with GB, which, with 10.7 wt %, possesses a significant potential for application as hydrogen source.

The thermal decomposition of GB was reported in a good yield, but the amount of ammonia in gas stream is problematic for fuel cell application. In contrast to thermal decomposition of GB, thermal decomposition of MGB showed a pure hydrogen gas stream up to 120 °C. Also, the catalytic dehydrocoupling of GB and MGB using wilkinson's and iron (II) chloride catalysts resulted in a pure H_2 stream. Thermal or catalytic decomposition of compounds MGB and GB, in contrast to that of ammonia borane, affords a series of well defined, solid products, but the reversibility is still a big challenge due to inslolubility of product and strong B-N bonding.

Due to our experience with ionic liquid as hydrogen storage material, we have developed other ionic liquids based on methyl guanidinium cation, which are explained in next chapter.

2.8 General Experimental Methodology

All reactions and product manipulations were performed under an atmosphere of dry argon using standard Schlenk techniques, or in an inert atmosphere glovebox. Diglyme was dried via molecular sieves 4 Å.

Guanidinium chloride, methyl guanidinium chloride, sodium borohydride, iron (II) chloride and $(PPh_3)_3RhCl$ were purchased and used as received. Solution NMR spectra were collected at room temperature using a Bruker ARX300 spectrometer.

^1H, ^{13}C NMR spectra are referenced to $SiMe_4$ by citing the residual solvent peak. ^{11}B NMR spectra were referenced externally to $BF_3.Et_2O$ at 0 ppm. Solid state $^{11}B\{^1H\}$ NMR spectra were performed at room temperature on a Bruker 300 MHz spectrometer. The solid sample was spun at 12 kHz, using 4 mm silicon nitride rotors filled in a glove box under an atmosphere of dry argon. Infrared spectra were recorded on a Bruker IFS55 FT-IR spectrometer at room temperature. DSC and TGA have been measured by DSCQ2000 and TGAQ5000 respectively from TA Instrument (Waters).

ESI-MS was carried out with a Varian 500 MS spectrometer with isopropanol as solvent.

Synthesis of methyl guanidinium borohydride (MGB)

Methyl guanidinium chloride (3 g) and sodium borohydride (1.06 g) were suspended in THF (20 mL) at room temperature in a 50 mL round-bottom flask. Under a flow of argon, the reaction was stirred for 18 h, the suspension turn to a homogenous particle distribution and the organic phase was removed by filtration under inert gas. The organic phase consisted of two different phases; after removing the upper phase, the solvent was removed under reduced pressure and washed twice with 10 ml of diethyl ether, giving pure MGB (81 %) as light yellow liquid.

^1H NMR (CD_2Cl_2-external standard, 300 MHz) δ = 6.78 (s, 5H, NH_2), 3.07 (s, 3H, CH_3), 0.11 (q, 4H, J = 79.2 Hz, BH_4); ^{11}B NMR (CD_2Cl_2-external standard, 300 MHz) δ = -37 (Pentett, J = 80.9 Hz, BH_4);

FTIR: 3327-3176 cm^{-1} (N-H); 2244 cm^{-1} (B-H);1646-1620 cm^{-1} (C-N, N-H); 1166 cm^{-1} (CH_3-N); 1084 cm^{-1} (B-H); 604 cm^{-1} (N-H).

Synthesis of guanidinium borohydride (GB)

Guanidinium chloride (3 g) and sodium borohydride (1.30 g) were suspended in THF (20 mL) at 0 °C in a 50 mL round-bottom Schlenk flask. Under a flow of argon, the reaction was stirred for 5 h at 0 °C, the apparent particle size of the suspended solid decreased, and the organic phase was then filtrated off under inert gas.

The organic phase consisted of two different phases; after removing the upper phase, the solvent was removed under reduced pressure and the solid was washed twice with 10 ml of diethyl ether affords to pure GB (82 %) as white solid.

^{1}H NMR (CD_3CN, 300 MHz) δ = 6.93 (s, 6H, NH_2), 0.13 (q, 4H, *J* = 81.2 Hz, BH_4); ^{11}B NMR (300 MHz, CD_3CN) δ = -40 (pentet, *J* = 81.5 Hz, BH_4); ^{13}C NMR (300 MHz, CD_3CN): δ = 157.9;

FTIR (KBr): 3150-3399 cm^{-1} (N-H); 2384, 2291, 2223 cm^{-1} (B-H);1641-1741 cm^{-1} (C-N, N-H); 1125 cm^{-1} (B-H); 516 cm^{-1} (N-H).

Elemental Analysis:

	Measured (%)	Calculated (%)
C:	17.00	16.30
H:	12.80	13.45
N:	55.29	56.09

Synthesis of 1,1,3,3-Tetramethylguanidine borane

A solution of $H_3B{\cdot}NMe_3$ (0.42 g, 5.7 mmol) in THF (30 mL) was slowly added by cannula to a stirred solution of 1,1,3,3-tetramethylguanidine (644 mg, 5.6 mmol) in toluene (20 mL). The reaction mixture was stirred for 18 h at 80 °C. The resulting solution was concentrated and stored at -20 °C to give colourless crystals of $H_3B{\cdot}N(H)C(NMe_2)_2$.

^{1}H NMR (C_6D_6, 300 MHz): δ = 4.57 (s, 1 H, NH), 2.78 (br. q, *J = 95* Hz, 3 H, BH_3), 2.53 (s, 6 H, Me_2N), 1.78 (s, 6 H, Me_2N) ppm. ^{11}B NMR (C_6D_6, 128.30 MHz): δ = –19.5 (q, J = 93 Hz, BH_3) ppm.

MS (EI+): m/z (%) = 128.2 $[C_5H_{15}BN_3]^+$, 126.2 $[C_5H_{13}BN_3]^+$

^{11}B and ^{13}C MAS spectra of dehydrogenation of MGB

^{11}B NMR

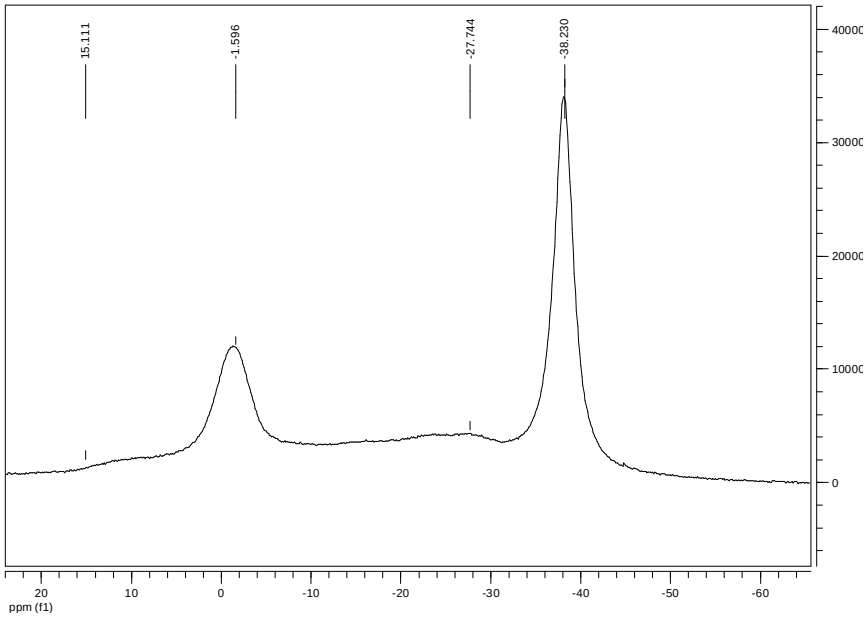

^{13}C NMR

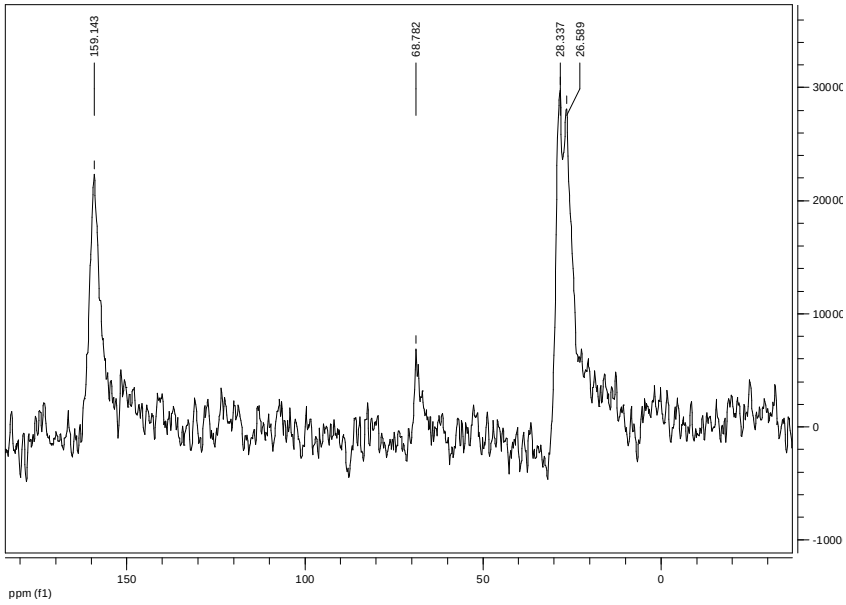

^{11}B and ^{13}C MAS spectra of dehydrogenation of GB

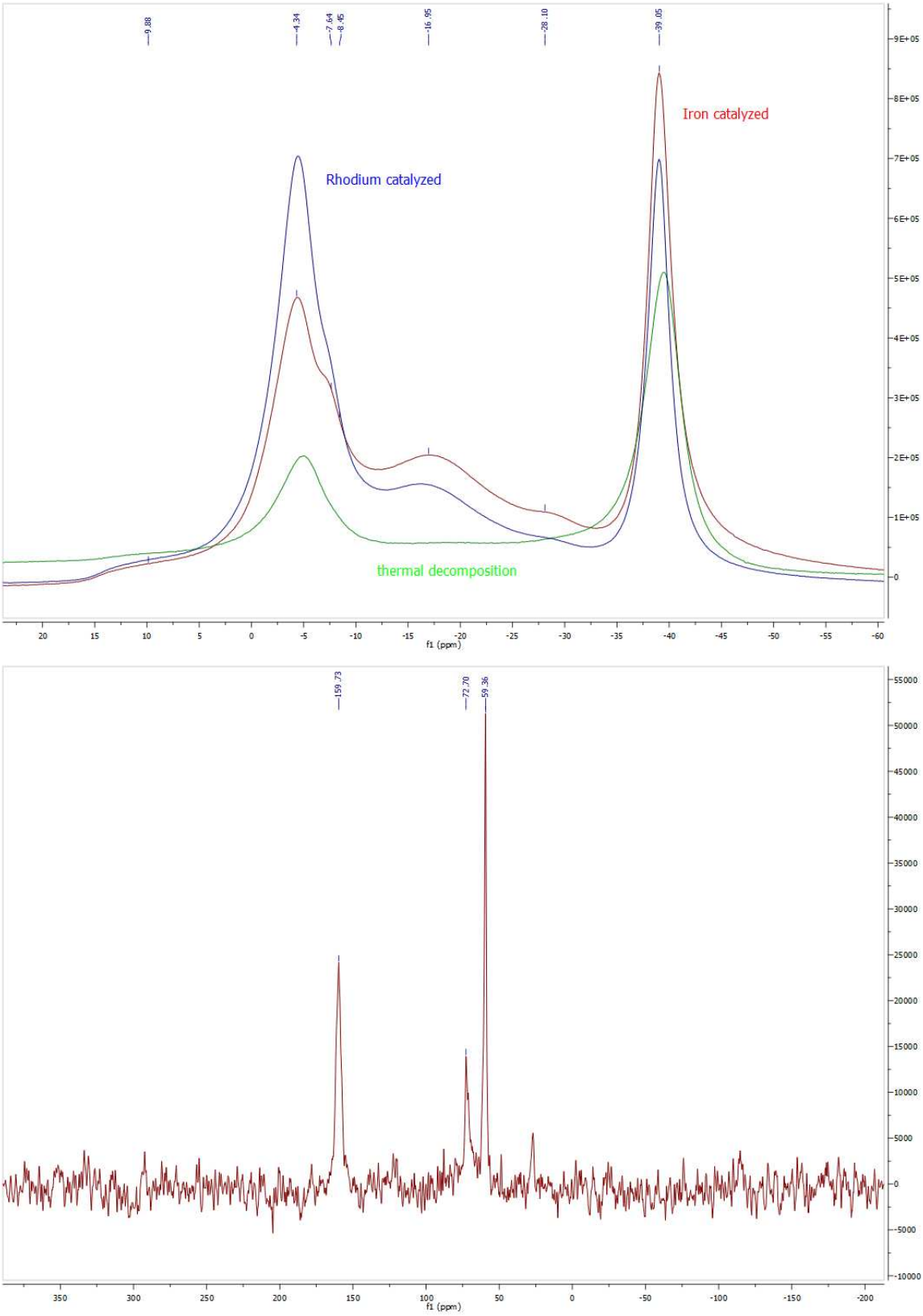

DCS and TGA Analysis

MGB:

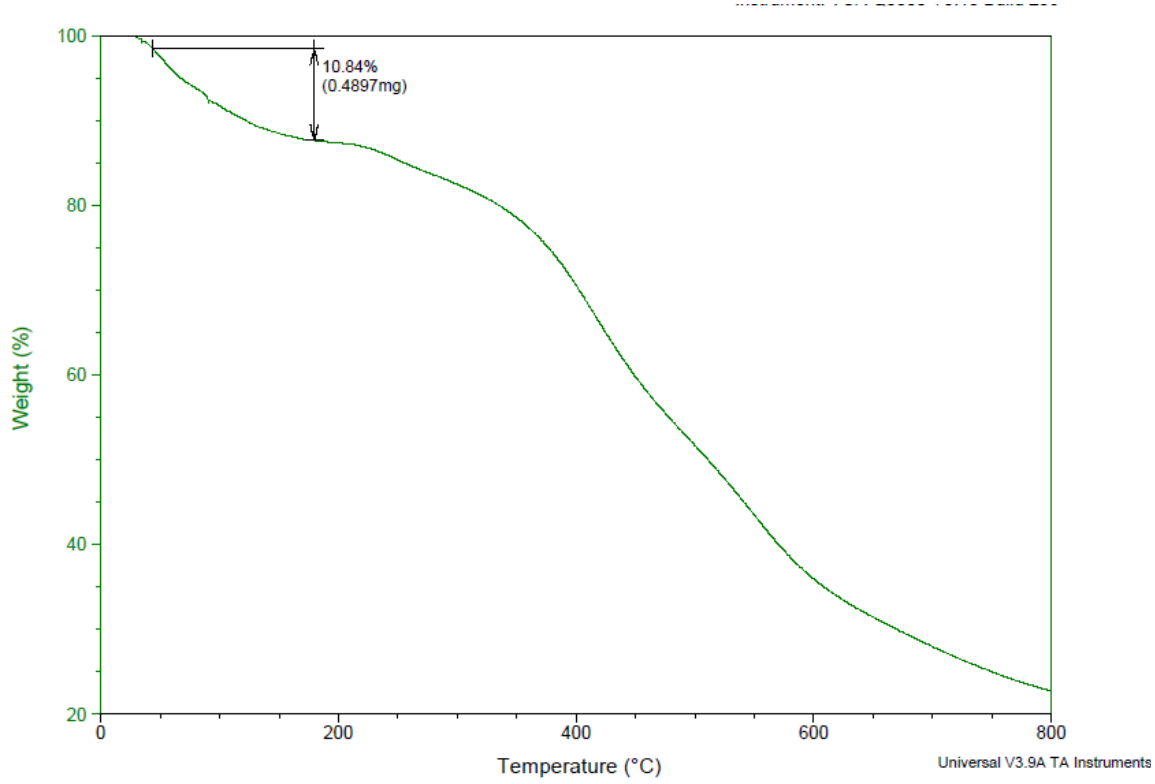

Chart S1: TGA curve of methyl guanidinium borohydride (MGB)

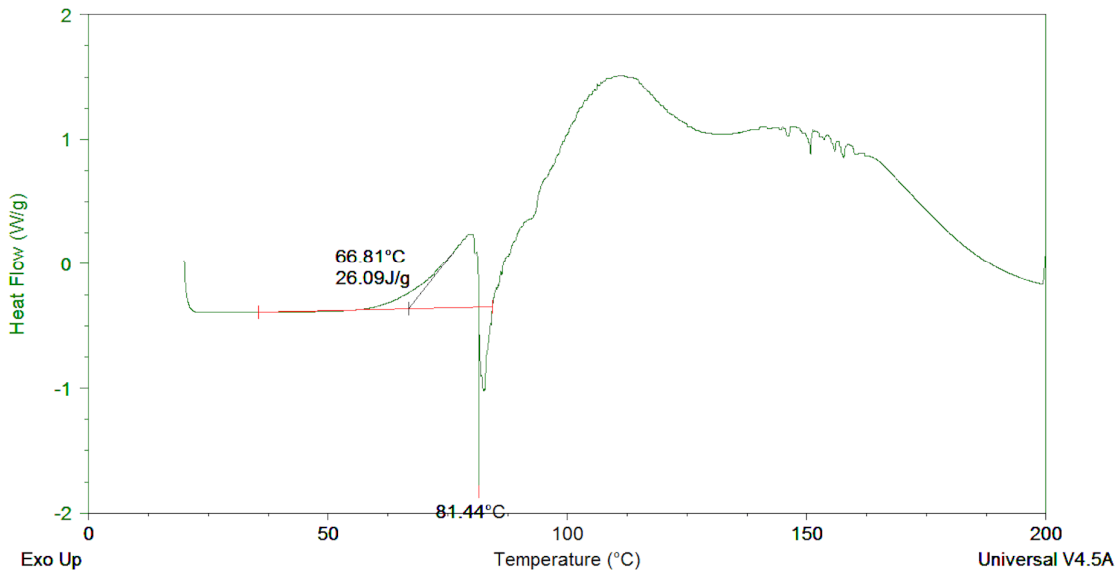

Chart S2: DSC Curve of methyl guanidinium borohydride (MGB).

GB:

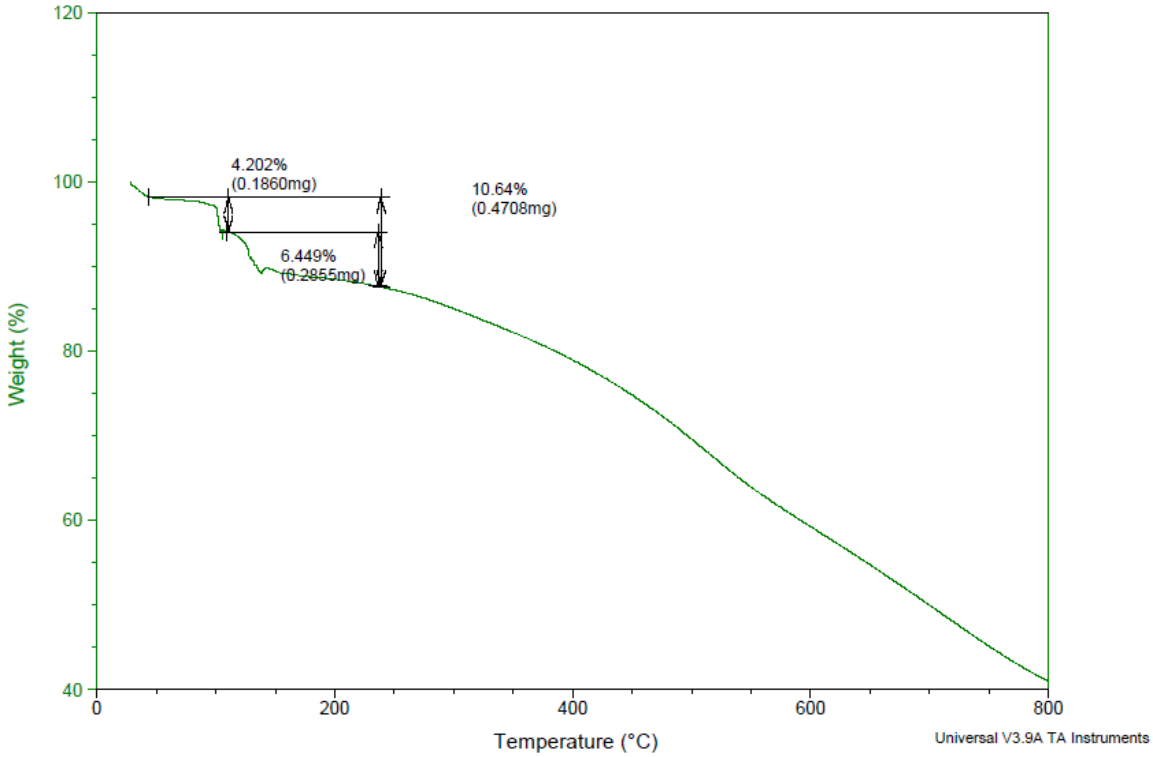

Chart S3: TGA curve of Guanidinium Borohydride (GB)

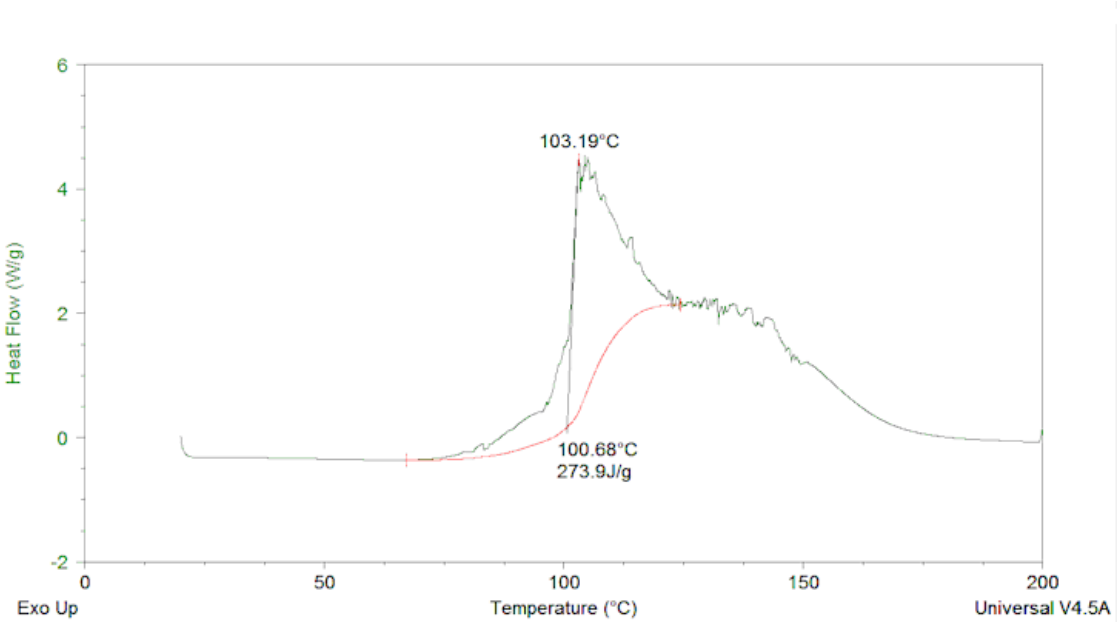

Chart S4: DSC curve of guanidinium borohydride (GB).

ESI-MS

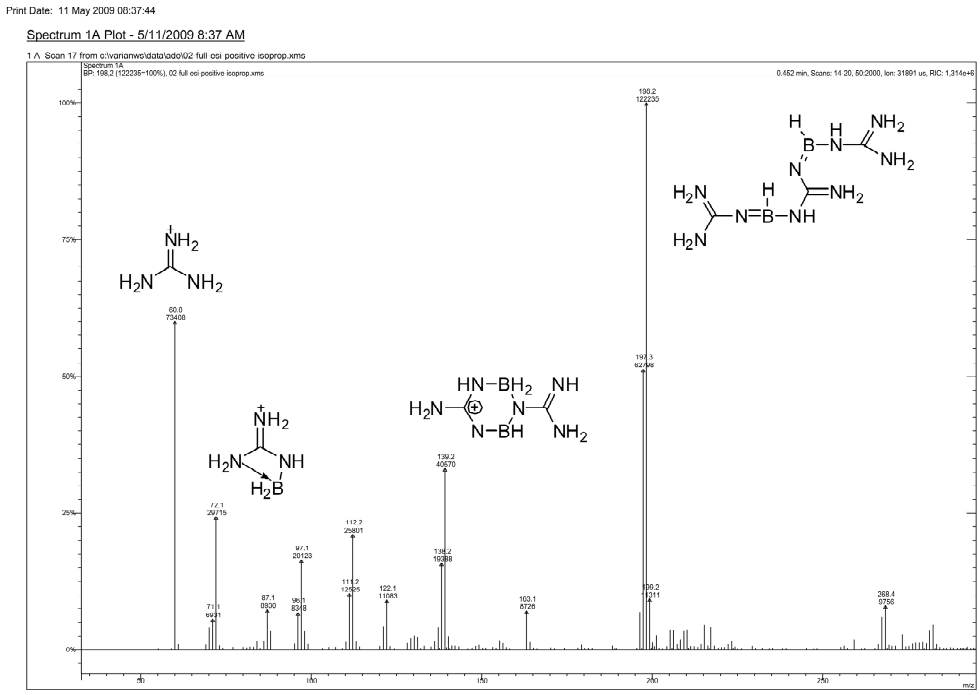

Chart S5: ESI-MS Spectra of the dehydrogenation products of GB**.**

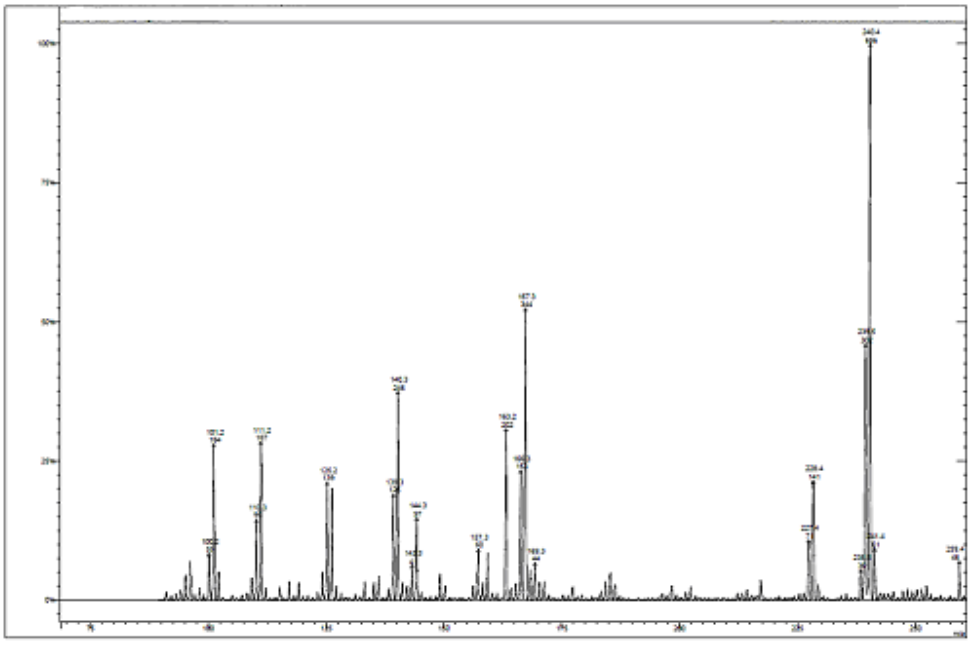

Chart S6: ESI-MS spectrum of the dehydrogenation products of MGB

Kinetic studies

In a typical experiment, $(PPh_3)_3RhCl$ (12.3 mg, 1 mol %) or $FeCl_2$ (13 mg, 1 mol %) and $(PPh_3)_3RhCl$ (1.2 mg, 0.1 mol %) or $FeCl_2$ (3.3 mg, 2 mol %) were dissolved in diglyme (2 ml, dried) in a 25 mL two-necked round-bottom flask and heated to 75 °C. The flask was stopped with a tight-fitting rubber septum. A solution of MGB (0.1 g, 1.33 mmol) in diglyme (1.5 mL) was transferred via syringe to the stirred catalyst solution heated at 75 °C.

The same experiment with $(PPh_3)_3RhCl$ (12.3 mg, 1 mol %) or $FeCl_2$ (13 mg, 1 mol %) was repeated for GB (0.1 g, 1.12 mmol) in diglyme (0.5 mL).

Immediate vigorous gas evolution was observed. The hydrogen gas was collected in a separating-funnel filled with $MgCl_2$ (aq. sat.) connected to a burette. The volume of collected hydrogen gas was measured periodically until the reaction was completed (Table a-e).

Table a. Equivalents of hydrogen collected compared with the original amount of GB using 1 mol % Wilkinsons Catalyst

Equiv. H_2 Collected	Time (min)
0	0
1.006	1
1.844	3
2.347	6
2.516	10
2.851	20
3.521	60
3.857	110
3.857	180

Table b. Equivalents of hydrogen collected compared with the original amount of GB using 2 mol % $FeCl_2$

Equiv. H_2 Collected	Time (min)
0	0
0.503	1
0.839	3
1.175	6
1.342	10
1.678	20

2.014	100
2.014	180

Table c. Equivalents of hydrogen collected compared with the original amount of MGB using 1 mol % Wilkinson`s Catalyst

Equiv. H_2 Collected	Time (min)
0	0
1.03	1
1.58	3
1.98	6
2.26	10
2.50	20
2.78	40
2.90	100

Table d. Equivalents of hydrogen collected compared with the original amount of MGB using 1 mol % $FeCl_2$

Equiv. H_2 Collected	Time (min)
0	0
0.97	1
1.19	3
1.58	6
1.78	10
2.18	20
2.38	40
2.46	100

Table e. Equivalents of hydrogen collected compared with the original amount of MGB by thermal decomposition

Equiv. H_2 Collected	Time (min)
0	0
0.51	1
0.79	3
0.99	6
1.23	10
1.50	20
1.74	40
2.18	100

MAS ^{11}B NMR spectroscopy

The precipitated solid resultinf from the thermal decomposition of MGB was rinsed several times with dry THF and the solid state ^{11}B NMR spectroscopy performed.

$^{11}B\{^1H\}$ NMR (300 MHz, solid) δ(B) = - 2 ppm, - 27 ppm, - 39 ppm

The precipitated solid resulting from the catalytic or thermal decomposition of GB was rinsed several times with dry diglyme and the solid state ^{11}B NMR spectroscopy performed.

Thermal

$^{11}B\{^1H\}$ NMR (300 MHz, solid) δ(B) = - 4 ppm, - 39 ppm

Elemental analysis (found): C: 17.34 %, H: 8.23 %, N: 46.31 %

$FeCl_2$

$^{11}B\{^1H\}$ NMR (300 MHz, solid) δ(B) 9 ppm, - 4 ppm, - 8 ppm, - 15 ppm, -28 ppm, - 39 ppm

$(PPh_3)_3RhCl$

$^{11}B\{^1H\}$ NMR (300 MHz, solid) δ(B) 9 ppm, - 4 ppm, - 8 ppm, - 15 ppm, - 28 ppm, - 39 ppm

Synthesis of Guanidinium octahydrotriborate (GOTB)

Sodium octahydrotriborate (1.44 g, 22.73 mmol) and guanidinium hydrochloride (2.28 g, 24 mmol) were suspended in isopropanol (20 mL) at room temperature in a 50 mL round-bottom flask. Under a flow of argon, the reaction was stirred for 18 h; the suspension turned to a homogenous particle distribution and the organic phase was removed by filtration under inert gas. The solvent was removed under reduced pressure and washed twice with 10 ml of diethyl ether, giving pure GOTB (81 %) as a white solid.

$^{11}B\{^{1}H\}$ NMR (300 MHz, CD_2Cl_2) δ(ppm) = – 25.88 (sept, B_3H_8, J_{B-H} = 32.78 Hz)

^{1}H NMR (300 MHz, CD_2Cl_2) δ(ppm) = - 0.12 (n, B_3H_8, J_{-H} = 32.78 Hz), δ 6.93 (s, 6H, NH_2)

Elemental Analysis:

	Measured (%)	Calculated (%)
C:	12.30	11.94
H:	14.78	14.03
N:	40.82	41.78

Synthesis of sodium octahydrotriborate

In an autoclave, sodiumborohydride (22.73 mmol) was added to a 50 ml one molar solution of THF-BH_3 (50 mmol). The mixture was heated at 70 °C for 6 h. The pressure was increased due to hydrogen generation. The solvent and nonreactive THF-BH_3 was removed under reduced pressure and washed twice with 10 ml of diethyl ether, giving pure sodium octahydrotriborate.

^{1}H NMR (300 MHz, THF-D_8) δ(ppm) = 0.07 (m, B_3H_8, J_{-H} = 32.31 Hz)
$^{11}B\{^{1}H\}$ NMR (300 MHz, THF-D_8) δ(ppm) = – 27.89 (n, B_3H_8, J_{B-H} = 32.31 Hz)

2.9 Literature

1) D. M. Heinekey, A. Lledos, J. M. Lluch, Chem. Soc. Rev. 33, 175 (2004).
2) G. S. McGrady, G. Guilera, Chem. Soc. Rev. 32, 383 (2003).
3) P. G. Jessop, R.H. Morris, Coord. Chem. Rev. 121, 155 (1992).
4) J. K. Burdett, O. Eisenstein, S. A. Jackson, in Transition Metal Hydrides: Recent advances in Theory and Experiment, A. Dedieu, Ed. (VCH, New York, 1991), P. 149.
5) R.H. Crabtree, Acc. Chem. Res. 23, 95 (1990).
6) G. J. Kubas, Acc. Chem. Res. 21, 120 (1988).
7) P. E. M. Siegbahn, Adv. Inorg. Chem. 56, 101 (2004).
8) M. Felderhoff, C. Weidenthaler, R. von Helmolt, U. Eberle, Phys. Chem. Phys., 9, 2643-2653 (2007); http://www.rsc.org/ej/CP/2007/b701563c.pdf
9) L. Schlapbach, MRS Bull. 2002, 27, 675).
10) (a) "Hydrogen Storage Materials Workshop Proceedings", United States Department of Energy, August 14 – 15, 2002. http://www.eere.energy.gov/hydrogenandfuelcells/pdfs/h2_stor_mat_-work_proceedings.pdf;

    b) "Basic Research Needs for the Hydrogen Economy", United States Department of Energy, report of the Basic Energy Sciences Workshop on Hydrogen Production, Storage, and Use, May 13 – 15, 2003. http://www.sc.doe.gov/ bes/hydrogen.pdf;

    c) E. Tzimas, C. Filiou, S. D. Peteves, J. B. Veyret, "Hydrogen Storage: State-of-the-Art and Future Perspective", European Commission DG JRC Institute for Energy, Petten 2003. http://www.jrc.nl/publ/2003_publ.html).
11) B. Wicke, presentation for the Hydrogen Storage Materials Workshop, United States Department of Energy, Argonne, IL, August 14 – 15, 2002.)
12) Kamiya, I.; Mori, R.; Kudo, M. Compressed Hydrogen Tank for Fuel Cell Vehicle. JP67457, Aug 31, 2007.
13) A. W. C. van den Berg and C. O. Area ´n, Chem. Commun., 2008,668.
14) A. D. Leonard, J. L. Hudson, H. Fan, R. Booker, L. J. Simpson, K. J. O'Neill, P. A. Parilla, M. J. Heben, M. Pasquali, C. Kittrell, J. M. Tour, J. Am. Chem. Soc., 2009, 131 (2), 723-728
15) G. G. Tibbetts, G. P. Meisner and C. H. Olk, Carbon, 2001, 39, 2291
16) J. Dong, X. Wang, H. Xu, Q. Zhao and J. Li, Int. J. Hydrogen Energy, 2007, 32, 4998

17) Z. Yang, Y. Xia and R. Mokaya, J. Am. Chem. Soc., 2007, 129,1673

18) a) P. M. Budd, A. Butler, J. Selbie, K. Mahmood, N. B. McKeown, B. Ghanem, K. Msayib, D. Book and A. Walton, Phys. Chem. Chem. Phys., 2007, 9, 1802; b) N. B. McKeown and P. M. Budd, Chem. Soc. Rev., 2006, 35, 675.

19) J.-Y. Lee, C. D. Wood, D. Bradshaw, M. J. Rosseinsky and A. I. Cooper, Chem. Commun. , 2006, 2670.

20) B. Bogdanovi´c, M. Schwickardi, J. Alloys Compd. 253, 1997, 1

21) a) L. Zaluski, A. Zaluska, J.O. Ström-Olsen, J. Alloys Compd. 290 (1999) 71. b) B. Bogdanovic, R.A. Brand, A. Marjanovic, M. Schwickardi, J. Tölle, J. Alloys Compd. 302 (2000) 36. c) R.A. Zidan, S. Takara, A.G. Hee, C.M. Jensen, J. Alloys Compd. 285 (1999) 119. d) G. Sandrock, K. Gross, G. Thomas, J. Alloys Compd. 339 (2002) 299.

22) S. Orimo, Y. Nakamori, J. R. Eliseo, A. Zu¨ ttel and C. M. Jensen, Chem. Rev., 2007, 107, 4111.

23) P. Chen, Z. Xiong, J. Luo, J. Lin and K. L. Tan, Nature, 2002, 420, 302

24) Renaudin, G.; Gomes, S.; Hagemann, H.; Keller, L.; Yvon, K. J.Alloys Compd. 2004, 375, 98.

25) Muller, A.; Havre, L.; Mathey, F.; Petit, V. I.; Bensoam. J. U.S. Patent 4,193,978, 1980.

26) E. Rönnebro and E. H. Majzoub, J. Phys. Chem. B, 2007, 111, 12045.

27) G. Soloveichik, J.-H. Her, P. W. Stephens, Y. Gao, J. Rijssenbeek, M. Andrus and J.-C. Zhao, Inorg. Chem., 2008, 47, 4290

28) G. H. Spikes, J. C. Fettinger and P. P. Power, J. Am. Chem. Soc., 2005, 127, 12232; Y. Peng, B. D. Ellis, X. Wang and P. P. Power, J. Am. Chem. Soc., 2008, 130, 12268.

29) O. Ciobanu, P. Roquette, S. Leingang, H. Wadepohl, J. Mautz and H.-J. Himmel, Eur. J. Inorg. Chem., 2007, 4530.

30) G. D. Frey, V. Lavallo, B. Donnadieu, W. W. Schoeller and G. Bertrand, Science, 2007, 316, 439

31) G. C. Welch, R. R. San Juan, J. D. Masuda and D. W. Stephan, Science, 2006, 314, 1124; Y. Guo and S. Li, Inorg. Chem., 2008, 47, 6212.

32) a) V. Sumerin, F. Schulz, M. Nieger, M. Leskela¨, T. Repo and B. Rieger, Angew. Chem., Int. Ed., 2008, 47, 6001; b) V. Sumerin, F. Schulz, M. Atsumi, C.Wang, M. Nieger,M. Leskela¨, T. Repo, P. Pyykko¨ and B. Rieger, J. Am. Chem. Soc., 2008, 130, 14117.

33) B. R. Hoffmann, J. Chem. Phys., 1964, 40, 2474

34) A. Doroodian, J. E. Dengler, A. Genest, N. Rösch, B. Rieger, Angewandte Chemie 2010, 122, 1915-1917,
35) L. R. Grant and J. E. Flanagan, US Pat., 4 381 206, 1983.
36) F. C. Gunderloy, Jr, B. Spielvogel and R. W. Parry, Inorg. Synth., 1967, 9, 13.
37) H. J. Emeleus and F. G. A. Stone, J. Chem. Soc., 1951, 840.
38) G. Kodama, R. W. Parry and J. C. Carter, J. Am. Chem. Soc., 1959, 81, 3534
39) W. Yoon and L. G. Sneddon, J. Am. Chem. Soc., 2006, 128, 13992
40) C. E. Nordman and C. Reimann, J. Am. Chem. Soc., 1959, 81, 3538.
41) W. V. Hough and J. M. Makhlouf, US Pat., 3 313 603, 1967.
42) J. E. Flanagan, US Pat., 4 166 843, 1979.
43) J. Williams, R. L. Williams and J. C. Wright, J. Chem. Soc., 1963, 5816
44) T. Yogo and S. Naka, J. Mater. Sci., 1990, 25, 374.
45) M. F. Hawthorne, S. S. Jalisatgi and A. Safronov, University of Missouri-Columbia's Progress Towards Chemical Hydrogen Storage Using Polyhedral Borane Anion Salts, DoE Hydrogen Annual Progress Report, 2007 (http://www.hydrogen.energy.gov/pdfs/progress07/iv_b_5d_hawthorne.pdf)
46) H. Nöth and H. Beyer, Chem. Ber., 1960, 93, 928.
47) B. Carboni and L. Monnier, Tetrahedron, 1999, 55, 1197
48) A. Staubitz, M. Besora, J. N. Harvey and I. Manners, Inorg.Chem., 2008, 47, 5910.
49) J. Dengler Dissertation: Hydrolytic Activation of Small Molecules Using Functional Catalysts.d
50) C. W. Hamilton, R. T. Baker, A. Staubitz, I. Manners, Chem. Soc. Rev. 2009, 38, 279–293.
51) P. A. Storozhenko, R. A. Svitsyn, V. A. Ketsko, A. K. Buryak and A. V. Ul'yanov, Russ. J. Inorg. Chem. (Transl. of Zh. Neorg. Khim.), 2005, 50, 980
52) M. Diwan, V. Diakov, E. Shafirovich and A. Varma, Int. J. Hydrogen Energy, 2008, 33, 1135.
53) a) H. C. Kelly, F. R. Marchelli and M. B. Giutso, Inorg. Chem.,1964, 3, 431; b) G. E. Ryschkewitsch, J. Am. Chem. Soc., 1960, 82, 3290; c) G. E. Ryschkewitsch and E. R. Birnbaum, J. Phys. Chem.,1961, 65, 1087; d) G. E. Ryschkewitsch and E. R. Birnbaum, Inorg. Chem., 1965, 4, 575; e) H. C. Kelly and V. B. Marriott, Inorg. Chem., 1979, 18, 2875; f) A. D'Ulivo, M. Onor and E. Pitzalis, Anal.Chem., 2004, 76, 6342.

54) a) M. Couturier, B. M. Andresen, J. L. Tucker, P. Dube´ , S. J. Brenek and J. T. Negri, Tetrahedron Lett., 2001, 42, 2763. b) M. Couturier, J. L. Tucker, B. M. Andresen, P. Dube´, S. J. Brenek and J. T. Negri, Tetrahedron Lett., 2001, 42, 2285. c) M. Couturier, J. L. Tucker, B. M. Andresen, P. Dube´ and J. T. Negri, Org. Lett., 2001, 3, 465; d) M. Couturier, B. M. Andresen, J. B. Jorgensen, J. L. Tucker, F. R. Busch, S. J. Brenek, P. Dube´ , D. J. am Ende and J. T. Negri, Org. Process Res. Dev., 2002, 6, 42. e) M. Chandra and Q. Xu, J. Power Sources, 2006, 156, 190. f) Q. Xu and M. Chandra, J. Power Sources, 2006, 163, 364. g) T. J. Clark, G. R. Whittell and I. Manners, Inorg. Chem., 2007, 46, 7522. h) P. V. Ramachandran and P. D. Gagare, Inorg. Chem., 2007, 46, 7810. i) S. B. Kalidindi, M. Indirani and B. R. Jagirdar, Inorg. Chem., 2008, 47, 7424. j) F. Cheng, H. Ma, Y. Li and J. Chen, Inorg. Chem., 2007, 46, 788. k) J.-M. Yan, X.-B. Zhang, S. Han, H. Shioyama and Q. Xu, Angew. Chem., Int. Ed., 2008, 47, 2287

55) F. Cheng, H. Ma, Y. Li and J. Chen, Inorg. Chem., 2007, 46, 788

56) D. A. Dixon and M. Gutowski, J. Phys. Chem. A, 2005, 109, 5129.

57) J. Zhang, S. Zhang and Q. S. Li, J. Mol. Struct. (THEOCHEM), 2005, 717, 33; Q. S. Li, J. Zhang and S. Zhang, Chem. Phys. Lett., 2005, 404, 100.

58) M. T. Nguyen, V. S. Nguyen, M. H. Matus, G. Gopakumar and D. A. Dixon, J. Phys. Chem. A, 2007, 111, 679.

59) J. Li, S. M. Kathmann, G. K. Schenter and M. Gutowski, J. Phys. Chem. C, 2007, 111, 3294; D. Jacquemin, E. A. Perpe` te, V. Wathelet and J.-M. Andre´ , J. Phys. Chem. A, 2004, 108, 9616.

60) M. H. Matus, K. D. Anderson, D. M. Camaioni, S. T. Autrey and D. A. Dixon, J. Phys. Chem. A, 2007, 111, 4411.

61) C. R. Miranda and G. Ceder, J. Chem. Phys., 2007, 126, 184703.

62) M. P. Brown, R. W. Heseltine and L. H. Sutcliffe, J. Chem. Soc. A, 1968, 612.

63) E. Framery and M. Vaultier, Heteroat. Chem., 2000, 11, 218.

64) O. T. Beachley, Inorg. Chem., 1967, 6, 870; M. E. Bowden, I. W. M. Brown, G. J. Gainsford and H. Wong, Inorg. Chim. Acta, 2008, 361, 2147.

65) a) M. G. Hu, R. A. Geanangel and W. W. Wendlandt, Thermochim. Acta, 1978, 23, 249; b) R. A. Geanangel and W. W. Wendlandt, Thermochim. Acta, 1985, 86, 375; c) V. Sit, R. A. Geanangel and W. W. Wendlandt, Thermochim. Acta, 1987, 113, 379; d)

G. Wolf, J. Baumann, F. Baitalow and F. P. Hoffmann, Thermochim. Acta, 2000, 343, 19; e) F. Baitalow, J. Baumann, G. Wolf, K. Jaenicke- Ro¨ sler and G. Leitner, Thermochim. Acta, 2002, 391, 159; f) J. Baumann, F. Baitalow and G. Wolf, Thermochim. Acta, 2005, 430, 9.

66) J. D. Carpenter and B. S. Ault, Chem. Phys. Lett., 1992, 197, 171.

67) A. C. Stowe, W. J. Shaw, J. C. Linehan, B. Schmid and T. Autrey, Phys. Chem. Chem. Phys., 2007, 9, 1831; M. Bowden, T. Autrey, I. Brown and M. Ryan, Curr. Appl. Phys., 2008, 8, 498.

68) S. De Benedetto, M. Carewska, C. Cento, P. Gislon, M. Pasquali, S. Scaccia and P. P. Prosini, Thermochim. Acta, 2006, 441, 184.

69) A. Gutowska, L. Li, Y. Shin, C. M.Wang, X. S. Li, J. C. Linehan, R. S. Smith, B. D. Kay, B. Schmid, W. Shaw, M. Gutowski and T. Autrey, Angew. Chem., Int. Ed., 2005, 44, 3578.

70) A. M. Feaver, S. Sepehri, P. J. Shamberger, A. C. Stowe, T. Autrey and G. Cao, J. Phys. Chem. B, 2007, 111, 7469

71) J. S. Wang and R. A. Geanangel, Inorg. Chim. Acta, 1988, 148, 185; W. J. Shaw, J. C. Linehan, N. K. Szymczak, D. J. Heldenbrandt, C. Yonker, D. M. Camaioni, R. T. Baker and T. Autrey, Angew. Chem., Int. Ed., 2008, 47, 7493.

72) M. E. Bluhm, M. G. Bradley, R. Butterick III, U. Kusari and L. G. Sneddon, J. Am. Chem. Soc., 2006, 128, 7748

73) F. H. Stephens, R. T. Baker, M. Hernandez-Matus, D. J. Grant and D. A. Dixon, Prepr. Pap. - Am. Chem. Soc., Div. Fuel Chem., 2006, 51, 573.

74) L. G. Sneddon, Amineborane Hydrogen Storage - New Methods for Promoting Amineborane Dehydrogenation- /Regeneration Reactions, DoE Hydrogen Annual Progress Report, 2007 (http://www.hydrogen.energy.gov/pdfs/progress07/iv_b_5e_sneddon.pdf).

75) L. G. Sneddon, Amineborane Based Chemical Hydrogen Storage, DoE Hydrogen Annual Merit Review, 2007 (http://www.hydrogen.energy.gov/pdfs/review07/st_27_sneddon.pdf).]

76) Y. D. Blum and R. M. Laine, US Pat., 4 801 439, 1989.

77) I. G. Green, K. M. Johnson and B. P. Roberts, J. Chem. Soc., Perkin Trans. 2, 1989, 1963.

78) Y. Jiang and H. Berke, Chem. Commun., 2007, 3571.
79) C. A. Jaska, K. Temple, A. J. Lough and I. Manners, Chem. Commun., 2001, 962; C. A. Jaska, K. Temple, A. J. Lough and I. Manners, J. Am. Chem. Soc., 2003, 125, 9424; C. A. Jaska and I. Manners, J. Am. Chem. Soc., 2004, 126, 9776.
80) Y. Chen, J. L. Fulton, J. C. Linehan and T. Autrey, J. Am. Chem. Soc., 2005, 127, 3254; J. L. Fulton, J. C. Linehan, T. Autrey, M. Balasubramanian, Y. Chen and N. K. Szymczak, J. Am. Chem. Soc., 2007, 129, 11936.
81) R. J. Keaton, J. M. Blacquiere and R. T. Baker, J. Am. Chem. Soc., 2007, 129, 1844.
82) Enders' carbene: 1,3,4-triphenyl-4,5-dihydro-1H-1,2,4-triazol-5- ylidene; IMes: 1,3-bis(2,4,6-trimethylphenyl)-1,3-dihydro-2Himidazol- 2-ylidene; IDipp: 1,3-bis(2,6-diisopropylphenyl)-1,3-dihydro- 2H-imidazol-2-ylidene.
83) T. J. Clark, C. A. Russell and I. Manners, J. Am. Chem. Soc., 2006, 128, 9582.
84) D. Pun, E. Lobkovsky and P. J. Chirik, Chem. Commun., 2007, 3297.
85) POCOP is k3-2,6-[OP(t-Bu)2]2C6H3.
86) M. C. Denney, V. Pons, T. J. Hebden, D. M. Heinekey and K. I. Goldberg, J. Am. Chem. Soc., 2006, 128, 12048.
87) Crestani, M. G.; Munoz-Hernandez, M.; Arevalo, A.; Acosta-Ramirez, A.; Garcia, J. J. J. Am. Chem. Soc. 2005, 127, 18066; Kawano, Y.; Haskiva, M.; Shimoi, M. Organometallics 2006, 25, 4420.
88) P. M. Budd, A. Butler, J. Selbie, K. Mahmood, N. B. McKeown, B. Ghanem, K. Msayib, D. Book and A. Walton, Phys. Chem. Chem. Phys., 2007, 9, 1802; N. B. McKeown and P. M. Budd, Chem. Soc. Rev., 2006, 35, 675.
89) A. Paul, C. B. Musgrave Angew. Chem. Int. Ed. 2007, 46, 8153 –8156
90) P. V. Ramachandran and P. D. Gagare, Inorg. Chem., 2007, 46, 7810.
91) L. G. Sneddon, Amineborane Based Chemical Hydrogen Storage, DoE Hydrogen Annual Merit Review, 2007 (http://www.hydrogen. energy.gov/pdfs/review07/st_27_sneddon.pdf).;;; S. Hausdorf, F. Baitalow, G. Wolf and F. O. R. L. Mertens, Int. J. Hydrogen Energy, 2008, 33, 608.
92) S. Hausdorf, F. Baitalow, G. Wolf and F. O. R. L. Mertens, Int. J. Hydrogen Energy, 2008, 33, 608.
93) F. M. Taylor and J. Dewing, US Pat., 3 103 417, 1963.
94) Jeffrey, G. A. An Introduction to Hydrogen Bonding; Oxford University Press:

Oxford, 1997.
95) Jeffrey, G. A.; Saenger, W. Hydrogen Bonding in Biological Structures; Springer-Verlag: Berlin, 1991.
96) Calhorda, M. J. Chem. Commun. 2000, 801.
97) Shubina, E. S.; Belkova, N. V.; Epstein, L. M. J. Organomet. Chem. 1997, 536-537, 17.
98) Crabtree, R. H.; Siegbahn, P. E. M.; Eisenstein, O.; Rheingold, A. L.; Koetzle, T. F. Acc. Chem. Res. 1996, 29, 348.
99) Crabtree, R. H. J. Organomet. Chem. 1998, 577, 111.
100) Alkorta, I.; Rozas, I.; Elguero, J. Chem. Soc. Rev. 1998, 27, 163.
101) Crabtree, R. H. Science 1998, 282, 2000.
102) Crabtree, R. H.; Eisenstein, O.; Sini, G.; Peris, E. J. Organomet. Chem. 1998, 567, 7-10.
103) Kelly, P.; Loza, M. Chem. Britain 1999, 35, 26.
104) Shubina, E. S.; Bachmutova, E. V.; Saitkulova, L. N.; Epstein, L. M. Mendeleev Commun. 1997, 83.
105) Epstein, L. M.; Shubina, E. S.; Bakhmutova, E. V.; Saitkulova, L. N.; Bakhmutov, V. I.; Chistyakov, A. L.; Stankevich, I. V. Inorg. Chem. 1998, 37, 3013.
106) Shubina, E. S.; Belkova, N. V.; Bakhmutova, E. V.; Saitkulova, L. N.; Ionidis, A. V Epstein, L. M. Russ. Chem. Bull. 1998, 47, 817.
107) CALABRESE, J., C.; GAINES, D. F.; HILDEBRANDT, S., J.; MORRIS, H. J. Am. Chem. SOC. 98, 1976, 5490.
108) M. P. Stracke, G. Ebeling, R. Catalun˜a, J. Dupont, Energy & Fuels, Vol. 21, No. 3, 2007.
109) L. V. Titov, M. D. Levicheva, Zh. Neorg. Khim. 1969, 14, 2886-2887.
110) L. V. Titov, M. D. Levicheva, G. N. Dubikhina, Zh. Neorg. Khim 1972, 17, 1181-1182.
111) a) R. Custelcean, J. E. Jackson, Chem. Rev. 2001, 101, 1963−1980.
b) T. J. Groshens, A. R. Hollins, Chem. Commun. 2009, 3089–3091.
112) a) R. Ahlrichs, M. Bär, M. Häser, H. Horn, C. Kölmel, Chem. Phys. Lett. 1989, 162, 165-169. b) F. Weigend, M. Häser, Theor. Chem. Acc. 1997, 97, 331- 340. c) M. Kollwitz, J. Gauss, Chem. Phys. Lett. 1996, 260, 639-646.

113) A. Schäfer, C. Huber, R. Ahlrichs, J. Chem. Phys. 1994, 100, 5829-5835.

114) G. Rasul, G. K. S. Prakash, G. A. Olah, Inorg. Chem. 1999, 38, 44-47; G. Rasul, G. K. S. Prakash, G. A. Olah, J. Mol. Struct. 2007, 818, 65-70; G. Rasul, G. K. S. Prakash, G. A. Olah, Inorg. Chem. 1999, 38, 44-47.

115) Titov, L. V.; Levicheva, M. D.; Dubikhina, G. N. Izvestiya Akademii Nauk SSSR, Seriya Khimicheskaya (1976), (8) 1856-9.

116) PETERS,C., R.; NORDMAN, C., E. J. Am. Chem. SOC. 82, 1960, 5758.

117) LIPPARD, S., . J.; MELMED, K. M. Inorg. Chem. 8, 1969, 2755.

118) ANDREWS, S., J.; WELCH, A., J.; JACOBSEN, G., B; M ORRIS, J., H. J. Chem SOC.,Chem. Commun. 1982, 749.

119) ANDREWS, S., J.; WELCH, A., J. Inorg. Chim. Acta 88, 1984, 153.

120) Deiseroth, H. J.; Sommer, O.; Binder, H.; Wolfer, K.; Frei, B. Zeitschrift fuer Anorganische und Allgemeine Chemie (1989), 571 21-8.

Chapter 3

Ionic Liquids

3.1 Introduction

The concept of ionic liquid (ILs) began in 1914 with an observation by Paul Walden, who reported the physical properties of ethylammonium nitrate ($[EtNH_3][NO_3]$ (mp 13–14 °C).[1]

Ionic liquids are most commonly defined as materials that are composed of cations and anions which melt at or below 100 °C. This temperature causes any chemical change.

After two decades of silence, ionic liquids appeared in a patent from 1934, which claimed that when halide salts of nitrogen-containing bases (such as 1-benzylpyridinium chloride, 1-ethylpyridinium chloride, etc.) were mixed with cellulose at temperatures above 100 °C, the cellulose was dissolved.[2]

After several years, ILs remerged in the patent literature[3] and afterwards in open literature[4], which described the application of mixture of aluminium chloride and 1-ethylpyridinium bromide to electrodeposition of aluminium.

In 1975, Osteryoung[5] and Gilbert[6] studied the chemical and physical properties of ILs made from 1-butylpyridinium chlorides and aluminium chloride. The room temperature liquid (20 °C) range occurs between about 60 and 67% mol per cent of aluminium chloride. The fundamental properties and application of the IL were reported; these were patented by United State Air Force. This report was a real breakthrough in the field, but unfortunately, the cation was easily reduced to use as battery electrolytes.

Wilkes and Hussey used computational studies to predict the LUMO energies for about 60 heterocyclic cations, and then correlated these with extant reduction potentials.[7] The result was a prediction that 1,3-dialkylimidazolium cations would be substantially more stable in reduction than the 1-alkylpyridinium cations. This led to the synthesis of the now archetypal ionic liquid system, $[C_2mim]Cl–AlCl_3$, and its subsequent characterisation.[8-12]

The phase diagram of this system is illustrated in Fig. 44. It is immediately clear that the liquid range of this system is very wide. It is a low viscosity liquid at room temperature from $X(AlCl_3)$ = 0.33 to $X(AlCl_3)$ = 0.67, where $X(AlCl_3)$ is the mole fraction of the aluminium(III) chloride content, although it should be clearly noted that there is no uncomplexed aluminium(III) chloride present.

Fig.44 The phase diagram for the $[C_2mim]Cl–AlCl_3$ system

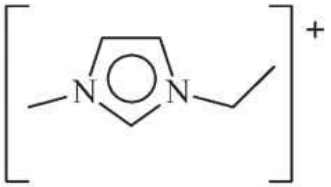

$[C_2mim]^+$

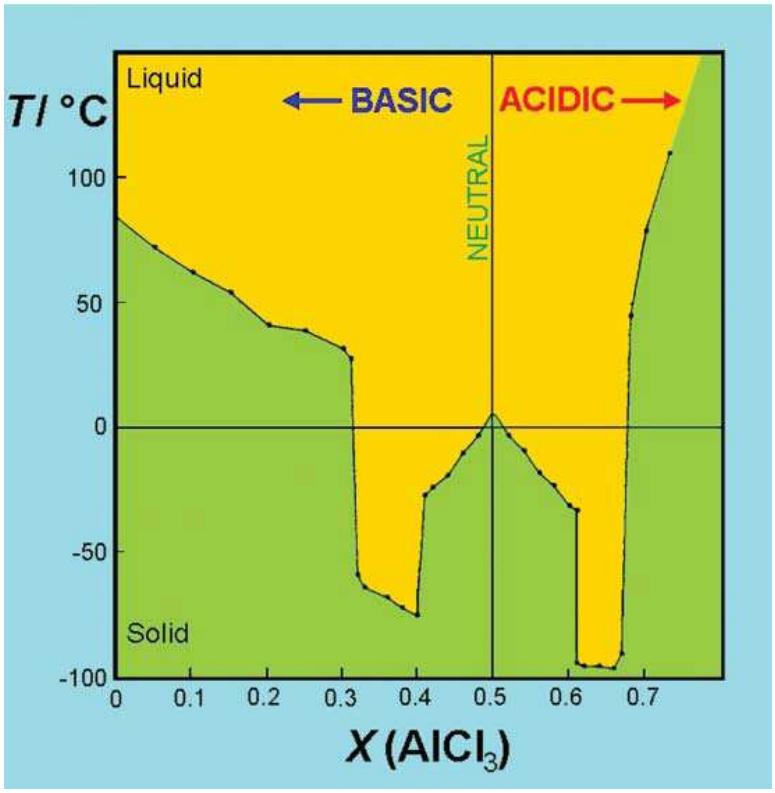

The IL is acidic $X(AlCl_3) > 0.5$, basic $X(AlCl_3) > 0.5$, or neutral $X(AlCl_3) = 0.5$ depending on the mole fraction of aluminium(III) chloride. The composition of the system depends on $X(AlCl_3)$ (Eq.9).

$$2[AlCl_4]^- \rightleftharpoons [Al_2Cl_7]^- + Cl^- \qquad \text{Eq. 9}$$

For very acidic systems, $X(AlCl_3) = 0.67–0.75$, a further equilibrium, Eq. (10), controls the anion concentration.

$$2\,[Al_2Cl_7]^- \rightleftharpoons [Al_3Cl_{10}]^- + [AlCl_4]^- \qquad \text{Eq. 10}$$

The $[Al_3Cl_{10}]^-$ anion has been detected by mass spectrometry.[13] Wilkes and Zaworotko reported[14] 1-ethyl-3-methylimidazolim based ILs containing a range of alternative anions such as $[CH_3CO_2]^-$, $[NO_3]^-$ or $[BF_4]^-$. These ILs are stable in the presence of air and moisture. Since 1992, a wide range of ILs has been developed containing many different anions, including hexafluorophosphate, ethanoate, trifluoroethanoate, sulfate, hydrogensulfate, alkylsulfate, nitrate, biscyanamide $[N(CN)_2]_2$, trifluoromethanesulfonate $[CF_3SO_3]_2$,bis{(trifluoromethyl)-sulfonyl}amide $[N(CF_3SO_2)_2]_2$, and tris{(trifluoromethyl)- sulfonyl}methanide $[C(CF_3SO_2)_3]_2$.

Over the years that followed, new classes of cations, based on phosphonium and pyrrolidinium were developed. It soon became clear that over one million simple ionic liquids could be synthesised.[15,16]

The melting points of inorganic salts are significantly above room temperature, thus they may be used as a medium for organic chemistry. Applying the understanding of lattice energies gained from the Kapustinskii equation,[17] the effect of increasing the size of the anion can be seen in Table 6.

Tab.6 Melting points of Group 1 chloroaluminates(III)

System	mol %	m.p./°C
$AlCl_3$	100	192
$LiCl\text{-}AlCl_3$	50-50	144
$NaCl\text{-}AlCl_3$	50-50	151
$KCl\text{-}AlCl_3$	50-50	256

The melting points of these simple tetrachloroaluminate(III) salts are in the range of the boiling points of high-boiling organic solvents. It is necessary to bring the melting point down even further. This can be done by increasing the size of the cations: replacing the simple inorganic cations with organic cations depresses the melting point to temperatures at or below room temperature. Moreover, the asymmetry of the cation has been long recognised[18] as an important factor in lowering the melting points. For example, salts of the 1-butyl-3-methylimidazolium cation (which has only C_1 symmetry) melt at lower temperatures (by about 100 °C) than the analogous salts of the 1-butylpyridinium cation (which has C_{2v} symmetry). Furthermore, conformational differences in the cations can frustrate crystallisation, leading to glass formation

and/or polymorphism.[19]

The effect of symmetry in melting points is also reflected in the higher melting points reported for 1,3-dimethylimidazolium and 1,3- diethylimidazolium salts in comparison with the more nonsymmetrical 1-ethyl-3-methylimidazolium or 1-butyl-3- methylimidazolium cation analogues.[20]

Most common ionic liquids are formed through the combination of an organic heterocyclic cation, such as dialkylimidazolium, and an inorganic or organic anion, such as nitrate or methanesulfonate. Typical cations and anions of ionic liquids, and their common abbreviations, are shown in Fig. 45. However, it should be remembered that, in principle, any singly charged cation or anion could be used.

Fig.45 Some commonly used ionic liquid systems

Most commonly used cations

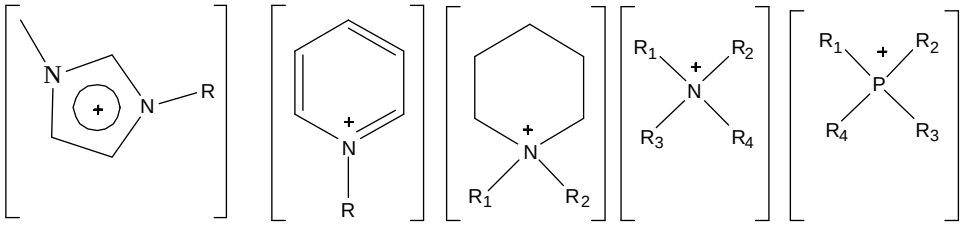

1-alkyl-3-methyl-imidazolium | N-alkyl-pyridinium | N-alkyl N-methyl piperidinium | Tetraalkyl ammonium | Tetraalkyl-phosphonium

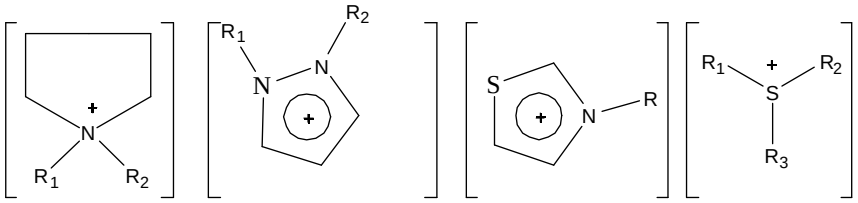

N-alkyl-N-methyl pyrrolidinium | 1,2-dialkyl-pyrazolinium | N-alkyl-thiazolium | Trialkyl-sulfonium

$R_{1,2,3,4} = CH_3(CH_2)_n$ (n = 1,3,5,7,9); aryl; etc.

Some possible anions

Water-immiscible ⟶ Water-miscible

$[PF_6]^-$	$[BF_4]^-$	$[CH_3CO_2]^-$
$[NTf_2]^-$	$[OTf]^-$	$[CF_3CO_2]^-$; $[NO_3]^-$
$[BR_1R_2R_3R_4]^-$	$[N(CN)_2]^-$	Br^-; Cl^-; I^-
		$[Al_2Cl_7]^-$; $[AlCl_4]^-$

Strong hydrogen bonds in the lattice influence melting point. In 1986, the presence of hydrogen bonding in the structures of 1-alkyl-3-methylimidazolium salt was reported.[21a] The report marked the first recognition of the existence of CH···X hydrogen bonds corresponding to the higher melting point in halogen containing ILs.

Since then, evidence for hydrogen bonding has been obtained from X-ray diffraction and mid-infrared and NMR spectroscopy. Local and directional interactions, such as hydrogen bonds, in imidazoliumbased ILs are indicated by shorter C-H···anion distances, redshifted C-H frequencies, and downfield-shifted C-H proton chemical shifts.[21b-l]

3.2 Metal-containing ionic liquids

In 1972, Parshall reported[22] the ILs of tetraalkylammonium chlorostannate with dissolved $PtCl_2$ as a reaction medium and catalyst for several homogeneous catalytic reactions of olefins. The interest in ILs as a reaction medium and catalyst increased after the success of Freidel–Crafts reaction in acidic [EMIM]Cl–$AlCl_3$ system.[23] Metal-containing ILs are potentially very useful as an ordered media, catalysts and catalyst precursors for chemical transformations.

The two isomorphous imidazolium salts $[EMIM]_2[MCl_4]$ (M=Co or Ni) with m.p. 90–100 °C were prepared directly by mixing the corresponding metal chloride with [EMIM]Cl under dry nitrogen atmosphere.[24] Crystal structure showed that extended hydrogen bonding networks were observed between the $[MCl_4]^{-2}$ chlorides and ring hydrogens (Fig. 46).

Fig.46 Local structure around a single cation in $[emim]_2[MCl_4]$

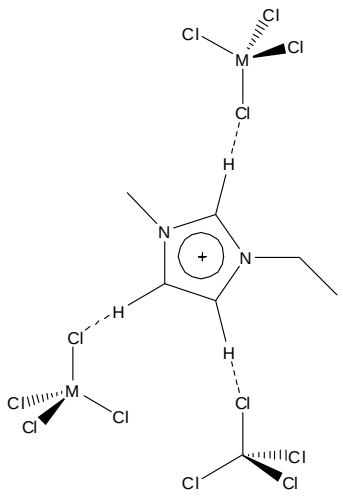

M = Ni, Co

Welton and co-workers reported[25] Vanadium-based salt $[EMIM]_2[VOCl_4]$, which was obtained from the reaction of [EMIM]Cl with $VOCl_2^-$ $(CH_3CN)_x$. In contrast to the crystal structures of similar compounds based on Ni and Co, no hydrogen bonding was detected.

Shreeve and co-workers found[26] that the reaction of mono or disubstituted (trimethyl-ammonium) ferrocene iodide with azole (imidazole or triazole) initially gave the ferrocene linked azoles.

Freeman and co-workers reported[27] ILs formed from [BMIM]Cl and $FeCl_2/FeCl_3$, in which $[BMIM][FeCl_4]/[Fe_2Cl_7]$, $[BMIM]_2[FeCl_4]$ and $[BMIM]/[Fe(II)/Fe(III)\text{-}Cl_n]$ were studied by Raman spectroscopy and ab initio calculations.

Furthermore, Sun et al.[28] demonstrated the use of [BMIM]Cl–$FeCl_3$ system for the alkylation of deuterated benzene with ethylene. A decrease in the intensity of 2-H of imidazolium ring after the reaction suggested that the proton for the initiation of the reaction was partly supplied by this 2-H of imidazolium ring.

Copper-based ILs were reported by Bolkan and Yoke.[29] Spectroscopic studies of mixture of [EMIM]Cl and CuCl showed that a broad variety such as $CuCl_3^{2-}$, $Cu_2Cl_3^-$, $CuCl^{4-}$, and polynuclear complexes $Cu_mCl_n^{-(n-m)}$ were formed.

Fernandez et. al. reported[55] the crystal structure of Bis(1-methylguanidinium) tetrachloro cuprate(II) (Fig. 47).

Fig.47 Molecular structure of Bis(1-methylguanidinium) tetrachloro cuprate(II)

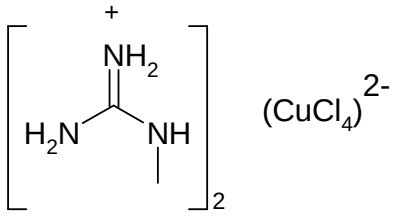

The geometry of the $[CuCl_4]^{2-}$ anion can be described as a flattened tetrahedron assuming the lowest energy structure for this kind of compound. Its symmetry in this case has a small deviation from D_{2d} (trans angle Cl-Cu-Cl = 130°) The N atoms help to keep the distorted geometry of the anion through several weak N-H···Cl bonds.

The use of $[EMIM]Cl/[ZnCl_2]$ ILs system in the electrodeposition of metals has been extensively studied by Sun and co-workers.[30] Mixing different ratios of [EMIM]Cl and $ZnCl_2$ produced

Lewis acidic ILs comprising [EMIM] cation with different chlorozincate anions ($ZnCl_3^-$, $Zn_2Cl_5^-$ and $Zn_3Cl_7^-$).

3.3 Scope of this work

As reported in chapter 2, our investigation of hydrogen storage materials led to methyl guanidinium borohydride, which is an IL with melting point of -20 °C. The purpose of this study is developing ILs and Metal-containing ionic liquids based on methyl guanidinium cation and exploring the properties due to strong hydrogen bonding.

This chapter illustrates the world of ionic liquid as a green solvent for organic, inorganic and catalytic reactions and combines the concept of catalysts and solvents based on ionic liquids.

3.4 ILs based on methyl guanidinium as cation

Three types of ILs have been prepared and investigated as hydrogen solvent. Methylguanidinium tetrafluoroborate, hexafluoro- phosphate and hexafluoroantimonate were prepared by ion exchange of corresponding sodium salt and methyl guanidinium chloride (Fig.48).

Fig.48 Preparation of ILs by ion methatesis

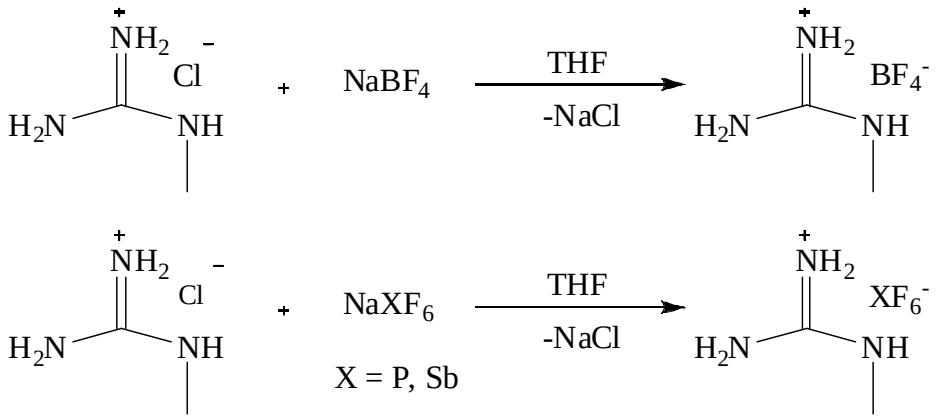

Melting point of these ILs increased with increasing the anion size (Tab. 7). As expected, the bigger the anion, the higher the melting point of ILs. The IL with tetrafluoroborate as anion is fluid at room temperature; however ILs with hexafluorophosphate and antimonite due to bigger anions at elevated temperature are light yellow liquids and stable with exposure to air.

Tab.7 Melting points of ILs.

Ionic liquids	m.p. °C
Methyl guanidinium tetrafluoroborate	-5
Methyl guanidinium hexafluorophosphate	63
Methyl guanidinium hexafluoroantimonate	80

In THF-d8, the ^{11}B NMR of methylguanidinium tetrafluoroborate exhibits a signal at -1.5 ppm. ^{19}F NMR shows two signals at -152.8 and -152.9 ppm, relative to the Et_2OBF_3 complex. The fine structure of the ^{19}F NMR spectrum is due to the spin-spin coupling with ^{10}B (I=3) and ^{11}B (I =3/2) nuclei. Although we detected two singlets, we expected a septet and a quartet, respectively. This is due to the fact that the spin-lattice relaxation times of the ^{10}B nuclei are shorter than those of the ^{11}B nuclei owing to the difference between the electric quadrupole moments of these nuclei.[31] ^{1}H NMR exhibited a doublet at 3 ppm (CH_3 with coupling constant of 4.9 Hz) and a broad signal at 7.1 ppm (amine), with the intensity ratio of 5 to 3, respectively.

The ILs based on methyl guanidinium were synthesized in this chapter. In the next step we have tried to use transition metal as anion to investigate the chemical reactions.

3.4.1 Metal containing protic ionic liquids

We will now report a series of metal-containing protic ionic liquids (MPILs), which constitute a promising class of technologically useful and fundamentally interesting materials, particularly in catalytic reactions. For instance, these compounds can be used as solvent and the catalyst simultaneously or they are suitable for application in two-phase catalytic reactions due to their insolubility in non-polar organic solvents. The strong hydrogen bonding between anion and cation, low melting point and catalytic activity are the interesting features of this class of materials. We report herein two MPILs, methyl guanidinium tetrachlorocobaltate (MGCC)(**1**) and methyl guanidinium tetrachlorozincate (MGCZ)(**2**) ionic liquids. These ionic liquids are interesting because of their activities at low temperature and strong hydrogen bonding. The ability of guanidinium derivates in protic ionic liquids to form strong hydrogen bonding was reported in our previous work[32] and confirmed by the crystal structures and far-IR of these ionic liquids, indicating strong hydrogen bonding between proton of methyl guanidinium, with strong acidic character, and chloride of metal anion. These MPILs are a type of ionic liquids formed by combining a Brønsted acid and a Brønsted base. The key property that distinguishes MPILs from other ILs is the presence of proton-donor and proton-acceptor sites, which can be used to build a hydrogen-bonded network and the catalytic ability of containing metal. This hydrogen-bonded network comprises the active metals, which can catalyse the CO_2 and propylen oxide cycloaddition. One of today's big challenges is the exhausted CO_2 gas, which can be utilized in chemical reaction for making new materials. One of the most important reactions is the coupling of CO_2 with ethylene or propylene oxide, to create a mixture of cyclic and polycarbonates.[33-40] The importance of cyclic carbonates is increased due to their expanded application—electrolytes in secondary batteries, valuable monomers of polycarbonates and polyurethanes, aprotic polar solvents, and raw materials in a wide range of chemical reactions. The mechanistic study and catalyst development for this has been reported in the literature.[41-45] Imidazolium-based ionic liquids have been introduced as effective catalysts for the synthesis of propylene carbonate from the coupling reaction of CO_2 and propylene oxide, but their catalytic activities expressed low turnover frequency (TOF = 10.63 for [bimim]Cl and 14.98 for [bimim]BF_4 at 110 $^{\circ}$C).[45] Previously, the cycloaddition reaction catalysed by ionic liquids based on zinc halides with higher TOF was reported.[46] These MPILs are catalytic active ILs and were synthesized and investigated for three dimensional hydrogen bonding in a solid state.

3.5 Results and discussion

3.5.1 Preparations

1 and **2** were prepared in high yields by reaction of methyl guanidinium chloride and $CoCl_2$ or $ZnCl_2$, respectively, as shown in Figure 49. The reactions were carried out at ambient temperature in isopropanol followed by washing with THF, which leads to blue and light yellow compounds for **1** and **2,** respectively. In contrast to metal chloride, methyl guanidinium chloride showed sparing solubility in isopropanol, but the visually decreasing quantity of the solid compound during reaction at room temperature in isopropanol implies continuance of the reaction. The solution mixture was filtered off, the solvent removed under vacuum and the resulting compound was rinsed with THF to seperate unreacted metal chloride. The mixture of these compounds and THF affords two discrete phases; the upper phase, consisting of THF and unreacted metal chloride; and the lower phase, comprising the products. The lower phase is comprised of **1** and **2** with 2.5 equivalents of THF (as determined by NMR spectroscopy, CD_2Cl_2 external standard). Removal of volatile components under vacuum affords **1** and **2** as solid compounds.

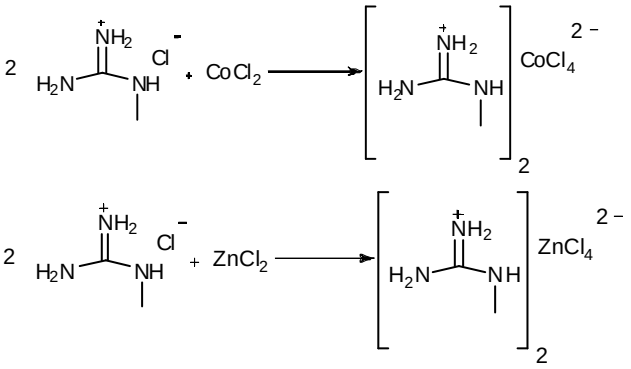

Fig.49 General synthetic route of **1**and **2**

These compounds can all be handled in air, and remain physically and spectroscopically unchanged after 24 h of exposure to air at room temperature. In addition, these compounds are highly soluble in all common alcohol solvents and water. However **1** shows symmetry changing from tetrahedral to octahedral in aqueous or alcohol solutions, which has been studied using UV-Vis measurements.

3.5.2 TGA and DSC studies

The melting point of an ionic liquid depends on its cation/anion composition. Generally, symmetric ions with a localized charge and strong interaction between ions result in good packing efficiency and hence a high melting point. Ionic liquids based on large, unsymmetric cations with a delocalized charge often have low melting points. Packing efficiency depends on interactions between ions, hydrogen bonding (or similar non-bonded interactions), which increases the order of the system and thus raises the melting point.[47]

DSC curves of **1** and **2** were obtained at a heating rate of 5 ºC min^{-1}. The melting temperatures determined from the broad DSC traces, 92.5 °C for **1** and 91.8 °C for **2**, respectively, which are clearly higher than imidazolium salts of these compounds. The melting peak is observed to be broad, over a range of several °K. This peak is too broad to regard this melting as a simple process. Due to the delay of heat transmission by rapid heating or cooling the DSC signals appear as broad signals. In this experiment, however, the amount of the sample was very small and the heating rate was slow enough to mimic an almost quasi-static process. We thus suggest that this apparent broad signal is due to pre-melting, which is characteristic of the present samples. The absorbed energy during the melting process of **1** and **2** was determined by integration of the exothermic DSC curves between 80 °C to 97 °C, which gives a value of ΔQ = 55.91 J/g for **1** and 45.87 J/g for **2**, respectively.

TGA analysis of **1** and **2** shows stable ionic liquids up to 280 °C for **1** and to 283 °C for **2**, respectively. In both cases, weight loss reached to 42 % approximately at 386 °C, which can be related to release of four equivalents HCl. The second step starts after a short plateau at 390 °C, and ends at 485 °C with 8 % weight loss.

3.5.3 Infrared studies and hydrogen bonding

The IR spectra (KBr) of **1** and **2** show some common features. The spectral bands between 3200 and 3408 cm^{-1} can be assigned to N-H stretching modes of N-H in methyl guanidinium. The signal at 2900 cm^{-1} refers to the C-H vibration of methyl group. The C-N and N-CH_3 vibrations can be detected at 1662 and 1166 cm^{-1}, respectively (Fig. 50).

The investigation of hydrogen bonding using far-IR carried out by measuring the low-frequency range below 600 cm^{-1}. This study shows characteristic intermolecular stretching and bending vibrational bands of hydrogen bonds between 70 and 200 cm^{-1}. This assignment was reported with supporting DFT-calculations by Ludwig et al.,[48] which gave wave numbers for the bending

and stretching modes of ion pairs and ion-pair aggregates in this frequency range.

Fig. 50 The IR spectra of **1**

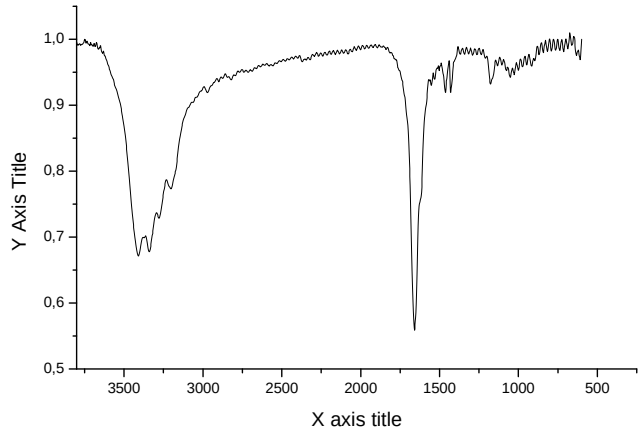

The low-frequency spectra for the neat protic ionic liquids **1** and **2** are shown in Figure 51, which shows the intermolecular hydrogen bonding over the range 100 and 200 cm^{-1}. This broad signal is shifted to higher wave numbers in comparison to the intermolecular hydrogen bonding in imidazolium-based ionic liquids, which indicates stronger hydrogen bonding. The measured H-Cl bond length in crystal structure confirms the strong interaction between acidic proton of methyl guanidinium and chloride of metal anions. This measurement demonstrates a strong extended network of hydrogen bonding in the solid, within position the metal centres.

The number of the observed signals related to M-Cl vibration depends on the symmetry of the anions.[49] The $[CoC1_4]^{2-}$ and $[ZnCl_4]^{2-}$ ions have an almost perfect tetrahedral structure, the four M-Cl distances being almost identical within experimental accuracy, and the bond angles being very close to the tetrahedral value of 109° 28'. For the ions $[CoCl_4]^{2-}$ and $[ZnC1_4]^{2-}$ of T_d symmetry, two vibrations of the F_2 species are expected, which are infrared active, but only one signal can be confidently assigned to **1** and **2** at 292 and 287 cm^{-1}, respectively. According to the literature,[50] the other signal should be detected at around 130 cm^{-1} but it is assumed to be overlapped by the broad signal at 150 cm^{-1}, which is assigned to intermolecular hydrogen bonding. The measurements at elevated temperatures up to 100 °C show no change in the observed signals.

In PILs **1** and **2**, each molecule has at least four donor and four acceptor sites to form a tetrahedral H-bond network.

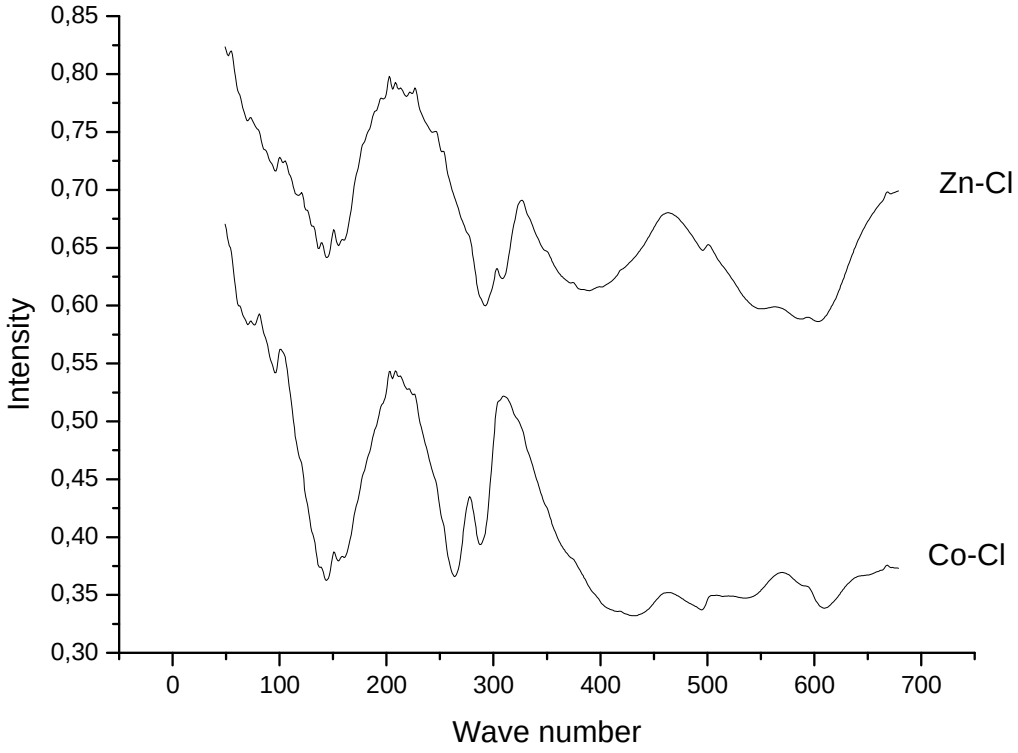

Fig.51 Low-frequency vibrational FTIR spectra of the protic ionic liquids

The characteristic bands for hydrogenbonding in the low-frequency set at 88, 130, 195, and 251 cm^{-1}, are obtained by fitting the structure of the connectivity band of water with a sum of four Gaussians.[51] These spectra can be related to measured bands in **1** and **2** at 120-160, 90-95 cm^{-1}, which confirm the three dimensional H-bond network.

3.5.4. UV-Vis studies

The UV-Vis absorption spectra for compound **1** in the region 300–800 nm were investigated in isopropanol. The broad split d-d band at 661 nm in absolute isopropanol (Fig. 52) is typical in wavelength and intensity for tetrahedral Co^{2+}, e.g. in $[CoCl_4]^{2-}$ ($^4A_2(F) \rightarrow {}^4T_1(P)$ transition)[52,53] In aqueous solution, this band is no longer visible (Fig. 53). Instead a much weaker transition is observed at 511 nm, which is typical for high-spin octahedral Co^{2+} ($^4T_{1g}(F) \rightarrow {}^4T_{1g}(P)$ transition.[54] The color change from blue to pink in water implicates a change in symmetry from tetrahedral to octahedral cobalt (II). In $[ZnCl_4]^{2-}$ anion no absorbance was detected, due to the absence of the d-d transition.

Fig. 52 UV measurement in isopropanol

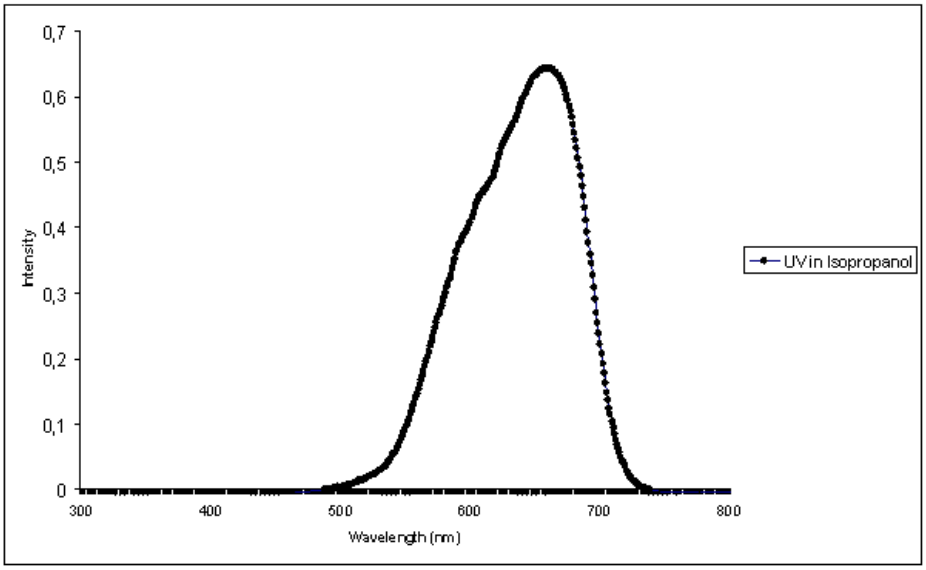

Fig. 53 UV measurement in water

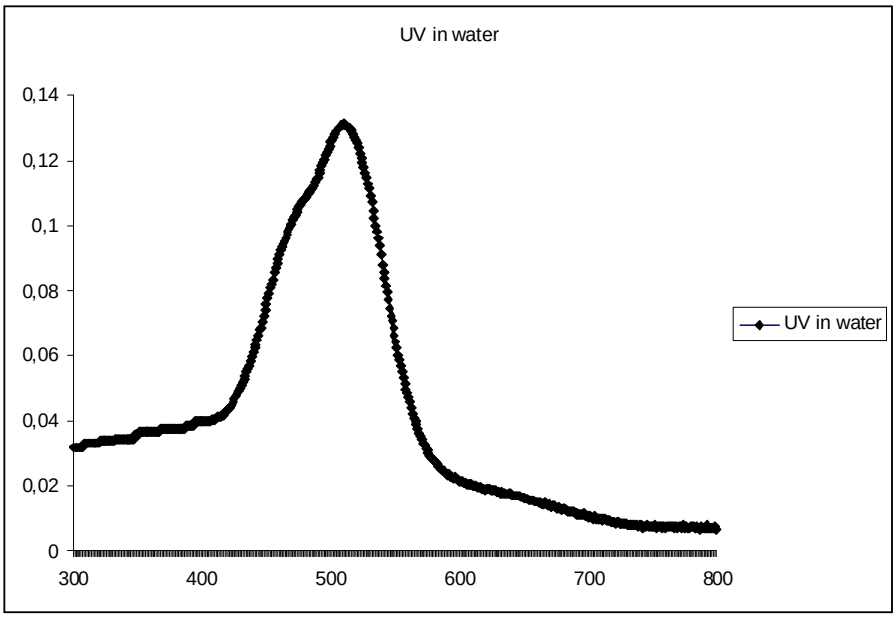

3.5.5 X-ray studies

X-ray quality crystals of **1** and **2** were obtained by slow diffusion of dichloromethane into the isopropanol solution of these compounds while oxygen-free conditions were maintained. The crystal structures of **1** and **2** consist of discrete $[MCl_4]^{2-}$ (M = Co, Zn) anions with two

monoprotonated $(C_2N_3H_8)^+$ cations, respectively. The anionic unit of **1** is comprised of discrete tetrahedral $[CoCl_4]^{2-}$ with a slight distortion from T_d symmetry in the asymmetric unit in space group P-1.

Tetrahedral $[CoCl_4]^{2-}$ anions and methylguanidinium cations are held together through N-H···Cl hydrogen-bonding interactions.

The zinc salt **2** is isomorphous with the zinc species at room temperature with two cations and one complete anion in the asymmetric unit in space group $P2_1/c$.

In a survey of neutron diffraction data, Taylor and Kennard[55] have demonstrated, that a contact shorter than 2.95 Å (C-H···O, C-H···N, and C-H···Cl) reliably indicates the presence of a hydrogen bond. The local structure around a single anion is shown in Fig. 54. The shortest contacts [H····Cl] of 2.45 Å for the $[CoC1_4]^{2-}$ salt and 2.59 Å for the $[ZnC1_4]^{2-}$, respectively, indicate that a strong, discrete hydrogen bond is formed between the proton of the methyl guanidinium and a chlorine atom of the anion.

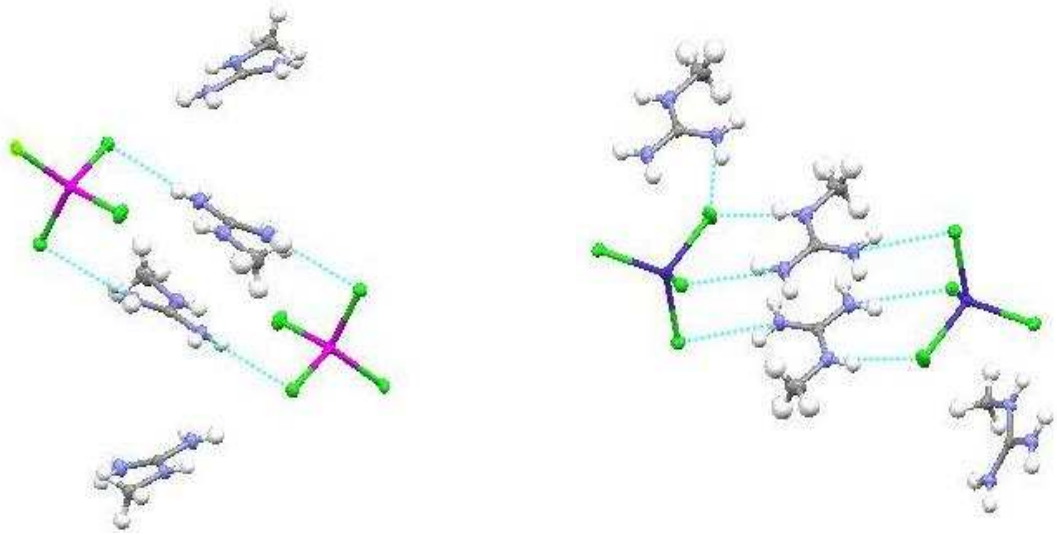

a) b)

Fig.54 Hydrogen bonding of a) $[ZnCl_4]^{2-}$ and b) $[CoCl_4]^{2-}$

3.5.6 Catalytic activity

The synthesis of cyclic carbonates by the coupling reactions of epoxides with carbon dioxide has attracted much attention with regard to the utilization of CO_2. Imidazolium-based ionic liquids have been introduced as effective catalysts for the synthesis of propylene carbonate from the coupling reaction of CO_2 and propylene oxide, but their catalytic activities expressed as turnover frequency (TOF: h^{-1}) were not very high (TOF = 10.63 for [bimim]Cl, 14.98 for [bimim]BF_4 at 110 °C. Recently, Jang and co-workers have reported[56] imidazolium zinc tetrahalide-based ionic liquids as an effective catalyst for this reaction as illustrated in Fig. 55. The catalytic activities of various bis(1-R-3-methylimidazolium) zinc tetrahalides were reported for the coupling reactions of CO_2 and ethylene oxide (EO) or propylene oxide (PO) at 100 °C for 1 h. We have tried this coupling reaction using our MPLIs at 100 °C. Interestingly, the MPLIs show catalytic activity to 54 and 50 % yield for **1** and **2**, respectively. The reaction was carried out in propylene oxide as solvent for 24 h at 100 °C. However, the yield of the reaction is satisfactory, but the TOF is very low (TOF = 18.12) due to the time of the reaction.

Jang and co-workers have reported[56] a high TOF for similar ionic liquids. Investigation of mechanism may be the answer to low TOF numbers.

Fig.55 Coupling reactions of propylenoxide with carbon dioxide

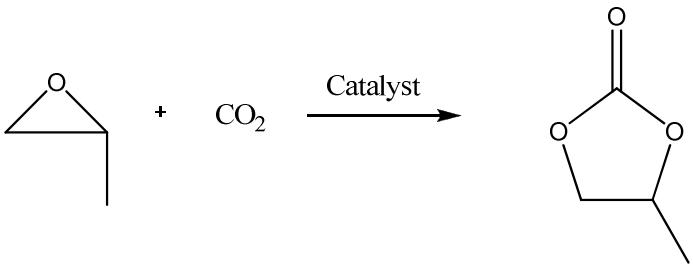

Varma et. al. reported[56] the NMR spectroscopic studies of mechanism for the coupling reaction catalyzed by tetrahaloindate(III)-Based Ionic Liquid (Fig. 56).

The initial active catalyst can be described as (1) in which Cl- forms H-bond with C(2) hydrogen of imidazolium cation. The coordination of PO to the Lewis acid site of indium to form the adduct (2), subsequent nucleophilic attack of Cl- on the less hindered carbon atom of the coordinated PO, followed by ring opening reaction leads to chloroalkoxy anion species (3), which

is stabilized through the H-bonding interaction. The insertion of CO_2 into O···H of (3) would produce chloroalkoxy carbonate intermediate.

Fig.56 Proposed mechanism of the coupling of carbon dioxide and epoxides by Varma et al.

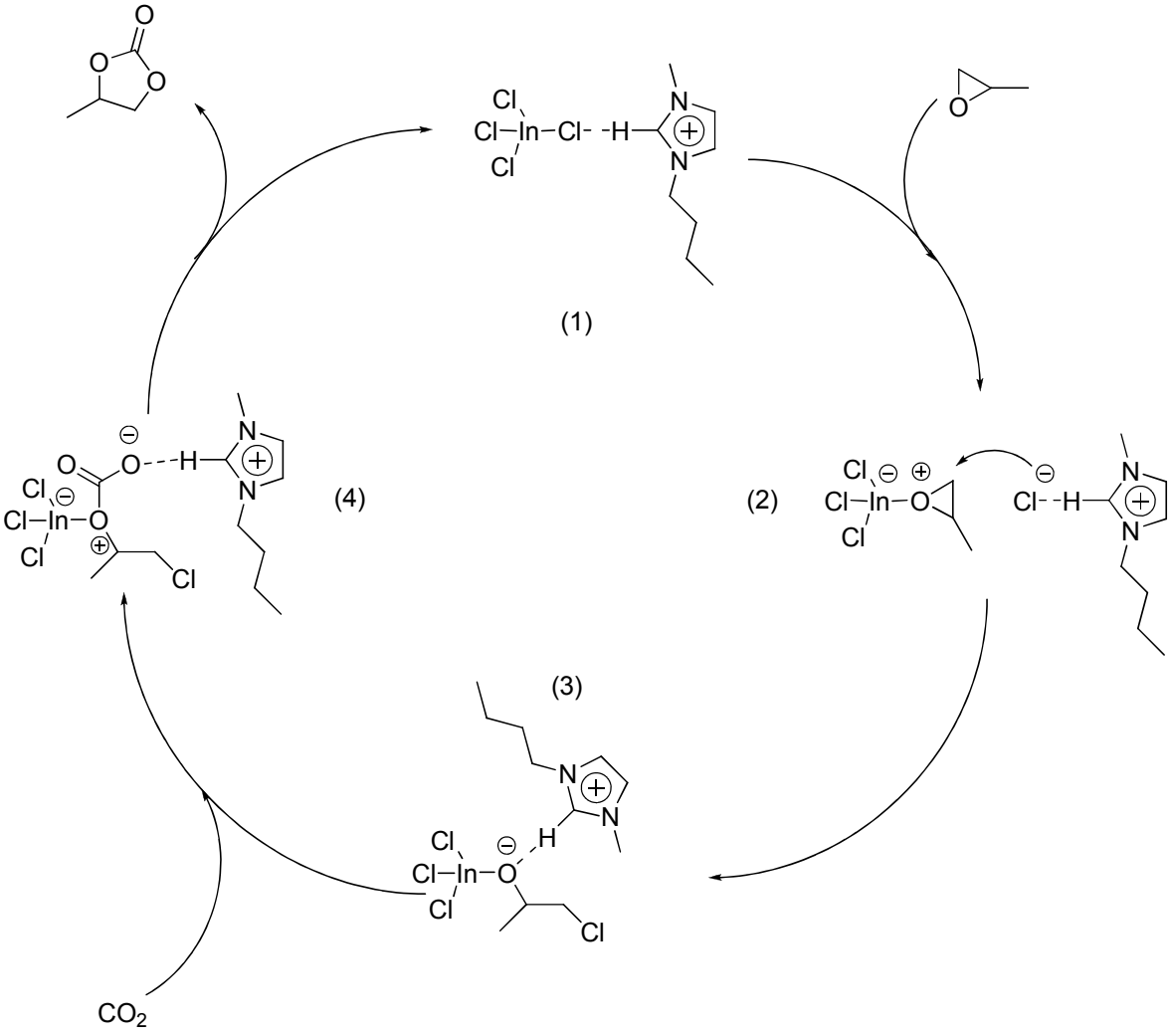

The intramolecular cyclic elimination (4) thus provides propylenecarbonate and regenerates the catalyst, (1). From a series of their experimental results using [Q][InCl4], it becomes clear that the ability to form H-bonding interaction is also an important factor influencing the catalytic activity.

Based on the above results and previous literature[57] a reasonable mechanism for the coupling reaction catalyzed by A is proposed (Fig. 57).

Fig. 57 proposed mechanism of coupling of carbon dioxide and epoxide

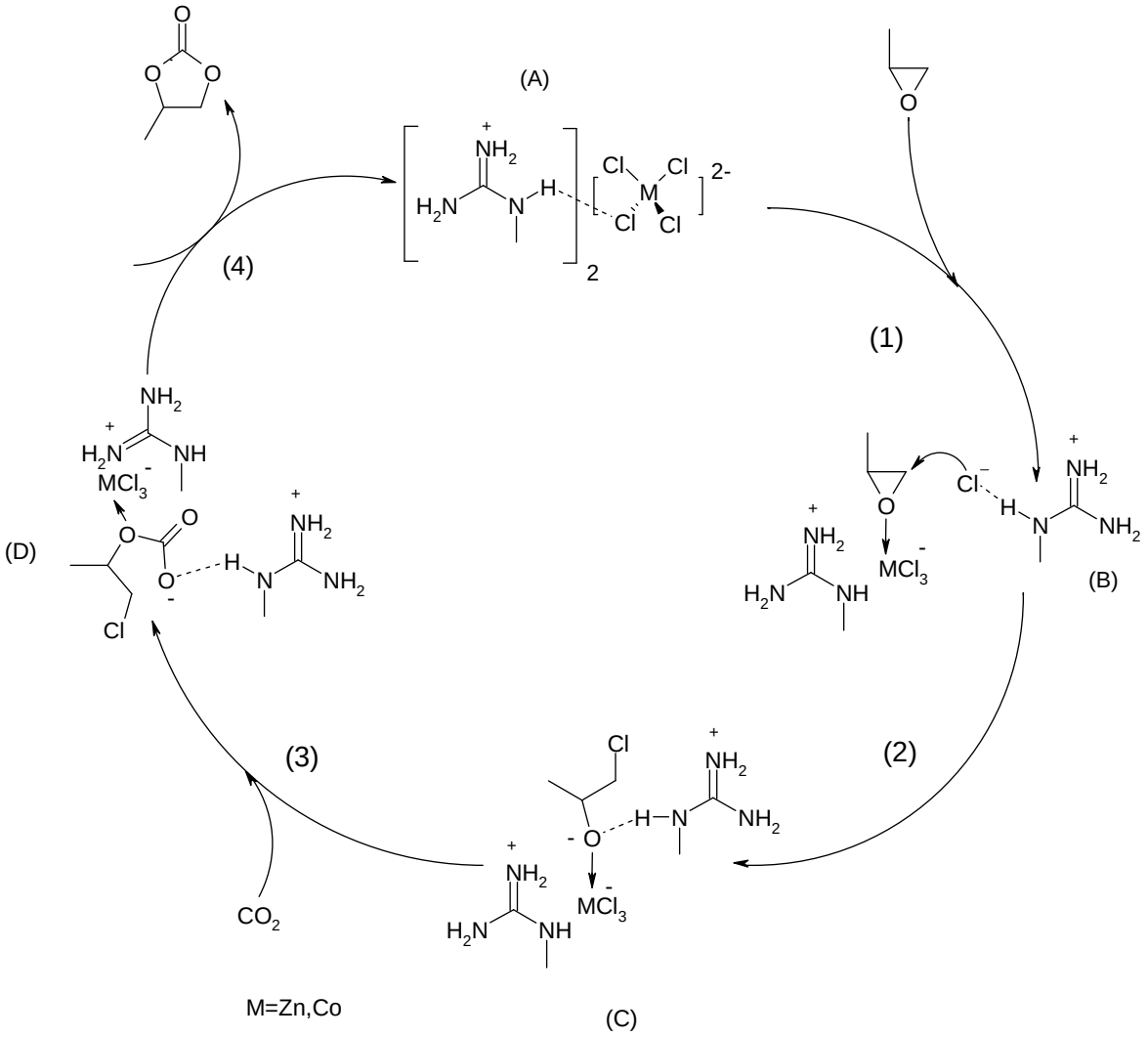

The initial active catalyst can be described as (A) in which Cl^- forms H-bond with hydrogen of methyl guanidinium cation. The coordination of propylene oxide to the Lewis acid site of transition metal forms the adduct, (B) , subsequent nucleophilic attack of Cl^- on the coordinated PO, followed by ring opening reaction leads to chloroalkoxy anion species, (C). The insertion of CO_2 into O···H of C would produce chloroalkoxy carbonate intermediate, (D).

The intramolecular cyclic elimination thus provides propylene carbonate and regenerates the catalyst. Kisch et al. reported that the coexistence of both Lewis acid and Lewis base is required to prepare alkylene carbonates from CO_2 and epoxides.[58]

It is resulted that the H-bonding property through the interaction with the halide ion and protons of guanidinium cation renders the dissociation of halide ion from metal and the coordination of epoxide much easier, thus facilitating the activation of coordinated epoxide to form haloalkoxy

species via ring-opening, which are also stabilized by the H-bonding interactions as illustrated in Fig 57.

The low yield in our reaction probably has its origin in stabilities of (B) or (D) compounds (Fig. 57). Because interaction between methylguanidinium cation and anions in (B) and (D) is strong, ring opening or ring closing reaction, may be slowing down.

3.6 Conclusion

Methylguanidinium is a suitable cation for ILs, in order to increase the interaction between anion and cation due to strong hydrogen-bridge bonding with anion. Methylguanidinium tetrafluoroborate, hexafluoro- phosphate and hexafluoroantimonate ILs have been prepared and investigated.

Methyl guanidinium tetrachlorocobaltate (MGCC) and methyl guanidinium tetrachlorozincate (MGCZ) metal containing protic ILs were prepared. The melting temperatures were evaluated by DSC measurements. These showed melting point of 92.5 °C for MGCC and 91.8 °C for MGCZ, respectively.

The investigation of hydrogen bonding using far-IR showed strong hydrogen bonding, which is confirmed by x-ray studies.

The catalytic activity was investigated by coupling of propyleneoxide and CO_2. However, the yield of the reaction is satisfactory, but the TOF is very low due to the time of the reaction.

The H-bonding interaction was also an important factor affecting the catalytic activity for the coupling reaction.

3.7 Experimental Section

General

All reactions and product manipulations were performed under an atmosphere of dry argon using standard Schlenk techniques or in an inert atmosphere glovebox. Isopropanol was dried over molecular sieves 4 Å. Solvents were refluxed over the appropriate drying agent, purged several times with argon during reflux, and distilled under argon (THF: CaH_2).

Methyl guanidinium chloride, cobalt chloride, zinc chloride, propylene oxide, sodium tetrafluoroborate, sodium hexafluorophosphate and sodium hexafluoroantimonite were purchased and used as received. Solution NMR spectra were collected at room temperature using a Bruker ARX300 spectrometer. ^{1}H, ^{13}C NMR spectra are referenced to $SiMe_4$ by referencing the residual solvent peak. Infrared spectra were recorded on a Bruker IFS55 FT-IR spectrometer at room temperature. ESI-MS was carried out with a Varian 500 MS spectrometer with isopropanol as solvent.

UV-Vis absorption spectra were recorded at ambient temperature using an HP 8453 UV-Vis spectrophotometer. GC-MS measurements were collected on a Varian 3900 GC-MS.

X-ray analysis was carried out by Dr. E. Herdtweck in the Anorganisch-chemische Institut at the Technischen Universitaet Muenchen. The single-crystal x-ray diffraction experiment was performed using a Bruker APEX2 diffractometer equipped with a Mo-anode (Mo-K_α radiation: λ = 7.1073 Å).

DSC-measurements were carried out by DSCQ2000 at room temperature from TA Instrument (Waters). Melting points were reported in °C.

Thermogravimetric mass spectrometry (TG-MS) were preformed on a TGAQ5000 system using ~10 mg sample heated at a ramp of 10 K per minute under argon or synthetic from room temperature.

Preparation of methylguanidinium tetrafluoroborate

Guanidinium chloride (2 g, 18.3 mmol) and sodium tetrafluoroborate (2g, 18.3 mmol) were slurried in 10 ml dry THF for 5 h at room temperature. The suspension turns to a homogenous particle distribution. The organic phase was then filtrated off under inert gas and the solvent was removed under reduced pressure. A light yellow liquid was isolated in 82 % yield.

^{1}H NMR (300 MHz, THF-d_8): δ(ppm) = 7.1-6.6 (m, 5H), 3.1 (d, J = 4.9 Hz, 3H)

^{11}B NMR (300 MHz, THF-d_8): δ(ppm) = -61.9, -62

^{19}F NMR (300 MHz, THF-d_8): δ(ppm) = -1.47

ESI-MS(+) 74 g/mol

ESI-MS(-) 87 g/mol

Elemental Analysis

	Measured (%)	Calculated (%)
C:	15.67	14.93
H:	5.78	5.01
N:	26.84	26.11

Preparation of methylguanidinium hexafluorophosphate

Guanidinium chloride (2 g, 18.3 mmol) and sodium tetrafluoroborate (3.06 g, 18.3 mmol) The same reaction processes similar to methylguanidinium tetrafluoroborate were applied.

^{1}H NMR (300 MHz, THF-d_8): δ(ppm) = 7.2-6.8 (m, 5H), 3.2 (d, J = 5 Hz, 3H)

ESI-MS(+) 74 g/mol

ESI-MS(-) 144 g/mol

Elemental Analysis:

	Measured (%)	Calculated (%)
C:	11.34	10.97
H:	4.12	3.68
N:	19.74	19.18

Preparation of methylguanidinium hexafluoroantimonite (Similar to hexafluoro-phosphate)

^{1}H NMR (300 MHz, THF-d_8): δ(ppm) = 7.2-6.8 (m, 5H), 3.2 (d, J = 5 Hz, 3H)

ESI-MS(+) 74 g/mol

ESI-MS(-) 235 g/mol

Elemental Analysis:

	Measured (%)	Calculated (%)
C:	8.13	7.75
H:	2.87	2.60
N:	14.10	13.56

Preparation of methyl guanidinium tetrachlorocobaltate (MGCC)(1)

Guanidinium chloride (1.68 g, 14.4 mmol) was slurried in 10 ml dry isopropanol. A solution of cobalt chloride (1 g, 7.7 mmol) in 10 mL dried isopropanol was added. The reaction was stirred for 5 h at room temperature, the apparent particle size of the suspended solid decreased. The organic phase was then filtrated off under inert gas and the solvent was removed under reduced pressure. The dark blue solid was washed twice with 10 mL THF. The organic phase consisted of two different phases; after removing the upper phase, the solvent was removed under reduced pressure and the solid was washed twice with 10 ml of diethyl ether affords to pure **1** (82 %) as blue solid.

ESI-MS(+) 74 g/mol

ESI-MS(-) 164 g/mol

Elemental Analysis:

	Measured (%)	Calculated (%)
C:	14.12	13.77
H:	5.44	4.62

N:	26.38	24.08
Cl:	38.40	40.64
Co:	15.66	16.89

IR-Measurements:

N-H 3200 and 3408 cm^{-1}; C-H 2900 cm^{-1}; C-N 1662 cm^{-1}; N-CH_3 1166 cm^{-1}

Far-IR: Co-Cl 265 cm^{-1}; NH···Cl 148 cm^{-1}

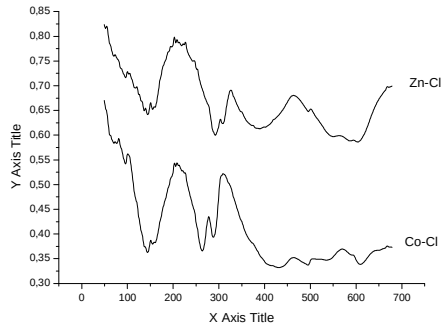

Crystal structure:

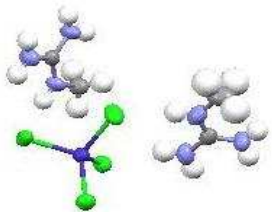

The molecular structure of **1**

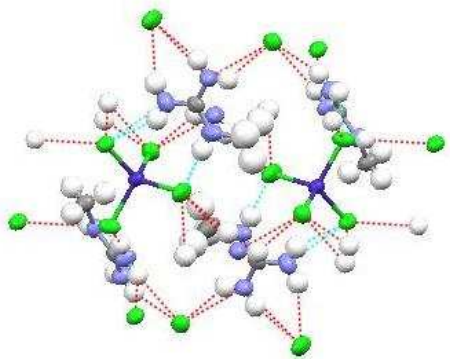

The molecular packing of the compound showing N—H···Cl interactions

$C_4H_{16}Cl_4CoN_6$

M_w = 346.95

Space group: P -1

a = 7.4168(3); b = 7.8242(4); c = 13.3978(6).

α 83.409(2); β 78.739(2); γ 72.329(2)

Cell volume 725.251

Room Temp. (283-303)

Fractional atomic coordinates

Number	Label	Xfrac + ESD	Yfrac + ESD	Zfrac + ESD
1	CO1	0.477518	0.623997	0.228718
2	CL1	0.752855	0.631905	0.122521
3	CL2	0.274019	0.539226	0.153257
4	CL3	0.317887	0.903264	0.28691
5	CL4	0.554153	0.414373	0.359036
6	N1	0.763259	0.208483	0.078055
7	H1	0.750354	0.319568	0.058634
8	N2	1.03847	0.20363	0.133739
9	H2	1.02364	0.314433	0.113008
10	H3	1.13537	0.145565	0.162382
11	N3	0.938286	-0.04806	0.154293
12	H4	0.857554	-0.102859	0.14709
13	H5	1.036	-0.104057	0.182768
14	C1	0.912149	0.122438	0.121559
15	C2	0.619652	0.131301	0.060286
16	H21	0.523843	0.221557	0.029115
17	H22	0.560543	0.086627	0.124009
18	H23	0.67894	0.034324	0.015902
19	N4	0.209337	0.246898	0.481805
20	H6	0.306376	0.271925	0.443324
21	N5	0.030562	0.385323	0.357935
22	H7	0.128477	0.412309	0.32169
23	H8	-0.077106	0.416601	0.336075
24	N6	-0.107148	0.25521	0.500443
25	H9	-0.100997	0.196123	0.558513
26	H10	-0.213091	0.288118	0.476809
27	C3	0.045634	0.295292	0.447721
28	C4	0.237067	0.153806	0.580332
29	H41	0.365207	0.140165	0.590831
30	H42	0.217854	0.037479	0.582152
31	H43	0.146467	0.222247	0.633134

Bond lengths:

Number	Atom1	Atom2	Length
1	CO1	CL1	2.2628(1)
2	CO1	CL2	2.2578(1)
3	CO1	CL3	2.2900(1)
4	CO1	CL4	2.2860(1)
5	N1	H1	0.8600
6	N1	C1	1.3124
7	N1	C2	1.4416
8	N2	H2	0.8600
9	N2	H3	0.8600
10	N2	C1	1.3240
11	N3	H4	0.8600
12	N3	H5	0.8600
13	N3	C1	1.3234(1)

14	C2	H21	0.9600
15	C2	H22	0.9600
16	C2	H23	0.9600
17	N4	H6	0.8600
18	N4	C3	1.3129
19	N4	C4	1.4525(1)
20	N5	H7	0.8600
21	N5	H8	0.8600
22	N5	C3	0.8600
24	N6	H10	0.8600
25	N6	C3	1.3167
26	C4	H41	0.9600
27	C4	H42	0.9600
28	C4	H43	0.9600

Bond angles:

Number	Atom1	Atom2	Atom3	Angle
1	CL1	CO1	CL2	113.13
2	CL1	CO1	CL3	109.99
3	CL1	CO1	CL4	108.16
4	CL2	CO1	CL3	107.12
5	CL2	CO1	CL4	106.52
6	CL3	CO1	CL4	111.93
7	H1	N1	C1	117.45
8	H1	N1	C2	117.45
9	C1	N1	C2	125.09
10	H2	N2	H3	120.00
11	H2	N2	C1	120.00
12	H3	N2	C1	120.00
13	H4	N3	H5	120.00
14	H4	N3	C1	120.00
15	H5	N3	C1	120.00
16	N1	C1	N2	121.01
17	N1	C1	N3	120.23
18	N2	C1	N3	118.75
19	N1	C2	H21	109.47
20	N1	C2	H22	109.47
21	N1	C2	H23	109.47
22	H21	C2	H22	109.47
23	H21	C2	H23	109.47
24	H22	C2	H23	109.47
25	H6	N4	C3	117.90
26	H6	N4	C4	117.90
27	C3	N4	C4	124.20
28	H7	N5	H8	120.00
29	H7	N5	C3	120.00
30	H8	N5	C3	120.00
31	H9	N6	H10	120.00
32	H9	N6	C3	120.00
33	H10	N6	C3	120.00
34	N4	C3	N5	120.49
35	N4	C3	N6	121.40
36	N5	C3	N6	118.11
37	N4	C4	H41	109.47
38	N4	C4	H42	109.47
39	N4	C4	H43	109.47
40	H41	C4	H42	109.47
41	H41	C4	H43	109.47
42	H42	C4	H43	109.47

Preparation of methyl guanidinium tetrachlorozincate (MGCZ)(2)

Guanidinium chloride (0.98 g, 9 mmol) was slurried in 10 ml dry isopropanol. A solution of zinc chloride (0.6 g, 4.4 mmol) in 10 mL dried isopropanol was added. The reaction was stirred for 5 h at room temperature, the apparent particle size of the suspended solid decreased. The organic phase was then filtrated off under inert gas and the solvent was removed under reduced pressure. The light yellow solid was washed twice with 10 mL THF. The organic phase consisted of two different phases; after removing the upper phase, the solvent was removed under reduced pressure and the solid was washed twice with 10 ml of diethyl ether affords to pure **2** (78 %) as light yellow solid.

ESI-MS(+) 74 g/mol

ESI-MS(-) 169 g/mol

Elemental Analysis:

	Measured (%)	Calculated (%)
C:	14.13	13.52
H:	5.11	4.54
N:	23.92	23.64
Cl:	40.34	39.90

IR-Measurements:

N-H 3200 and 3408 cm^{-1}; C-H 2900 cm^{-1}; C-N 1662 cm^{-1}; N-CH_3 1166 cm^{-1}

Far-IR: Zn-Cl 275 cm^{-1}; NH$^{\cdots}$Cl 146 cm^{-1}

Crystal structure:

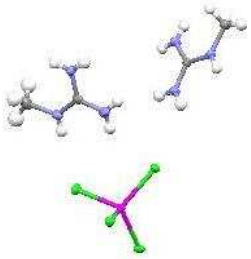

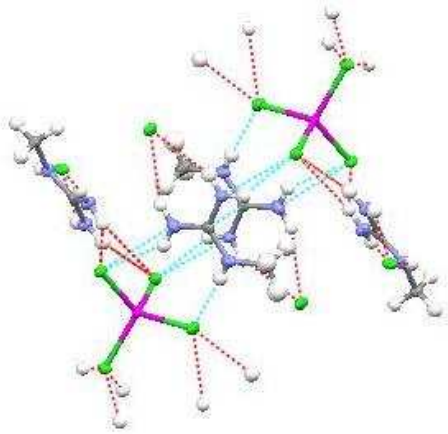

The molecular packing of the compound showing N—H···Cl interactions

$C_4H_{16}Cl_4ZnN_6$

M_w = 351.95

Space group: P -1

a = 7.2438(4); b = 7.8150(4); c = 13.4120(7)

α 85.073(2); β 77.020(2); γ 71.932(2)

Cell volume 703.266

Room Temp. (283-303)

Fractional atomic coordinates

Number	Label	Xfrac + ESD	Yfrac + ESD	Zfrac + ESD
1	ZN1	0.983303	0.635608	0.224382
2	CL1	1.06332	0.43609	0.356156
3	CL2	0.774539	0.545894	0.15361
4	L3	0.812686	0.917179	0.289476
5	CL4	1.26283	0.642311	0.110716
6	N1	0.538504	0.216949	0.140589
7	N2	0.433546	-0.035325	0.160573
8	N3	0.269435	0.215342	0.076008
9	C1	0.412593	0.133235	0.125311
10	C2	0.125179	0.133445	0.057525
11	H1	0.528078	0.32303	0.121676
12	H2	0.627546	0.162134	0.173876
13	H3	0.371802	-0.093189	0.14554
14	H4	0.535161	-0.088797	0.185012
15	H5	0.263517	0.314746	0.056186
16	H21	0.198322	0.027632	0.014553
17	H22	0.032678	0.22101	0.021961
18	H23	0.058402	0.094405	0.120729
19	N4	0.544685	0.391322	0.362382
20	N5	0.396647	0.253922	0.501018
21	N6	0.722801	0.247794	0.48401
22	C3	0.556249	0.296798	0.449389
23	C4	0.743614	0.151891	0.580907
24	H6	0.642534	0.406802	0.327256
25	H7	0.443308	0.414248	0.340912
26	H8	0.289531	0.299213	0.480378
27	H9	0.395642	0.207088	0.555959
28	H10	0.809052	0.275808	0.452459
29	H41	0.875475	0.135175	0.589645
30	H42	0.729323	0.035092	0.578102
31	H43	0.650195	0.225771	0.637729

Bond lengths:

Number	Atom1	Atom2	Length
1	ZN1	CL1	2.3058(1)
2	ZN1	CL2	2.2575(1)
3	ZN1	CL3	2.3000(1)
4	ZN1	CL4	2.2566(1)
5	N1	C1	1.3338(1)
6	N1	H1	0.8312
7	N1	H2	0.8509
8	N2	C1	1.3354(1)
9	N2	H3	0.7917

10	N2	H4	0.8473
11	N3	C1	1.3217(1)
12	N3	C2	1.4565(1)
13	N3	H5	0.7906
14	C2	H21	0.9847
15	C2	H22	0.9736
16	C2	H23	0.9532
17	N4	C3	1.3311(1)
18	N4	H6	0.7952
19	N4	H7	0.8117
20	N5	C3	1.3301(1)
21	N5	H8	0.8446
22	N5	H9	0.7937
23	N6	C3	1.3238(1)
24	N6	C4	1.4574(1)
25	N6	H10	0.7533
26	C4	H41	0.9557(1)
27	C4	H42	0.9548
28	C4	H43	0.9867

Bond angles:

Number	Atom1	Atom2	Atom3	Angle
1	CL1	ZN1	CL2	107.42
2	CL1	ZN1	CL3	109.51
3	CL1	ZN1	CL4	109.71
4	CL2	ZN1	CL3	107.15
5	CL2	ZN1	CL4	112.42
6	CL3	ZN1	CL4	110.53
7	C1	N1	H1	121.88
8	C1	N1	H2	118.87
9	H1	N1	H2	119.14
10	C1	N2	H3	120.96
11	C1	N2	H4	118.05
12	H3	N2	H4	118.82
13	C1	N3	C2	123.78
14	C1	N3	H5	116.72
15	C2	N3	H5	119.49
16	N1	C1	N2	118.91
17	N1	C1	N3	120.68
18	N2	C1	N3	120.41
19	N3	C2	H21	107.71
20	N3	C2	H22	108.61
21	N3	C2	H23	109.94
22	H21	C2	H22	110.24
23	H21	C2	H23	108.66
24	H22	C2	H23	111.60
25	C3	N4	H6	119.43

26	C3	N4	H7	118.69
27	H6	N4	H7	120.72
28	C3	N5	H8	117.62
29	C3	N5	H9	120.63
30	H8	N5	H9	120.23
31	C3	N6	C4	123.66
32	C3	N6	H10	117.10
33	C4	N6	H10	119.17
34	N4	C3	N5	118.59
35	N4	C3	N6	120.58
36	N5	C3	N6	120.82
37	N6	C4	H41	107.84
38	N6	C4	H42	109.74
39	N6	C4	H43	109.65
40	H41	C4	H42	107.20
41	H41	C4	H43	107.98
42	H42	C4	H43	114.20

DSC:

A. MGCC: (**1**)

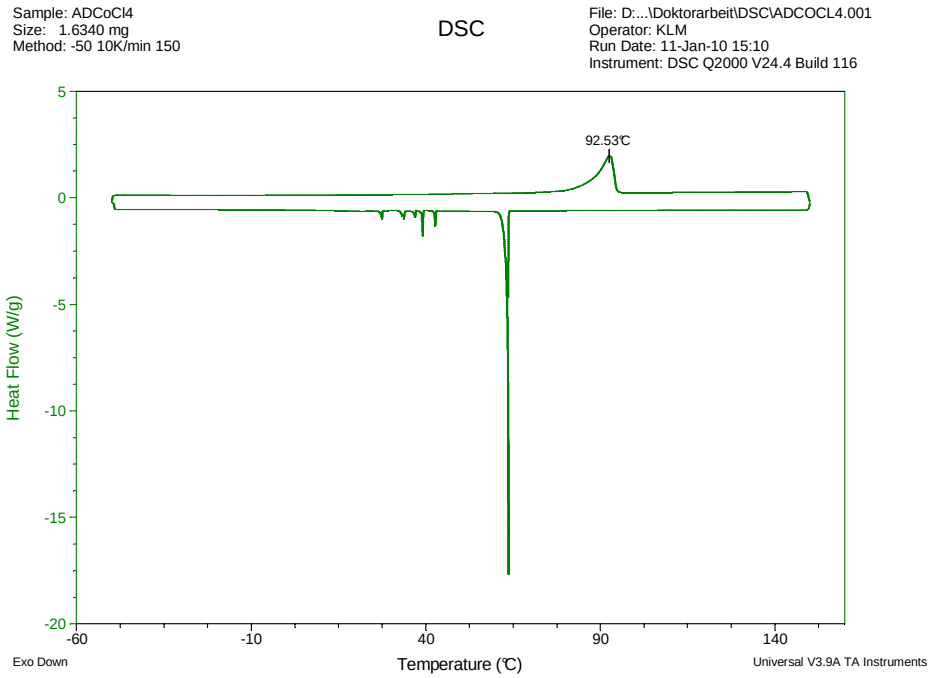

B. MGCZ: (**2**)

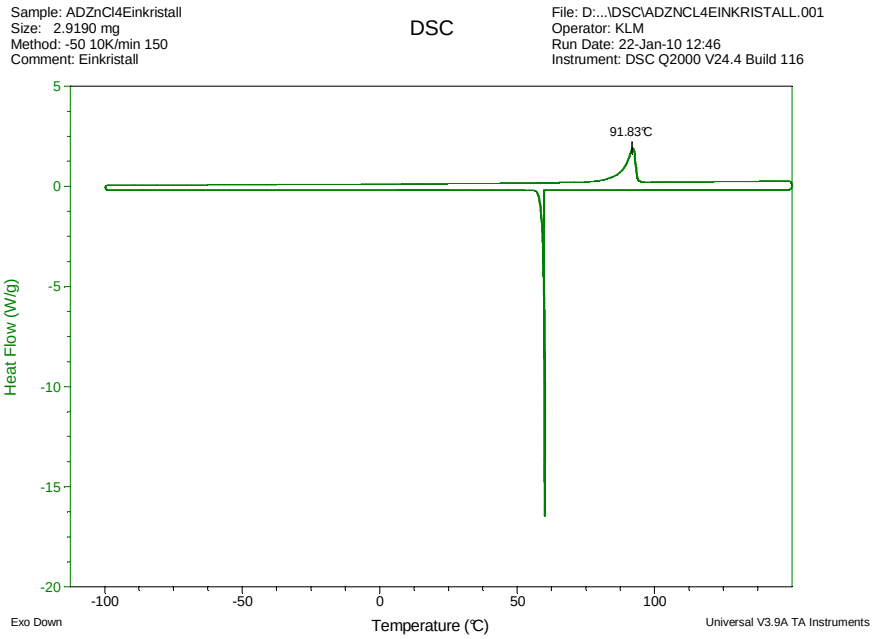

TGA:

A. MGCC: (**1**)

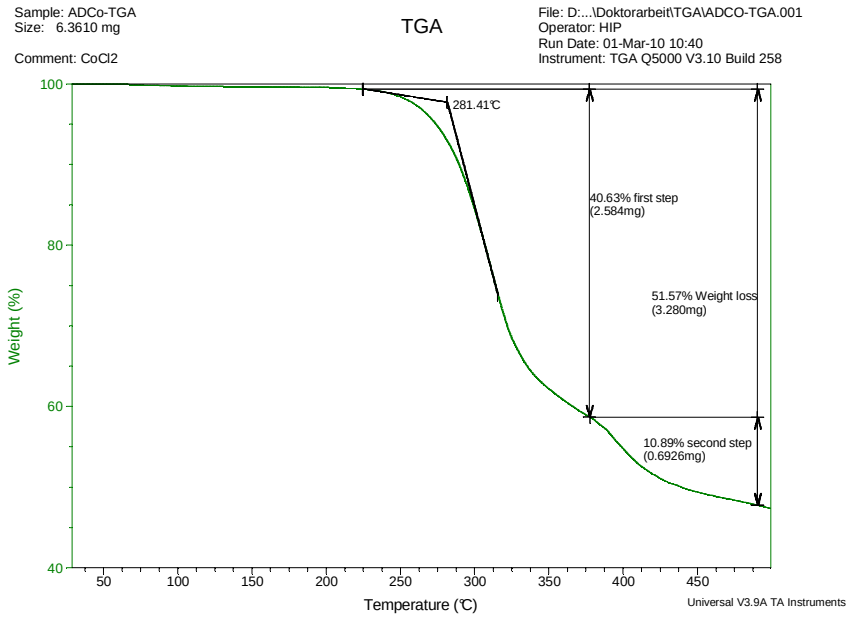

B. MGCZ: (**2**)

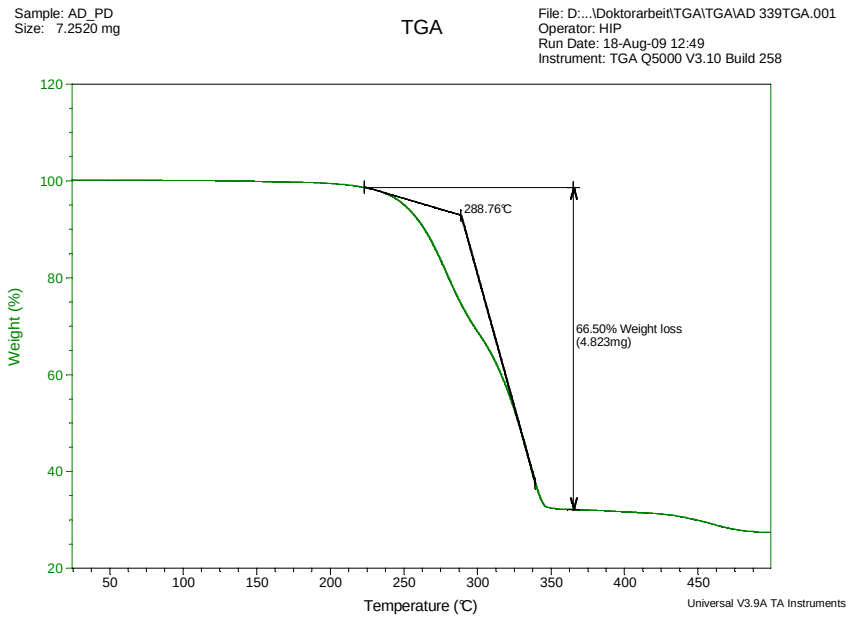

Coupling reaction

All the coupling reactions were conducted in a 200-mL stainless-steel bomb reactor equipped with a magnet bar and an electrical heater. The reactor was charged with an appropriate catalyst and an epoxide and pressurized with CO_2 (40 bar). The bomb was then heated to 100 °C with the addition of CO_2 from a reservoir tank to maintain a constant pressure. After the reaction, the bomb was cooled to room temperature, and the remaining epoxide was removed under reduced pressure. The mixture was treated by CH_2Cl_2/H_2O and the organic phase was removed under vacuum, then the mixture was investigated by ^1H and IR.

^1H-NMR ($CDCl_3$/TMS): δ 1.4 (d, 3H), δ 3.9~4.1 (q, 1H), δ 4.4~4.6 (t, 1H), δ 4.7~4.9 (m, 1H).

IR: $\upsilon_{C=O}$ 1793 cm^{-1}, υ_{C-O} 1183, 1120, 1075, 1052 cm^{-1}

3.8 Literature

1) W. Hückel, Chem. Ber., 1958, 91, XIX–LXVI.

2) C. Graenacher, Cellulose solution, US Pat., 1943176 (1934).

3) F. H. Hurley, Electrodeposition of Aluminum, US Pat., 4,446,331 (1948); T. P. Wier, Jr., US Pat., 4,446,350 (1948); T. P. Wier, Jr. and F. H. Hurley, US Pat., 4,446,349 (1948).

4) F. H. Hurley and T. P. Wier, J. Electrochem. Soc., 1951, 98, 207–212; F. H. Hurley and T. P. Wier, J. Electrochem. Soc., 1951, 98, 203–206.

5) H. L. Chum, V. R. Koch, L. L. Miller and R. A. Osteryoung, J. Am. Chem. Soc., 1975, 97, 3264–3265.

6) R. J. Gale, B. Gilbert and R. A. Osteryoung, Inorg. Chem., 1978, 17, 2728–2729.

7) J. S. Wilkes, in 'Ionic Liquids: Industrial Applications to Green Chemistry', ed. R. D. Rogers and K. R. Seddon, ACS Symp. Ser, American Chemical Society, Washington D.C., 2002, vol. 818, pp. 214–229; J. S. Wilkes, Green Chem., 2002, 4, 73–80.

8) C. J. Dymek, C. L. Hussey, J. S. Wilkes and H. A. Øye, J. Electrochem. Soc., 1987, 134, C510.

9) A. M. Elias and J. S. Wilkes, J. Chem. Eng. Data, 1994, 39, 79–82; A. A. Fannin, L. A. King, D. J. Stech, R. L. Vaughn, J. S. Wilkes and J. L. Williams, J. Electrochem. Soc., 1982, 129, C122; H. A. Oye, M. Jagtoyen, T. Oksefjell and J. S. Wilkes, Mater. Sci. Forum, 1991, 73–75, 183–190; J. S. Wilkes, J. A. Levisky, J. L. Pflug, C. L. Hussey and T. B. Scheffler, Anal. Chem., 1982, 54, 2378–2379; J. S. Wilkes, J. S. Frye and G. F. Reynolds, Inorg. Chem., 1983, 22, 3870–3872.

10) A. A. Fannin, D. A. Floreani, L. A. King, J. S. Landers, B. J. Piersma, D. J. Stech, R. L. Vaughn, J. S. Wilkes and J. L. Williams, J. Phys. Chem., 1984, 88, 2614–2621.

11) A. A. Fannin, L. A. King, J. A. Levisky and J. S. Wilkes, J. Phys. Chem., 1984, 88, 2609–2614.

12) C. L. Hussey, T. B. Scheffler, J. S. Wilkes and A. A. Fannin, J. Electrochem. Soc., 1986, 133, 1389–1391.

13) A. K. Abdul-Sada, A. M. Greenway, K. R. Seddon and T. Welton, Org. Mass Spectrom., 1993, 28, 759–765; A. K. Abdul-Sada, A. M. Greenway, K. R. Seddon and T. Welton, Org. Mass Spectrom., 1989, 24, 917–918.

14) J. S. Wilkes and M. J. Zaworotko, J. Chem. Soc., Chem. Commun., 1992, 965–967.

15) K. R. Seddon, in 'The International George Papatheodorou Symposium: Proceedings', ed. S. Boghosian, V. Dracopoulos, C. G. Kontoyannis and G. A. Voyiatzis, Institute of Chemical Engineering and High Temperature Chemical Processes, Patras, 1999, pp. 131–135.

16) A. Stark and K. R. Seddon, in 'Kirk-Othmer Encyclopaedia of Chemical Technology', ed. A. Seidel, John Wiley & Sons, Inc., Hoboken, New Jersey, 2007, vol. 26, pp. 836–920.

17) A. F. Kapustinskii, Q. Rev. Chem. Soc., 1956, 10, 283–294.

18) K. R. Seddon, Kinet. Katal., 1996, 37, 743–748; K. R. Seddon, Kinet. Catal., 1996, 37, 693–697.

19) J. D. Holbrey, W. M. Reichert, M. Nieuwenhuyzen, S. Johnston, K. R. Seddon and R. D. Rogers, Chem. Commun., 2003, 1636–1637.

20) K. R. Seddon, J. Chem. Technol. Biotechnol., 1997, 68, 351–356.

21) a) A. K. Abdul-Sada, A. M. Greenway, P. B. Hitchcock, T. J. Mohammed, K. R. Seddon J. A. Zora, J. Chem. Soc., Chem. Commun., 1986, 1753–1754.

b) P. B. Hitchcock, K. R. Seddon, T. J.Welton, J. Chem. Soc. Dalton Trans. 1993, 2639 – 2643.

c) J. D. Holbrey, W. M. Reichert, M. Nieuwenhuyzen, S. Johnston, K. R. Seddon, R. D. Rogers, Chem. Commun. 2003, 1636 – 1637.

d) J. D. Holbrey,W. M. Reichert, M. Nieuwenhuyzen, O. Sheppard, C. Hardacre, R. D. Rogers, Chem. Commun. 2003, 476 – 477.

e) P. Bonh_te, A.-P. Dias, N. Papageorgiou, K. Kalynasundaram, M. Gr_tzel, Inorg. Chem. 1996, 35, 1168 – 1178.

f) J. D. Tubbs, M. M. Hoffmann, J. Solution Chem. 2004, 33, 381 – 394.

g) R.W. Berg,M. Deetlefs, K. R. Seddon, I. Shim, J. M. Thompson, J. Phys. Chem. B 2005, 109, 19018 – 19025.

h) S. Katsyuba, E. E. Zvereva, A. Vidisˇ, Paul J. Dyson, J. Phys. Chem. B 2007, 111, 352 – 370.

i) A. Dominguez-Vidal, N. Kaun, M. J. Ayora-Ca_ada, B. Lendl, J. Phys. Chem. B 2007, 111, 4446 – 4452.

j) T. K_ddermann, C. Wertz, A. Heintz, R. Ludwig, ChemPhys- Chem 2006, 7, 1944 –

1949.

k) A. Wulf, K. Fumino, D. Michalik, R. Ludwig, ChemPhysChem 2007, 8, 2265 –2269.

l) A. Yokozeki, D. J. Kasprzak, M. B. Shiflett, Phys. Chem. Chem. Phys. 2007, 9, 5018 – 5026.

22) G.W. Parshall, J. Am. Chem. Soc. 94 (1972) 8716.

23) J.A. Boon, J.A. Levisky, J.L. Pflug, J.S. Wilkes, J. Org. Chem. 51 (1986) 480.

24) P.B. Hitchcock, K.R. Seddon, T. Welton, Dalton Trans. (1993) 2639.

25) P.B. Hitchcock, R.J. Lewis, T. Welton, Polyhedron 12 (1993) 2039.

26) Y. Gao, B. Twamley, J. Shreeve, Inorg. Chem. 43 (2004) 3406.

27) M.S. Sitze, E.R. Schreiter, E.V. Patterson, R.G. Freeman, Inorg. Chem. 40 (2001) 2298.

28) X.W. Sun, S.Q. Zhao, R.A. Wang, Chin. J. Catal. 25 (2004) 247.

29) (a) S.A. Bolkan, J.T. Yoke, J. Chem. Eng. Data 31 (1986) 194;

(b) S.A. Bolkan, J.T. Yoke, Inorg. Chem. 25 (1986) 3587.

30) (a) P.-Y. Chen, M.-C. Lin, I.-W. Sun, J. Electrochem. Soc. 147 (2000) 3350;

(b) P.-Y. Chen, I.-W. Sun, Electrochim. Acta 46 (2001) 1169;

(c) M.-C. Lin, P.-Y. Chen, I.-W. Sun, J. Electrochem. Soc. 148 (2001) C653;

(d) J.-F. Huang, I.-W. Sun, J. Electrochem. Soc. 149 (2002) E348;

(e) J.-F. Huang, I.-W. Sun, J. Electrochem. Soc. 150 (2003) E299;

(f) J.-F. Huang, I.-W. Sun, J. Electrochem. Soc. 151 (2004) C8;

(g) J.-F. Huang, I.-W. Sun, Electrochim. Acta 49 (2004) 3251.

31) R. K. Mazitov, V. V. Evsikov, M. N. Buslaeva, Teoretical and experimental chemistry, 1976, 11, 336-340.

32) A. Doroodian, J. E. Dengler, A. Genest, N. Rösch, B. Rieger, Angew. Chem. 2010, 122, 1915 –1917.

33) Luinstra, G. A.; Haas, G. R.; Molnar, F.; Volker, B.; Eberhardt, R.; Rieger, B.; Chem. Eur. J. 2005, 11, 6298 – 6314.

34) Eberhardt R.,Allmendinger M., Rieger, B.; Macromol. Rapid Commun. 2003, 24, 194-196.

35) Rokicki, G.; Kuran, W.; Marciniak B. P.; Monatshefte für Chemie 1984, 115, 205-214.

36) Ji, D; Lu, X.; Ren, H.; Applied Catalysis A General 2000, 203(2), 329–333.

37) Kim, H. S.; Kim, J., J.; Byung, G. L.;Jung, O. S., Jang, H. G.;Kang, S. O.; Angew. Chem. Int. Ed. 2000, 39, 4096-4098.

38) Mai, T.; Davis R. J.; Journal of Catalysis 2001, 199(1), 85-91.

39) Matsuda, H.; Ninagawa, A.; Nomura, R.; Chemistry Letters 1979, 10, 1261-1262.

40) Peng, J.; Deng, Y.; New J. Chem. 2001, 25, 639.

41) H.S. Kim, J.J. Kim, H.N. Kwon, M.J. Chung, B.G. Lee, H.G. Jang, J. Catal. 205 (2002) 226.

42) V. Calo, A. Nacci, A. Monopoli, A. Fanizzi, Org. Lett. 4 (2002) 2561.

43) R.L. Paddock, S. Nguyen, J. Am. Chem. Soc. 123 (2001) 11498.

44) H.S. Kim, J.J. Kim, B.G. Lee, O.S. Jung, H.G. Jang, S.O. Kang, Angew. Chem. Int. Ed. 39 (2000) 4096.

45) K. Yamaguchi, K. Ebitani, T. Yoshida, H. Yoshida, K. Kaneda, J. Am. Chem. Soc. 121 (1999) 4526.

46) Kim, H. S; Kim, J. J.; Kim, H.; Jang, H. G.; Journal of Catalysis 2003, 220, 44–46.

47) Stenzel O, Raubenheimer HG & Esterhuysen C J. Chem. Soc., Dalton Trans., 2002, 1132–1138.

48) Alexander Wulf, Koichi Fumino, and Ralf Ludwig, Angew. Chem. Int. Ed. 2010, 49, 449 -453.

Koichi Fumino, Alexander Wulf, and Ralf Ludwig Angew. Chem. Int. Ed. 2009, 48, 3184 –3186.

49) D. F. Hornig, J. Chem. Phys. 16, 1063 (1948); H. Winston and R. S. Halford, ibid., 17, 607 (1941)

50) J. Am. Chem. Soc., 1964, 86 (1), pp 17–20.

51) J.-B. Brubach, A. Mermet, A. Filabozzi, A. Gerschel, P. Roy, J. Chem. Phys. 2005, 122, 184509

52) H. L. Schläfer, G. Gliemann, Basic Principles of Ligand Field Theory, Wiley-Interscience, London 1969, p. 86.

53) B. Wisser,C, Janiak; Z. Anorg. Allg. Chem. 2007, 633, 1796-1800.

54) T. W. Swaddle, L. Fabes, Can. J. Chem. 1980, 58, 1418-1426.

55) a) R. C. Suarez, I. Doaz, S. G. Granda, V. Fernandez Acta Cryst. (2000). C56, 385-387.
b) R. Taylor and 0. Kennard, J. Am. Chem. SOC., 1982,104, 5063.

56) a) H. S. Kim, J. J. Kim, H. Kim, H. G. Jang, Journal of Catalysis 220 (2003) 44–

46.

b) Y. J. Kim, R. S. Varma, J. Org. Chem, Vol. 70, No. 20, 2005, 7882-91.

57) a) V. Calo, A. Nacci, A. Monopoli, A. Fanizzi, Org. Lett. 4 (2002) 2561.

b) F.W. Li, L.F. Xiao, C.G. Xia, B. Hu, Tetrahedron Lett. 45 (2004), 8307.

c) J. Palgunadi, O. Kwon, H. Lee, J.Y. Bae, B.S. Ahna, N.Y. Min, H.S. Kim, Catal. Today 98 (2004) 511.

d) Y.J. Kim, R.S. Varma, J. Org. Chem. 70 (2005) 7882.

58) a) Ratzenhofer, M.; Kisch, H. Angew. Chem., Int. Ed. Engl. 1980, 19, 317-318.

b) Dümler, W.; Kisch, H. Chem. Ber. 1990, 123, 277-283.

Zusammenfassung:

Diese Dissertation ist in drei Kapitel aufgeteilt. Am Anfang wurde die Wasserstoffaktivierung zwischen bifunktionellen sterisch anspruchsvollen Lewissäuren und Lewisbasen wie 1,6-bis(bis(perfluorophenyl)boryl)hexan (1) und 1,3-bis (diphenylphosphino)propan (2) untersucht. Eine Lösung von 1 und 2 in Toluol wurden gemischt und ein weißer Feststoff wurde nach kurzer Zeit herauskristallisiert. Eine spektroskopische Untersuchung (31P NMR) in CDCl3 zeigt eine Lewissäure/Lewisbase Addukt. Die Ursache ist ein zu geringer sterischer Anspruch, der zu einer Lewis-paar Wechselwirkung führt. Deshalb wurden sterisch anspruchsvollere Borane wie Tris-(pentafluorophenyl)boran eingesetzt, um den sterischen Effekt auf Borverbindungen zu erhöhen. Die Lewissäure/Lewisbase Wechselwirkung wurde in dem Fall auch spektroskopisch festgestellt. Die Untersuchung der Kristallstruktur von 2 zeigt eine starke Nukleophilie, welche die Wechselwirkung mit Lewis Säure vereinfacht. Diisoproylsulfid wurde als ein weiters, starke Nukleophil in Wechselwirkung mit $B(C_6F_5)_3$ untersucht. Dabei fällt ein weißer Feststoff nach kurzer Zeit aus der Lösung aus. Die spektroskopische Untersuchung zeigt wieder die Lewis-Paar-Wechselwirkung.

Aufgrund unserer Erfahrung in der Wasserstoffaktivierung und -speicherung haben wir die Aminoboranderivaten als Wasserstoffspeichermaterialien in dem zweiten Kapitel untersucht. Es wurde eine neue ionische Flüssigkeit auf Basis von Methylguanidinium vorgestellt.

Die ionische Flüssigkeit Methylguanidiniumborhydrid kann unter thermischen und katalytischen Bedingungen theoretisch 9 Gew.-% Wasserstoff freisetzen. Die thermodynamischen Eigenschaften der Verbindung sowie die bei der dehydrierenden Zersetzung entstehenden Produkte wurden vorgestellt.

In dem letzten Kapitel wurden ionische Flüssigkeiten auf Basis des Methylguanidinium Kations mit unterschiedlichen Anionen wie Tetrafluoroborat hergestellt.

Diese Verbindungen auf Basis von Übergangsmetallen wurden produziert, um die Wasserstoffbrückenbindungen und die daraus resultierende katalytische Aktivität zu untersuchen. Die Kristallstruktur und IR-Messungen in fernen Infrarotbereich zeigen starke Wasserstoffbrücken zwischen dem Metallchlorid und Wasserstoff von Methylguanidinium. Die katalytische Aktivität wurde bei der Zyklisierung von CO_2 und Propylenoxid zu zyklischen Carbonaten untersucht.